TECHNISCHE UNIVERSITÄT MÜNCHEN

Wissenschaftszentrum Weihenstephan für Ernährung, Landnutzung und Umwelt

Lehrstuhl für Technische Mikrobiologie

Formation and structure of exopolysaccharides of meat starter cultures

Roman Maximilian Prechtl

Vollständiger Abdruck der von der Fakultät Wissenschaftszentrum Weihenstephan für Ernährung, Landnutzung und Umwelt der Technischen Universität München zur Erlangung des akademischen Grades eines

Doktors der Naturwissenschaften (Dr. rer. nat.)

genehmigten Dissertation.

Vorsitzender: Prof. Dr. Wolfgang Liebl

Prüfende der Dissertation:
1. Prof. Dr. Rudi F. Vogel
2. Prof. Dr. Wilfried Schwab

Die Dissertation wurde am 16.01.2019 bei der Technischen Universität München eingereicht und durch die Fakultät Wissenschaftszentrum Weihenstephan für Ernährung, Landnutzung und Umwelt am 05.04.2019 angenommen.

DANKSAGUNG

Mein besonderer Dank an dieser Stelle gilt meinem Doktorvater Herrn Prof. Rudi F. Vogel für das in mich gesetzte Vertrauen, sowie die uneingeschränkte Unterstützung und lehrreichen Diskussionen zu jedem Zeitpunkt der Promotion. Herzlichen Dank dafür, Rudi!

Weiterhin möchte ich mich in besonderem Maße bei meinem Betreuer Dr. Frank Jakob bedanken, der mich zu jeder Zeit mit hilfreichen Anmerkungen, anregenden Diskussionen und seiner fachlichen Expertise unterstützt hat.

Bei Frau Angela Seppeur möchte ich mich explizit für die Übernahme der Verwaltungsaufgaben im Rahmen meines Projektes, v.a. die finanziellen Angelegenheiten, bedanken.

Herrn Dr. Daniel Wefers, Dr. Jürgen Behr und Frau Dr. Christina Ludwig danke ich für die schnelle, unkomplizierte und vor allem erfolgreiche Realisierung unserer wissenschaftlichen Kooperationen.

Besonderer Dank gilt außerdem Di Xu und Evelin Wigmann, die stets für eine angenehme Stimmung im Ost-Büro gesorgt haben! Danke meine Mädels für viele unvergessliche Momente! Dieser Dank gilt natürlich auch meinen übrigen Kolleginnen und Kollegen im Labor, egal ob Student, Doktorand oder TA, welche den Laboralltag tagtäglich mit ihrer Anwesenheit und angenehmen Art bereichert haben.

Ganz besonders bedanken möchte ich mich auch bei meinen Freunden Björn und Sabine, Gabriel und Evelin, Claudia, Melli, Raini und Dani für das regelmäßige Bereitstellen von Übernachtungsmöglichkeiten und viele schöne gemeinsame Stunden in Freising!

Nicht zuletzt möchte ich mich aber vor allem bei meiner Familie bedanken, die einen wesentlichen Anteil daran trägt, dass ich heute hier stehe: Meinen Großeltern Franz und Marianne, die diesen Tag leider nicht mehr miterleben kann, sowie Rosi und Robert für die finanzielle Unterstützung während des Studiums. Und natürlich meinen Eltern Angela und Hubert, sowie meinen Geschwistern Hubert, Sabine, Maria und Simon für die liebevolle und aufopferungsvolle Erziehung, bzw. den kompromisslosen Zusammenhalt aller Geschwister!

INDEX

ABBREVIATIONS

%	percentage
°C	degrees celsius
µg	microgram
aa	amino acids
AAB	acetic acid bacteria
ADP	adenosine diphosphate
AF4	asymmetric flow field flow fractionation
AST	antimicrobial susceptibility testing
ATP	adenosine triphosphate
av.	average
BLAST	basic local alignment search tool
bp	base pair
bP	bisphosphate
CDM	chemically defined medium
CDS	coding sequences
CFU	colony forming units
chr	chromosome
COSY	correlated spectroscopy
CPS	capsular polysaccharide
Da	dalton
DexB	glucan-1,6-alphaglucosidase
dH$_2$O	demineralized water
dn/dc	refractive index increment
Dsr	dextransucrase
EC	enzyme commision (number)
EPS	exopolysaccharide
fin. conc.	final concentration
Fru	fructose

FruA	PTS fructose transporter subunit IIABC
FruK	1-phosphofructokinase
FruR	fructose operon repressor
g	gramm
Gal	galactose
GH	glycoside hydrolase
Glc	glucose
GTF	glycosyltransferase
h	hour
HePS	heteropolysaccharide
HGAP 3	hierarchical genome-assembly process version 3
HoPS	homopolysaccharide
HPAEC	high performance anionic exchange chromatography
HPIC	high performance ion chromatography
HPLC	high performance liquid chromatography
HSQC	Heteronuclear single quantum coherence
kb	kilobases
kDa	kilodalton
L	liter
L.	*Llactobacillus*
LAB	lactic acid bacteria
Lc.	*Lactococcus*
Ln.	*Leuconostoc*
LS	light scattering
LTA	lipoteichoic acid
M	molarity
Mal	maltose
MALDI-TOF MS	matrix assisted laser desorption ionization-time of flight mass spectrometry
MALS	multi angle light scattering
Man	mannose

MBp	basal medium with peptone
MDa	megadalton
mg	milligram
MIC	minimal inhibitory concentration
min	minute
mL	milliliter
mm	millimeter
mmol	millimole
mMRS	modified de Man, Rogosa and Sharpe medium
M_W	(weight average) molecular weight
NCBI	National Center for Biotechnology Information
nm	nanometer
NPS	Nitrit-Pökelsalt (curing salt)
OD	optical density
P	phosphate
PAD	pulsed amperiometric detection
PCA	perchloric acid
PDI	polydispersity index
PEP	phosphoenole pyruvate
PFK	phosphofructokinase
PGI	phosphoglucose isomerase
pl	Plasmid
PMAA	partially methylated alditole acetate
RAST	rapid annotation using subsystems technology
Rha	rhamnose
RI	refractive index
RMS	root mean square radius
rpm	rotations per minute
RSM	Rohwurst-Simulations-Medium (simulation medium for raw-fermented sausages)
RT	room temperature

R$_W$ (geo)	(weight average) geometric radius
s	second
S.	*Streptococcus*
ScrA	PTS beta-glucoside transporter subunit IIBCA
ScrB	sucrose-6-phosphate hydrolase
ScrK	fructokinase
ScrR	sucrose operon repressor
seq	sequence
SMRT	single molecule realtime
sp.	species
spp.	speciales
Suc	sucrose
TCA	trichloroacetic acid
TFA	trifluoroacetic acid
TMW	Technische Microbiologie Weihenstephan
TOCSY	total correlated spectroscopy
UV	ultraviolet
WGS	whole genome shotgun sequence
WTA	wallteichoic acid
w/w	weight by weight
x g	times gravity

1. INTRODUCTION

1.1. Exopolysaccharide formation by lactic acid bacteria

The production of exopolysaccharides (EPS) is quite common among lactic acid bacteria (LAB) and has been extensively studied in the past (Han, 1990; van Geel-Schutten et al., 1998; De Vuyst and Degeest, 1999; Monsan et al., 2001). According to their monomeric composition, which may contain only one or different types of sugar monomers, they are classified in homopolysaccharides (HoPS) and heteropolysaccharides (HePS) and they may either occur in a cell-bound or a cell-free form (Sutherland, 1979; Looijesteijn and Hugenholtz, 1999; van Geel-Schutten et al., 1999; Tieking et al., 2005; Schwab and Gänzle, 2006; van Hijum et al., 2006).

Several physiological roles of the EPS formation have been discussed in the literature, and especially the cell surface associated EPS were reported to play an important role in the modulation of bacterial interactions with their surrounding environment (Zeidan et al., 2017). Besides their contribution to biofilm formation, this includes primarily the protection of the producing strain against adverse external factors such as toxic molecules (i.e. ethanol, antibiotics), hydrolyzing enzymes (i.e. lysozyme), desiccation or phage infection (Sutherland, 1979; Monsan et al., 2001; Badel et al., 2011; Zannini et al., 2016). Since most strains are lacking the enzymes required for the degradation of the produced EPS, it is generally believed that they do not serve as an energy reserve for the producing strains (Cerning, 1990).

Apart from that, EPS have been suggested to mediate interactions between the producing bacteria and their host in that they facilitate the adherence to various surfaces including eukaryotic cells and the intestinal mucosa (Ryan et al., 2015; Zeidan et al., 2017). In this context, several EPS have been reported to function as immunomodulators, while antitumor and even cholesterol-lowering activities have been described as well (De Vuyst and Degeest, 1999; Ruas-Madiedo et al., 2002; Badel et al., 2011). As opposed to these beneficial properties, however, EPS produced by LAB can also have negative effects for the host: The water-insoluble mutans produced by some *Streptococcus (S.)* spp., for example, were shown to play a vital role in the bacterial adhesion to the tooth surface, thereby causing dental plaque formation and eventually cariogenesis (Hamada and Slade, 1980; De Vuyst and Degeest, 1999).

1.1.1. Synthesis of homopolysaccharides

Types of homopolysaccharides

By definition, homopolysaccharides (HoPS) are composed of only one type of sugar monomer. Although several exceptions exist, for example β-glucans produced by some *Pediococcus* spp. or polygalactans produced by a *Lactococcus* (*Lc.*) *lactis* strain (De Vuyst and Degeest, 1999; Ruas-Madiedo et al., 2002; Fraunhofer et al., 2018), HoPS are generally synthesized by extracellular enzymes, which use sucrose as glycosyl donor and are composed of either glucose (glucans) or fructose (fructans) (Monsan et al., 2001). Hence, in contrast to the majority of polysaccharides, no activated sugar precursors are required for their synthesis, as the energy for polymerization is obtained from the hydrolysis of the glycosidic α,β-1,2-linkage in the sucrose molecule. Accordingly, the involved enzymes are not designated as glycosyltransferases but transglycosylases (glycansucrases), which belong to the GH70 family (CAZy database), and they are further specified depending on their polymer product as glucan- or fructansucrases, respectively (De Vuyst and Degeest, 1999; Monsan et al., 2001). A more detailed classification of both homopolysaccharides and corresponding enzymes can be performed according to the chemical linkages present in the polysaccharides (Figure 1).
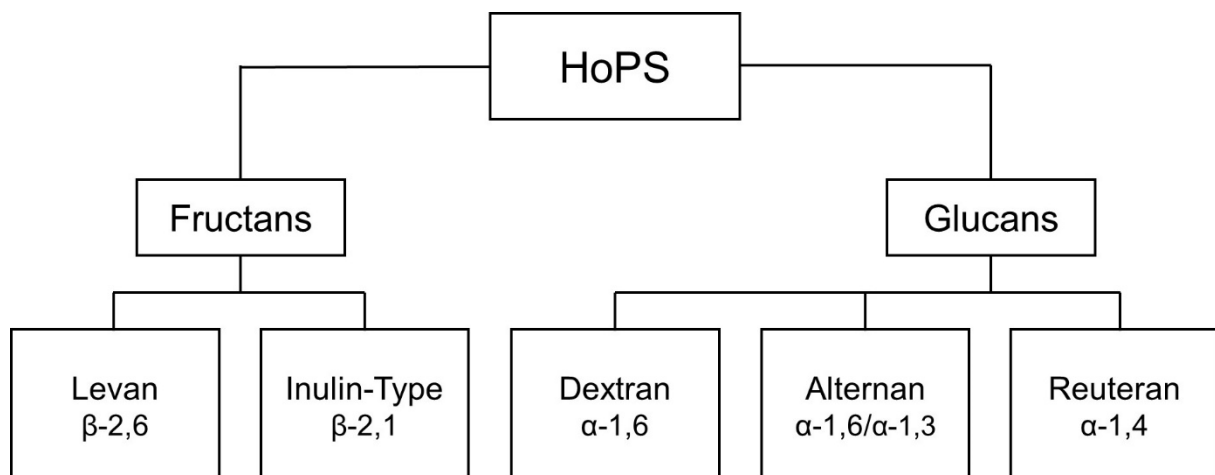
Figure 1 Classification of homopolysaccharides produced by *Lactobacillus* spp. with predominant backbone linkages.

Depending on the producing species and strains, all HoPS may contain branchings at various positions, while the degree of branchings and also their position are characteristic and depend on the producing strain (Monsan et al., 2001; Badel et al., 2011).

Structural composition of glucansucrases

In contrast to fructansucrases (FS), which are evolutionarily related to sucrose-hydrolyzing invertases, the glucansucrases (GS) are related to α-amylase type enzymes and share the same structural organization of the catalytic core, which is made up of three domains (A, B, C) being homologous to their counterparts in GH13 enzymes (van Hijum et al., 2006). Like many members of the related GH13 family, glucansucrases harbor a heptacoordinated Ca^{2+} ion between the core domains A and B, which was demonstrated to be crucial for a proper enzymatic activity (Vujicic-Zagar et al., 2010). In addition to the three core domains, two extra domains IV and V are attached to the core domains and complete the structural composition of GS, which may reach high molecular weights of 120-200 kDa or even larger (Leemhuis et al., 2013). The catalytic site of GS is located in the core domain A, which is arranged in a $(\beta/\alpha)_8$ barrel structure, and involves three catalytic residues forming a catalytic triad: (i) an aspartate (catalytic nucleophile), (ii) glutamate (general acid/base catalyst) and (iii) a second aspartate (transition state stabilizer) (Leemhuis et al., 2013). In addition, four other amino acid residues, which are involved in substrate orientation and transition state stabilization, are conserved in the active site of both GH13 enzymes and GS. These include an arginine, an aspartate and two histidine residues, whereas one of the latter was replaced by a glutamine residue in GS (van Hijum et al., 2006; Leemhuis et al., 2013). While the function of domain IV remains unclear and was discussed to constitute a 'hinge' region between the core domains ABC and domain V (Ito et al., 2011), the latter is formed by the N- and C- terminus of the polypeptide chain and contains a variable number of glucan binding domains (GBD). These GBD were not only discussed to be involved in glucan product binding, but might also mediate interactions of the GS with carbohydrates present in the cell wall of bacteria. This is supported by the fact, that several GS were shown to contain a C-terminal LPxTG cell wall anchor motif (Rühmkorf, 2012; Prechtl et al., 2018a).

Enzymatic mechanism of glucan synthesis

The enzymatic mechanism of glucan synthesis was described in detail by Vujicic-Zagar et al., who also provided a model for the incorporation of branchings at various positions (Vujicic-Zagar et al., 2010). Briefly, the glycosidic oxygen in the α,β-1,2 glycosidic linkage of sucrose is protonated by the general acid/base catalyst (Glu) upon coincidental nucleophilic attack of the anomeric carbon atom C1 in the substrate by the catalytic nucleophile Asp, which eventually leads to the release of fructose and the formation of a covalent glycosyl-enzyme intermediate. In the second part of the reaction mechanism, the enzyme-linked glucosyl moiety is transferred to the acceptor substrate. The formation of the new glycosidic

linkage (retaining mechanism) is again favoured by the general acid/base catalyst Glu, which is now acting as base and deprotonates the linkage-forming hydroxyl group of the acceptor molecule, thereby increasing its nucleophilic potential (Vujicic-Zagar et al., 2010). Three different types of acceptor molecules are possible, thereby defining the three reaction types being catalyzed by glucansucrases: (i) Polymerization reaction (acceptor= growing α-glucan chain), (ii) hydrolysis reaction (acceptor = water molecule) and (iii) acceptor reaction (acceptor = other than α-glucan, e.g. maltose, isomaltose, etc.) (Leemhuis et al., 2013).

Macromolecular structure of glucans

In regard to the macromolecular structure, the α-glucans synthesized by *Lactobacillus* (*L.*) spp. (e.g. *L. curvatus*, *L. sakei*, *L. hordei*, etc.) represent high molecular weight polymers with average molecular weights of up to even more than 1×10^8 Da (Rühmkorf et al., 2012; Nacher-Vazquez et al., 2017b; Prechtl et al., 2018b; Xu et al., 2018). In contrast, the glucans (mainly dextrans or alternans) produced by *Leuconostoc* (*Ln.*) spp. are commonly smaller and reach average molecular weights of ca. 10^6-10^7 Da (Kim et al., 2003; Miao et al., 2015).

However, it is important to know that the molecular weight of produced glucans (and also fructans) as well as their branching degree are influenced by external parameters such as pH and temperature (Shamala and Prasad, 1995; Ua-Arak et al., 2017a; Prechtl et al., 2018b).

1.1.2. Synthesis of heteropolysaccharides

HePS biosynthesis in LAB

Besides the different monomer composition, which includes more than only one type of carbohydrate monomer, the HePS biosynthesis process itself varies greatly from that of HoPS and is far more complex. Most importantly, HePS biosynthesis does *not* occur extracellularly but in the cytoplasm, and more specifically at the cell membrane (De Vuyst and Degeest, 1999). Secondly, HePS biosynthesis relies on activated sugar precursors and involves a number of various glycosyltransferases (GTs), which assemble the oligosaccharide precursors and may incorporate various branchings (De Vuyst and Degeest, 1999; Schmid et al., 2015). So far, three different mechanisms have been described for HePS biosynthesis in bacteria: (i) the Wzx/Wzy dependent pathway, (ii) the ATP-binding cassette (ABC) transporter-dependent pathway and (iii) the synthase-dependent pathway (Schmid et al., 2015). Since LAB mostly use the Wzx/Wzy dependent pathway for HePS synthesis (Zeidan et al., 2017), it will be discussed in more detail in this section.

Wzx/Wzy-dependent HePS biosynthesis clusters

The available data for HePS synthesis clusters of LAB suggest a rather conserved modular organization of ca. 15-20 kb clusters in which three modulatory genes (*wzd, wze, wzh*) form a tyrosine phosphoregulatory circuit and are followed by a varying number of GTs responsible for repeating unit synthesis (Groot and Kleerebezem, 2007; Zeidan et al., 2017). Apart from that, other transferases may be part of the cluster and catalyze the derivatization of the repeat unit with non-sugar moieties (e.g. acetyl-groups). Furthermore, a flippase (*wzx*) and a polysaccharide polymerase (*wzy*) enable translocation and interconnection of the repeating units, respectively (Figure 2).
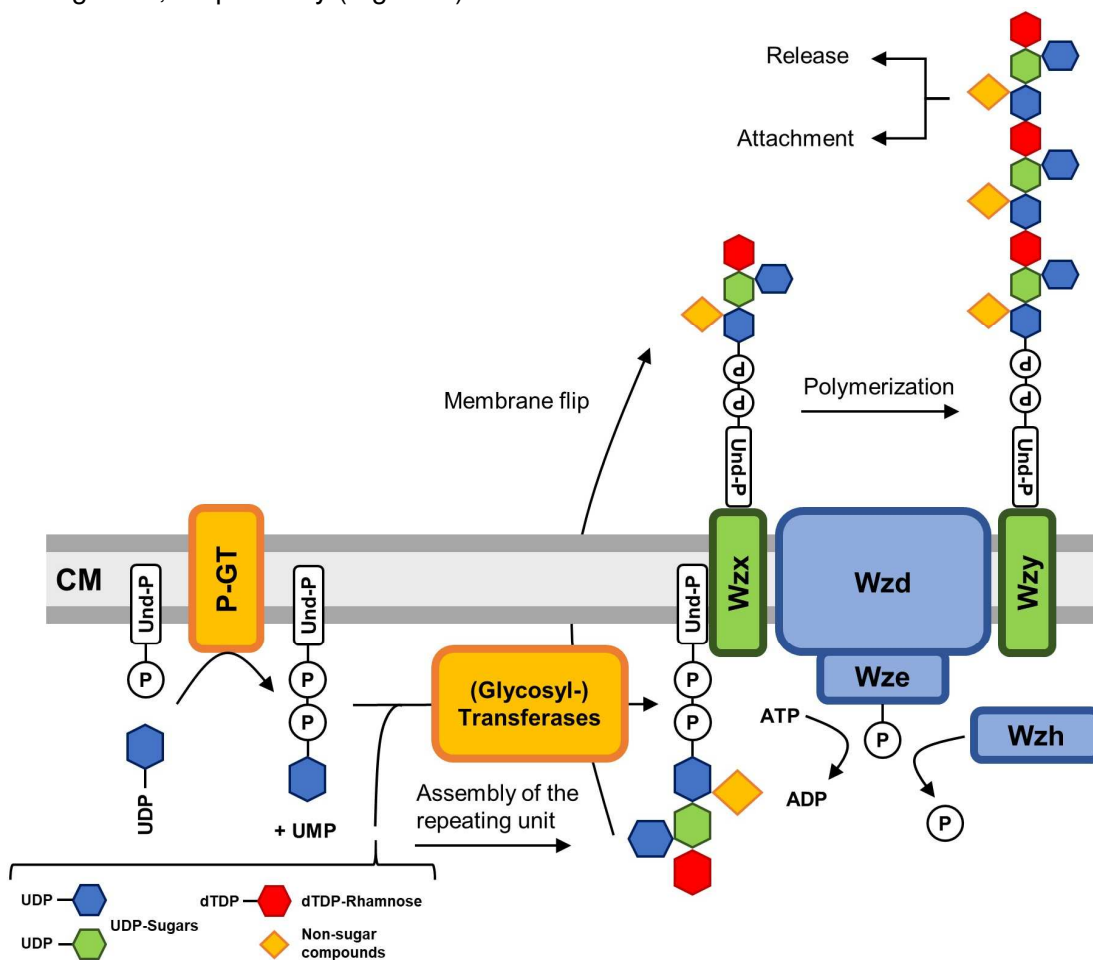
Figure 2 Model for HePS biosynthesis in LAB via to the Wzx/Wzy dependent pathway. This figure is based on Figure 5 published by Zeidan et al. (2017). The priming glycosyltransferase (P-GT) is anchored in the cellular membrane (CM) and catalyzes the first step in repeating unit synthesis by transferring a sugar moiety to the lipid carrier undecaprenylphosphate (Und-P). Afterwards, several (glycosyl-) transferases complete the repeating unit by sequential addition of sugar and non-sugar residuals, where the former requires activated sugar precursors (uridine diphosphate = UDP-sugars or deoxythymidine diphosphate = dTDP-rhamnose). The repeating unit is flipped across the membrane by the flippase Wzx and polymerized by Wzy. The modulatory proteins Wzd, Wze and Wzh form a phosphoregulatory circuit, where Wzd initiates autophosphorylation of Wze, whereas Wzh catalyzes dephosphorylation of Wze. The precise mechanism of HePS biosynthesis regulation by Wzd, Wze and Wzh remains unexplored and an additional role of Wzd as scaffold for the HePS biosynthesis machinery (P-GT, Wzx, Wzy) was discussed as well. The polymerized HePS can be either released in the extracellular space or linked with the peptidoglycan layer to form a capsular polysaccharide, which putatively requires an additional enzyme (Zeidan et al., 2017).

While modulatory enzymes, flippase and polysaccharide polymerase, as well as the priming glycosyltransferase (P-GT, catalyzing the first step in repeat unit synthesis via transfer of a monosaccharide to the lipid carrier undecaprenyl-phosphate, Und-P) usually share homology on amino acid level to other members of these protein families, the GTs were found to be highly diverse, reflecting the enormous structural variety of HePS produced by LAB (Zeidan et al., 2017). As a result of this complex biosynthesis mechanism, the HePS yields obtained from bacteria cultivated at non-optimized culture conditions are usually lower than 0.350 g/L, whereas the amounts of HoPS are in the range of up to several grams per liter (De Vuyst and Degeest, 1999; Monsan et al., 2001).

Structures of HePS produced by LAB

Many studies were focused on the structural analysis of HePS by means of monomer- and methylation analysis, as well as various NMR techniques (e.g. TOCSY, HMBC). Numerous repeat unit structures of usually 3-8 types of monosaccharides, distinct linkage types and various decorative elements (e.g. acetate, phosphate) were detected in these studies (Zeidan et al., 2017). For example, HePS of the industrially exploited yoghurt starter culture *S. thermophilus* Sfi6 is composed of a tetrameric repeating unit containing galactose, glucose and N-acetylgalactosamine (2:1:1). In contrast, *Lc. Lactis* NIZO produces a phosphorylated (and thus negatively charged) HePS comprising galactose, glucose and rhamnose (2:2:1) (Stingele et al., 1996; van Kranenburg et al., 1997). Among *Lactobacillus* species, the HePS produced by *L. delbrueckii ssp. bulgaricus* Lfi5 and *L. rhamnosus* RW-9595M are well characterized, and both are constituted of a heptameric repeating unit containing galactose, rhamnose and glucose in different ratios, whereas the HePS of *L. rhamnosus* RW-9595M is additionally decorated with a pyruvate moiety (Lamothe et al., 2002; Van Calsteren et al., 2002). Moreover, some structural data are available for HePS produced by *L. plantarum* species. While the HePS of *L. plantarum* MTCC9510 was composed of a linear trimeric repeating unit containing glucose and mannose residues, *L. plantarum* C88 was demonstrated to produce a structural complex HePS with a branched pentameric repeating unit containing glucose, galactose and an O-acetyl group (Ismail and Nampoothiri, 2010; Fontana et al., 2015). Apart from that, Remus et al. investigated the surface glycan composition of *L. plantarum* WCFS1, which was shown to contain rhamnose, glucosamine and galacturonic acid next to the common monosaccharides glucose and galactose (Remus et al., 2012). The molecular mass of the polymers is commonly determined by means of chromatographic methods (e.g. size exclusion chromatography) and usually yields magnitudes of 10^4-10^6 Da (Stingele et al., 1999; Pham et al., 2000; Remus et al., 2012).

1.2. Exopolysaccharides in industrial products

The use of exopolysaccharides as natural hydrocolloids caught the attention of the food and chemical industry many years ago (Sutherland, 1979; Cerning et al., 1992; Marshall et al., 1995; De Vuyst and Degeest, 1999). Because of their physicochemical properties, exopolysaccharides function as natural stabilizers, thickeners and gelling agents, which establishes their use in various industrial products including cosmetic and medical substances, pharmaceutical compounds or foods (Han, 1990; van Geel-Schutten et al., 1998; Zeidan et al., 2017). Furthermore, several EPS were even demonstrated to exhibit health-promoting effects, namely antioxidant or anti-tumor activities (Freitas et al., 2011; Ryan et al., 2015). Apart from that, EPS can be chemically modified, which gives rise to even more industrial applications. Controlled hydrolysis of *Ln. mesenteroides* dextran, for example, results in the formation of low molecular weight fractions, which are used in the manufacturing of supports for gel permeation chromatography columns (Sephadex®), while sulfated dextrans are used as antiviral agents (Monsan et al., 2001; Freitas et al., 2011).

However, the occurrence of EPS can also be disadvantageous especially in food products and lead to spoilage, such as the formation of β-glucan by *L. brevis* in beer (Fraunhofer et al., 2018). Moreover, EPS can be involved in pathogenicity, which is related to their key role in capsule and biofilm formation of pathogenic bacteria such as *S. pneumoniae* (Yother, 2011).

1.3. Lactic acid bacteria as starter cultures in the food industry

The manufacturing of fermented food products is known since centuries and dates even back to prehistoric times, where fermentation processes guaranteed the preservation of foods of animal and plant origin. One of the most important mechanisms of preservation is the acidification of the food matrix, which is accomplished by acetic acid bacteria (AAB) or LAB and inhibits the growth of pathogenic or food spoilage bacteria (Buckenhüskes, 1993). However, other mechanisms have been elucidated as well, including the synthesis of antimicrobial peptides (i.e. bacteriocins), which were demonstrated to suppress the growth of undesired or pathogenic bacterial species. While the presence of microbes was unknown in those days and the fermentation processes were driven by the autochthonous microbiota, their existence and role in food fermentation processes has been discovered and extensively studied in the past century. As a result, customized and commercially available starter culture preparations have been developed, which are now specifically added in the manufacturing of fermented food products to assure both safety and quality parameters of the final product in standardized processes. Typical fermented food products, the ripening processes of which are based on LAB activity, are raw-fermented sausages (e.g. salami), fermented vegetables (e.g. sauerkraut) as well as dairy products (e.g. yoghurt), for example.

1.3.1. LAB as meat starter cultures

Typical meat starter culture preparations include representatives of the genera *Staphylococcus, Micrococcus, Pediococcus* and *Lactobacillus* (Buckenhüskes, 1993; Vignolo et al., 2010). Species of these genera are commonly isolated from traditionally (spontaneously) fermented sausages and are obviously adapted to the stringent conditions of both the meat ecosystem and the ripening process (Vignolo et al., 2010). Characteristic ecological determinants in these products are the presence of sodium chloride, nitrate/nitrite and a limited nutrient content, which mainly extends to (purine) nucleosides, certain amino acids (e.g., arginine), glucose and ribose (Champomier-Verges et al., 2001; Chaillou et al., 2005; Rimaux et al., 2012). Furthermore, the temperature is typically decreased during the ripening process of fermented meat products, which represents another decisive factor for meat starter cultures (Feiner, 2006). Apart from the inhibition of the growth of pathogens such as *Salmonella* spp. or *Listeria* spp., the pH decrease by lactic acid formation leads to secondary effects, which are important for the ripening process of fermented meat products: As a result of the acidification, the meat proteins start to coagulate, which leads to the typical firmness and sliceability of dry sausages, for example, and contributes to the reduction of the water content, thereby prolonging the shelf-life of the product (Feiner, 2006). Another

important objective of starter cultures in meat products is their contribution to the reddening process (formation of nitrosomyoglobin) during the ripening, which is favored at low pH values and may require the presence of nitrit-reductases provided by the starter cultures to form nitrite from nitrate (Buckenhüskes, 1993).

1.3.2. EPS-forming LAB starter cultures

The use of exopolysaccharide forming starter cultures is well known in the dairy industry, where the formed biopolymers function as natural, structure-forming hydrocolloids (Jolly et al., 2002; Ruas-Madiedo et al., 2002). Conditioned by their physicochemical properties, they interact with the food matrix and serve as natural thickeners and stabilizers, thereby ensuring the rheological and textural characteristics of yoghurt and cheese products, for example (Badel et al., 2011; Torino et al., 2015; Zannini et al., 2016). It is worth mentioning at this point, that structural effects mediated by EPS do not only depend on their abundance, but to a substantial extent on their structural properties. The functional effects are the result of specific interactions between the polysaccharides, the bacterial cells and/or other macromolecules in the product matrix (e.g. proteins) (Schellhaass and Morris, 1985; Cerning et al., 1992; De Vuyst and Degeest, 1999; Mozzi et al., 2006), and due to the close structure-function relationship, these interactions are predominantly determined by both the macromolecular and molecular structure of EPS, including their molar mass, monomer composition, possible charges and degree of branching, for example (Vandenberg et al., 1995; Jakob et al., 2013). As a result, despite the markedly lower production levels as compared to HoPS, HePS can induce decisive structural changes in yoghurt, the creamy structure of which is mainly depending on HePS produced by *S. thermophilus* or *Lc. lactis* (Marshall et al., 1995; Degeest et al., 2001; Mozzi et al., 2006). Apart from that, new consumer demands for low-fat or gluten-free food have given rise to explore the potential of *in situ* produced EPS to replace these functional ingredients in "clean label" products (Perry et al., 1997; Tieking et al., 2003; Rühmkorf et al., 2012; Ua-Arak et al., 2017b).

Interestingly, applications of EPS-forming starter cultures in processed meat products remain widely unexplored, although structure-forming, water binding and fat-replacing properties of EPS could be exploited in these products as well and e. g. could possibly facilitate the manufacturing of spreadable, raw-fermented sausages with reduced fat content similar to applications in low-fat cheese. However, it is not yet clear whether EPS production is feasible in such harsh environments, which are commonly dominated by cold temperatures and increasing salt concentrations.

2. MOTIVATION, HYPOTHESES AND APPROACHES

New consumer demands for fat-reduced food products have raised the question if *in situ* produced EPS by appropriate meat starter cultures may replace this functional ingredient in "clean labelled" manufactured meat products, such as German Teewurst. However, such meat starter cultures and their EPS have neither been identified nor investigated, respectively, and it is not yet clear whether a sufficient EPS production is feasible in such environments, which are commonly characterized by low temperatures and high salt concentrations. Above that, the production conditions of manufactured meat products are commonly defined by technological aspects, and both production and structure (and thus functionality) of EPS *in situ* may differ from that one determined under optimal laboratory conditions. Moreover, the application of HoPS forming LAB starter cultures would require sucrose as carbon source instead of the usually applied glucose, and the general physiological response of HoPS forming LAB strains to this carbohydrate was well as active metabolic pathways during HoPS synthesis are not characterized in that environment. The present work should address this lack of knowledge under consideration of the following working hypotheses:

- Suitable EPS forming meat starter cultures can be identified in the in-house strain collection
- The use of the identified starter cultures does not constitute any health risk
- The macromolecular and chemical structure of formed EPS can be elucidated
- EPS biosynthesis is genetically encoded, and the responsible genes can be identified
- Environmental parameters have an impact on production and structure of formed HoPS
- HoPS forming starter cultures show a specific physiologic response to sucrose as carbon source

From these working hypotheses, the following approaches were derived:

- LAB strains isolated from meat or cold-stored, salt containing food products (e.g. sauerkraut) should be screened for EPS formation
- Promising strains should be identified in competitive growth experiments
- Any health risk due to transferable antibiotic resistances or formation of biogenic amines should be excluded by means of appropriate screening experiments

- Macromolecular and chemical structure of the EPS should be investigated by means of various analytical techniques, including HPAEC-PAD, AF4-MALS and NMR
- The genetic principle of both HePS and HoPS biosynthesis should be elucidated via whole genome sequencing and comparative genomics
- HoPS should be produced at defined cold- and salt stress parameters and investigated as described above
- The physiologic response to sucrose in relation to glucose should be investigated by means of a quantitative proteomics approach and monitoring of the fermentation metabolites

3. MATERIALS AND METHODS

3.1. General microbiological techniques

3.1.1. Strains and culture conditions

Initially, 77 strains of the species *L. sakei*, *L. curvatus*, *L. plantarum*, *Lc. piscium* and *Ln. gelidum* were used in this study. Bacterial isolates were recovered from cryo-cultures (-80 °C, 80% w/w glycerol) on modified MRS (mMRS) agar (Stolz et al., 1995) by incubation for 48 h at 30 °C or 25 °C (*Lc. piscium* and *Ln. gelidum* spp.). The composition of mMRS medium and used vitamin-mix are specified in Table 1 and Table 2.

Table 1 Recipe for the preparation of mMRS medium.

Compound	Final concentration in dH_2O
Peptone	10 g/L
Yeast extract	5 g/L
Meat extract	5 g/L
$K_2HPO_4 \cdot 3\ H_2O$	4 g/L
KH_2PO_4	2,6 g/L
NH_4Cl	3 g/L
Cystein-HCl	0.5 g/L
Tween-80	0,5 g/L
(Agar)	15 g/L
HCl	ad pH 6.2
Sugar mix (fructose, glucose, maltose) [a]	5, 5, 10 g/L
Vitamin-Mix (1000x) [b]	1 mL/L

[a] depending on the experiment, the sugars were replaced by glucose, sucrose, or a mixture of glucose, galactose and lactose (see below).

[b] the vitamin mix was sterilized by filtration (0.2 µm) and added after autoclaving. Recipe: Table 2.

The solution was sterilized by autoclaving (121 °C, 20 min) and cooled, before vitamin-mix and sugar solution (both sterilized by vacuum filtration, 0.2 µm) were added. For regular precultures and strain recovery on agar plates, fructose, glucose and maltose were applied at final concentrations of 5 g/L, 5 g/L and 10 g/L, respectively, and this composition is further denoted as standard mMRS medium. If necessary, these sugars were replaced by glucose (20 g/L), sucrose (50/80 g/L), or a mixture of glucose, galactose and lactose (20 g/L each) (3.1.3, 3.1.4, 3.2.1).

Table 2 Recipe for the preparation of the vitamin-mix.

Compound	Final concentration in dH_2O
$MgSO_4 \cdot 7\ H_2O$	0.2 g/mL
$MnSO_4 \cdot H_2O$	0.038 g/mL
Thiamin	0.2 mg/mL
Niacin	0.2 mg/mL
Folic acid	0.2 mg/mL
Pyridoxal	0.2 mg/mL
Pantothenic acid	0.2 mg/mL
Cobalamin	0.2 mg/mL

To prepare precultures, 15 mL mMRS medium were inoculated with single colonies from mMRS agar plates and incubated at 30/25 °C for 36-48 h at micro-aerobic conditions (sealed tubes, Sarstedt AG & Co., Germany) without shaking.

3.1.2. Strain verification with MALDI-TOF MS

Strain verification on species level was carried out using matrix assisted laser desorption ionization-time of flight mass spectrometry (MALDI-TOF MS). Single colonies were smeared onto a stainless steel target (Bruker Daltonics, Germany) and overlaid with 1 µl formic acid (70%, Sigma-Aldrich GmbH, Germany) and 1 µl of a α-cyano-4-hydroxycinnamic acid matric solution (Bruker Daltonics, Germany). The mass spectra were generated with a Microflex LT MALDI-TOF MS (Bruker Daltonics, Germany) equipped with a nitrogen laser (λ = 337 nm), whereas operation was performed in a linear positive ion detection mode under the control of Biotyper Automation Control 3.0 (Bruker Daltonics, Germany) (Usbeck et al., 2013).

3.1.3. Determination of viable cell counts

To determine viable cell counts in CFU/mL, 50 µl of appropriate cell culture dilutions in saline (0.9% NaCl) were spread on mMRS agar (20 g/L glucose) with sterile glass beads (2.7 mm, Carl Roth GmbH, Karlsruhe, Germany) and incubated at 30/25 °C for 48 h.

3.1.4. Visual screening for EPS formation on mMRS and RSM agar

To screen for exopolysaccharide (EPS) formation, bacterial strains were recovered from cryo-cultures on mMRS agar (3.1.1) and subsequently transferred with a sterile tooth-pick to appropriate agar plates, which allowed for a visual identification of EPS positive strains by mucoid/ropy phenotypes. Sucrose dependent EPS production (i.e. production of HoPS) was detected on mMRS agar (Table 1) supplemented with sucrose (80 g/L). Screening for sucrose independent EPS production was performed on mMRS agar containing increased amounts of yeast and meat extract (10 g/L each) as well as glucose, galactose and lactose (20 g/L each), to facilitate a potential formation of HePS (Polak-Berecka et al., 2014). Finally, EPS positive strains were identified after incubation for up to 48 h at 30/25 °C. To confirm the EPS formation at mild stress conditions, the strains were additionally screened on an agar simulating the conditions of raw-fermented sausage fermentation (Rohwurstsimulations-medium, RSM) (Table 3). The RSM agar was supplemented with sucrose or glucose/galactose/lactose (depending on whether sucrose dependent or independent EPS formation was to be screened, respectively, as described above), and mucoid/ropy phenotypes were identified after incubation at 20 °C for 120 h.

Table 3 Recipe for the preparation of RSM (agar).

Compound	Final concentration in dH_2O
Meat extract	100 g/L
Tween 80	1 g/L
Nitrite curing salt (0.5% w/w $NaNO_3$ in NaCl) [a]	30 g/L
Sodium ascorbate [a]	0.6 g/L
Glucose [a, b]	3 g/L
Lactic acid	ad pH 5.8
(Agar)	15 g/L

[a] these compounds were sterilized by filtration (0.2 µm) and added after autoclaving (121 °C, 20 min).
[b] standard RSM contained glucose (3 g/L) and was used in growth experiments (3.1.5). In EPS screening experiments, glucose was replaced by sucrose (80 g/L) or a mix of glucose, galactose and lactose (20 g/L each).

3.1.5. Determination of characteristic growth parameters

The determination of maximum growth rates μ_{max} and lag-phases λ was performed in 96 well microtest plates (flate base, polystyrene; Sarstedt, Germany). 200 µL of the respective medium were inoculated from pre-cultures with an initial OD_{600} of 0.05, subsequently covered with 100 µl sterile paraffin oil and incubated various temperatures until the stationary growth phase was reached. The optical densities were recorded in regular intervals by means of a microplate reader (SPECTROstar Nano, BMG Labtech, Germany) at a wavelength of 600 nm, and the plates were shaked (500 rpm, 30 s) in the *double orbital* mode before each measurement. The growth data were evaluated with the software tool RStudio (R Development Core Team, 2010; RStudio Team, 2016) using the R package *grofit* (Kahm et al., 2010) to determine the maximum growth rates μ_{max} and the lag-phases λ by parametric (*logistic, gompertz, mod. gompertz, richards*) or non-parametric (*spline*) curve fitting, whichever fitted best. The maximum growth rate represented the maximum increase of cell density (OD_{600}) per time unit during the exponential growth phase, while λ corresponded to the inflection point of the fitted curve. In total, three to four replicates were analyzed for each strain or condition, while μ_{max} and λ were calculated for each replicate separately and finally averaged.

To determine the maximum turbidity, 15 mL liquid medium in sealed tubes were inoculated with 150 µL of a preculture and incubated statically for up to one week at various temperatures. The optical densities were measured in regular intervals in cuvettes (1 mL sample) with the use of a spectrophotometer (Novaspec Plus, GE Healthcare Company, Germany) at 600 nm, where each sample was measured in triplicate.

3.1.6. Screening for biogenic amine formation

The formation of biogenic amines from selected amino acid precursors was screened on decarboxylase agar (Bover-Cid and Holzapfel, 1999), the composition of which is presented in Table 4.

Table 4 Recipe for the preparation of decarboxylase agar.

Compound	Final concentration in dH$_2$O
Tryptone	5 g/L
Yeast extract	5 g/L
Meat extract	5 g/L
NaCl	2.5 g/L
Glucose [a]	0.5 g/L
Tween 80	1 g/L
MgSO$_4$ • 7 H$_2$O	0.2 g/L
MnSO$_4$ • 7 H$_2$O	0.05 g/L
FeSO$_4$ • 7 H$_2$O	0.04 g/L
Diammonium hydrogen citrate	2 g/L
Thiamine [a]	0.01 g/L
K$_2$HPO$_4$	0.2 g/L
CaCO$_3$	0.1 g/L
Bromcresol purple	0.06 g/L
Amino acid [b]	10 g/L
HCl/NaOH	ad pH=5.6
Agar	20 g/L

[a] glucose and thiamine were added after autoclaving (121 °C, 20 min).

[b] histidine, tyrosine, phenylalanine, lysine, ornithine and arginine.

On each agar plate, up to four different strains were screened for the formation of biogenic amines from a certain amino acid by pipetting 10 µL of the corresponding precultures on the agar surface and incubating the plates for 24-48 h at 30 °C. As the amino acids were present in excess, their decarboxylation could be visually detected by the development of a dark blue color, which was caused by the applied indicator upon alkalization of the medium.

3.1.7. Antimicrobial susceptibility testing (AST)

To investigate the susceptibility of selected strains towards various antibiotic agents, an agar diffusion assay was performed on lactobacillus susceptibility test medium (LSM, Table 5), while the inhibition zone diameters were determined as suggested by the M100-S22 document, which had been published by the Clinical and Laboratory Standards Institute

(CLSI) (CLSI, 2012). Accordingly, the pathogenic strain *Staphylococcus aureus* ATCC 25923 was used as quality control throughout the experiment to verify its validity.

Table 5 Recipe for the preparation of *Lactobacillus* susceptibility test medium (LST).

Compound	Amount in final LSM
mMRS medium (pH 6.2)	10 % (v/v)
Iso-Sensitest Broth [a]	90 % (v/v)
Agar	16.7 g/L

[a] sterilized by autoclaving (121 °C, 20 min). Iso-Sensitest Broth was obtained from Thermo Fisher Scientific, Germany and prepared as described in the manufacturers protocol, while the pH was adjusted to 6.7 with HCl/NaOH before autoclaving.

Cell suspensions in saline with a final OD_{600} of 0.1 (corresponds to ~ 0.5 McFarland standard solution) were prepared from liquid precultures and subsequently streaked on the agar plates with sterilized Q-tips. For *L. curvatus* TMW 1.50 and TMW 1.624, the concentration was increased to an OD_{600} of 0.2. After drying the agar plates on air for a few minutes, they were loaded with up to four antibiotic containing disks (SensiDisks, Oxoid LTD, United Kingdom), where two disks each were containing the same antibiotic. The plates were incubated at appropriate temperatures (30 °C or 37 °C) for up to 48 h, and the diameters of formed inhibition zones were determined after 24 h and 48 h.

In total, the susceptibility of a particular strain against a certain antibiotic was investigated for two biological replicates (i.e. two independent precultures), while two disks were used for each replicate and antibiotic, respectively (technical replicates).

3.2. Production and purification of EPS

3.2.1. Production and purification of HoPS

To produce HoPS, 50 mL or 15 mL mMRS medium supplemented with sucrose (50 g/L or 80 g/L) as sole carbon source were inoculated from liquid precultures (3.1.1) with either 1% v/v or a final OD_{600}=0.1 and incubated at 30 °C (25 °C for *Ln. gelidum* spp.) for up to 48 h at micro-aerobic conditions (sealed tubes) without shaking. Culture supernatants were obtained by centrifugation (6000 x g, 20 min) and the EPS were precipitated with two volumes of chilled denatured ethanol overnight. Afterwards, EPS were collected by centrifugation (13000 x g, 30 min, 4 °C), air dried and dissolved in an appropriate volume of dH_2O. Next, the solutions were dialyzed (dialysis tubings with 3.5 kDa MWCO, Membra-Cell™, Serva,

Germany) against dH_2O in 5 L buckets for at least two days at 4 °C, whereby the water was exchanged at least five times. Finally, the dialyzed HoPS solutions were freeze dried (FreezeZone™, Labconco, US) and stored at -20 °C or room temperature until further usage. Quantification was performed gravimetrically from freeze-dried samples.

3.2.2. Production and purification of HePS

3.2.2.1. HePS production and purification from MBp medium

For preliminary analyses, putatively HePS producing strains were cultivated in a basal medium with peptone as sole complex nitrogen source (MBp), to avoid a contamination with polymer substances contained in yeast extract. The composition is presented in Table 6.

Table 6 Composition of MBp medium.

Compound	Final concentration in dH_2O
Peptone	5 g/L
$K_2HPO_4 \cdot 3\ H_2O$	2,5 g/L
$(NH_4)_2$-Hydrogen-Citrate	2 g/L
Tween 80	1 g/L
Sodium-Acetate $\cdot$ 3 H_2O	8 g/L
Acetic acid (conc.)	ad pH 6.2

The solution was sterilized by autoclaving at 121 °C for 20 min. After cooling, a vitamin-mix (1 mL/L; Table 2) and a sugar solution (both sterilized by vacuum filtration) containing glucose, galactose and lactose were added (fin. conc. in the medium: 20 g/L each).

To produce HePS, 200 ml MBp medium were inoculated with 1% v/v of a liquid preculture (3.1.1) and incubated for 6 d at 20 °C at micro-aerobic conditions (closed glass bottles) without shaking. Isolation and purification of HePS from the supernatant was performed as described for HoPS, which had been produced in mMRS medium (3.2.1). Quantification was performed gravimetrically from freeze-dried samples.

3.2.2.2. HePS production and purification from chemically defined medium (CDM)

For detailed structural analyses, HePS were produced in a chemically defined medium (CDM), to avoid any contamination with unknown polymer substances contained in complex

nitrogen sources such as yeast extract or peptone. The composition of the CDM is presented in Table 7. Sterilization was realized by vacuum filtration (0.22 µm).

Table 7 Composition of the chemically defined medium (CDM).

Compound	Final concentration in dH_2O
KH_2PO_4	3 g/L
$K_2HPO_4 \cdot 3 H_2O$	3 g/L
Na-Acetate	5 g/L
Tween 80	1 g/L
Diammonium hydrogen citrate	1.5 g/L
$MgSO_4 \cdot 7 H_2O$	0.2 g/L
$MnSO_4 \cdot H_2O$	20 mg/L
$FeSO_4 \cdot 7 H_2O$	20 mg/L
100x mix (nuclein bases, amino acids, vitamins) [a]	100 mL/L
Glucose, galactose, lactose [b]	10 g/L each
Acetic acid	ad pH=6.2

[a] according to (Hébert et al., 2004).

[b] the sugar mix was based on the results of (Polak-Berecka et al., 2014).

The medium was inoculated from precultures with a final OD_{600} of 0.1 (~ 1 x 10^7 CFU/mL) and incubated at 20 °C for up to 96 h. To liberate the loosely associated HePS from the cell wall, the cultures were heated for up to 2 h at 60 °C in a water bath and vortexed several times prior to pelletization (13000 x g, 20 min) according to literature data (Looijesteijn and Hugenholtz, 1999). If necessary, slimy cell pellets were diluted with 0.9% NaCl and centrifugation was repeated.

Finally, the HePS were isolated, purified and quantified as described in 3.2.1. If detailed structural analyses should be performed, co-precipitated proteins were removed prior to dialysis by precipitation with trichloroacetic acid (10%) on ice for 30 min, followed by centrifugation (15 min, 13000 x g, 4 °C).

3.2.3. Dextran synthesis with resuspended cells in buffer solution

To investigate the analysis of dextran formation at comparable conditions, dextrans were produced with resting cells in buffer solutions by native (cell-bound) glycosyltransferases

similar to van Geel-Schutten et al. (van Geel-Schutten et al., 1999). Liquid cultures in standard mMRS medium (15 mL) were inoculated from pre-cultures with a final OD_{600} of 0.1 and incubated at 30 °C for several hours until a pH of 5.0, which corresponded to the mid-exponential growth phase (according to preliminary experiments). The cultures were subsequently centrifuged (2000 x g, 5 min, 4 °C), washed with saline (5 mL) by gently pipetting up and down and resuspended in 15 mL buffer solution (*vide infra*) for dextran production. Since preliminary experiments had demonstrated that cells which had been obtained from cultures in standard mMRS (without sucrose) produced equal amounts of dextran in buffer solution as those from cultures containing sucrose, the former setup was chosen to avoid a carry-over of dextrans into the buffer solutions.

To improve the comparability of the results with those of fermentation experiments, the solute concentration in the buffer solution had been adjusted to the mMRS medium, while complex constituents had been omitted to facilitate dextran quantification. The buffer was composed of K_2HPO_4 (17.5 mM), KH_2PO_4 (19.1 mM), NH_4Cl (56 mM), $CaCl_2$ (1 mM), lactic acid (pH adjusted to 5.0) and sucrose (50 g/L). If salt stress should be simulated in buffer solutions, 9.5% (w/v) NaCl were added. Bacterial growth was prevented through inhibition of DNA and RNA synthesis by the antifolate trimethoprim (10 µg/mL), against which *L. sakei* TMW 1.411 was shown to be susceptible (4.1.4). The cell suspensions were incubated for 20 h at 30 °C and 10 °C, respectively, and the supernatants were collected after centrifugation (5000 x g, 10 min). Afterwards, 5 mL of the supernatants were dialyzed as described (3.2.1). Negative controls were prepared in buffer without sucrose and uninoculated buffer solutions served as control for complete sucrose removal during dialysis.

3.3. Analytical methods

3.3.1. Acid hydrolysis of EPS

3.3.1.1. Hydrolysis of HoPS

To hydrolyze HoPS prior to HPLC analysis, 10 mg of a freeze-dried EPS sample were dissolved in 930 µl deionized water (dH$_2$O) and 70 µl of perchloric acid (PCA, 70% w/w) were added to the solution (812 mM fin. conc. PCA). For mild acid hydrolysis of EPS (e.g. to detect fructans), EPS solutions (2.5 mg/mL) were hydrolyzed with 81 mM PCA in 2 mL reaction tubes. In each case, hydrolysis was performed for 4 h at 100 °C. Subsequently, the samples were centrifuged (13000 rpm, 10 min) to remove any precipitated matter and the cooled supernatant was filtered (0.22 µm nylon filters, Phenomenex, USA). Finally, the filtered supernatants were subjected to HPLC analysis (3.3.2).

3.3.1.2. Hydrolysis of HePS

To hydrolyze HePS produced in MBp medium, 15 mg of a freeze-dried EPS sample were dissolved in 930 µl deionized water (dH$_2$O) and 70 µl of perchloric acid (PCA, 70% w/w) were added to the solution (8% w/w fin. conc. PCA). Hydrolysis was performed for 5 h at 100 °C. Subsequently, the samples were treated as described for HoPS (3.3.1.1).

HePS which had been produced in CDM and should be subjected to HPAEC-PAD monomer analysis were hydrolyzed with a different protocol: 1.5 mg HePS were hydrolyzed with 4 M trifluoroacetic acid (TFA) at 100 °C for 2 h and subsequently centrifuged (13000 x g, 10 min) to remove any precipitated material. Diluted supernatants were filtered (0.2 µm nylon filters, Phenomenex Inc., USA) and finally subjected to HPAEC-PAD analysis as described in 3.3.3.

3.3.2. Determination of sugar monomers in EPS with HPLC-RI

To determine the sugar monomers in isolated HoPS and putative HePS, 20 µl of hydrolyzed and pretreated samples (3.3.1) were automatically injected (AS 50 autosampler, Thermo Fisher, USA) into a HPLC system (Dionex Ultimate 3000, Thermo Fisher, USA) coupled to a refractive index (RI) detector (Shodex, Showa Denko, Japan). The separation of monosaccharides was achieved on a Rezex™ RPM Pb^{2+} monosaccharide column at 85 °C and a flow-rate of 0.6 mL/min using filtered dH$_2$O as isocratic eluent. Peak identification was realized with the Chromeleon™ software (v. 6.8, Thermo Fisher, USA) by means of appropriate standard solutions.

3.3.3. Analysis of HePS monomer composition with HPAEC-PAD

HPAEC-PAD analysis was carried out using a Dionex Series ICS5000 system equipped with an analytical CarboPac™ PA20 column (3 x 150 mm, 6.5 µm particle size; Thermo Scientific Dionex, USA). The monosaccharides were separated by isocratic elution (8 mM NaOH, 0.5 ml/min) within 15 min, and subsequently quantified by means of appropriate standard solutions. To regenerate the column after each sample, it was flushed with 200 mM NaOH as well as 1 M sodium acetate supplemented with 200 mM NaOH for 10 min each, followed by equilibration with 8 mM NaOH for 20 min.

To assess the statistical significance of differences in the HePS monomer composition for samples which had been harvested after different culturing times, a one-way ANOVA was performed (p=0.05), whereas the Tukey test served as post-hoc test to compare the mean values.

3.3.4. Analysis of macromolecular EPS structures with AF4-MALS

3.3.4.1. Analysis of HoPS

Lyophilized EPS were dissolved in 50 mM $NaNO_3$ at a concentration of 0.5 mg/mL by vortexing and incubating over night at 4 °C. Up to 25 µg were injected into the separation channel, which was equipped with a 10 kDa regenerated cellulose membrane (Superon, GmbH, Germany), using a Dionex HPLC autosampler and pump system (Dionex Ultimate 3000, Thermo Fisher Scientific, USA). Proper separation of the polysaccharides was achieved at a detector flow rate (v_d) of 1 mL/min and a linear cross-flow (v_x) gradient of 3 to 0.1 mL/min for 15 min following the focussing step. After the gradient, v_x was kept at 0.1 mL/min for 20 min and finally set to 0 mL/min for 5 min, to elute any remaining particles. The data were evaluated with the ASTRA 6.1 software (Wyatt Technology, Germany), whereas the weight average geometric radii ($R_{w\,(geo)}$) were calculated from the MALS signals only (*particle mode*) using the sphere model for globular particles, as this yielded the best fit. Concentration signals required for the calculation of weight average molar masses (M_w) were recorded on-line with a UV detector (Dionex Ultimate 3000, Thermo Fisher Scientific, USA) at 400 nm, as previously described for levan particles (Ua-Arak et al., 2017a) and a dn/dc value of 0.146 mL g^{-1} was used to calculate the weight-average molecular weight (Rühmkorf et al., 2012). The specific UV extinction coefficients ($\varepsilon_{400\,nm}$; [mL mg^{-1} cm $^{-1}$]) of the dextran were calculated as the slopes of calibration curves which had been obtained from the UV extinction values of respective concentration series (0.5-2.5 mg/mL) according to the Beer-Lambert law.

3.3.4.2. Analysis of HePS

HePS solutions (0.5 mg/mL) in 50 mM NaNO$_3$ were prepared by vigorous vortexing, incubation overnight (4 °C) and subsequent centrifugation (13000 x g, 30 min) to remove any undissolved matter. Finally, 100 µl were analyzed as described in 3.3.4.1. In contrast to HoPS, the RMS radii were determined directly from the MALS signals (*particle mode*) using the Zimm model. The average molecular mass was estimated with a commercial dextran standard (M$_r$=2 x 10^6; *Ln. mesenteroides*).

3.3.5. Chemical structure analyses of EPS

These experiments were performed in cooperation by Dr. Daniel Wefers at the Department of Food Chemistry and Phytochemistry, which is affiliated to the Institute of Applied Biosciences of the Karlsruhe Institute of Technology (KIT).

3.3.5.1. Determination of absolute monosaccharide configuration with GLC-MS

Hydrolysis of HePS was performed with 2 M TFA for 30 min, and after evaporation of the acid, monosaccharides were derivatized by using 150 µL of (*R*)-2-octanol and 5 µL of TFA. The solvent was removed, and the octyl-glycosides were silylated by using 80 µL of *N,O*-bis(trimethylsilyl)trifluoroacetamide and 20 µL of pyridine. The silylated octyl-glycosides were then analyzed on a GLC-MS system (GC-2010 Plus and GC-MS-QP2010 Ultra, Shimadzu, Japan) equipped with a Rxi-5Sil MS column (30 m x 0.25 mm i.d., 0.25 µm film thickness, Restek, Germany). The applied conditions were as follows: initial column temperature, 150 °C; ramped at 1 °C/min to 200 °C; ramped at 15 °C/min to 300 °C. Split injection was used at a split ratio of 10:1 and the injection temperature was 275 °C. As carrier gas, helium was applied at a rate of 40 cm/sec, and the transfer line was held at 275 °C. The peaks were assigned by comparison with the derivatives of the corresponding monosaccharides.

3.3.5.2. Methylation analysis

The present glycosidic linkages in HePS were analyzed by methylation analysis according to procedures described in the literature (Nunes et al., 2008; Fels et al., 2018). Briefly, the sample was dissolved in dimethyl sulfoxide and permethylated by using freshly ground sodium hydroxide and methyl iodide. Subsequently, the methylated polysaccharides were extracted into dichloromethane and washed with 0.1 sodium thiosulfate and water. After evaporation and drying, the residue was incubated with 2 M TFA at 121 °C for 90 min. TFA was removed by evaporation and the partially methylated monosaccharides were reduced by using sodium borodeuteride. The reaction was terminated by using glacial acetic acid and

acetylation was performed by using 1-methylimidazole and acetic anhydride. The partially methylated monosaccharides (PMAA) were then extracted by using dichloromethane and residual water was removed by freezing overnight. Analysis of the PMAAs was carried out by means of GLC-MS on a DB-5MS column (30 m x 0.25 mm i.d., 0.25 µm film thickness, Agilent Technologies, CA) using the following conditions: Initial column temperature 140 °C, held for 2 min; ramped at 1 °C/min to 180 °C, held for 5 min; ramped at 10 °C/min to 300 °C, held for 5 min. As carrier gas, helium was used at a rate of 40 cm/sec. The transfer line was held at 275 °C, and electron impact mass spectra were recorded at 70 eV. Split injection with a split ratio of 30:1 was used and the injection temperature was 250 °C. Semiquantitative analysis of the PMAAs was performed by using a GLC-FID system (GC-2010 Plus, Shimadzu) and the same conditions as described for GLC-MS, with the exception of a reduced split ratio of 10:1. Nitrogen was used as makeup gas and the FID temperature was 240 °C. Analysis was performed in duplicate and molar response factors were used to calculate the portions of the PMAAs (Sweet et al., 1975).

3.3.5.3. NMR analyses

NMR spectroscopy was performed with a Bruker Ascend 500 MHz spectrometer equipped with a Prodigy cryoprobe (Bruker, Rheinstetten, Germany). Ca. 2 mg samples were dissolved in D_2O and standard parameter sets provided by Bruker were used to acquire ^1H, Correlated Spectroscopy (COSY), Total Correlated Spectroscopy (TOCSY), Heteronuclear Single Quantum Coherence (HSQC), HSQC-Nuclear Overhauser Enhancement Spectroscopy (HSQC-NOESY), HSQC-TOCSY, and Heteronuclear Multiple Bond Correlation (HMBC) experiments at 298 K. To improve resolution of the HMBC spectrum, 2048 points were recorded in the f2 dimension and 512 points were recorded in the f1 dimension. Acetone was used as internal reference (^1H: 2.22 ppm, ^{13}C: 30.89 ppm) (Gottlieb et al., 1997).

3.3.5.4. Endo-dextranase assay of glucans

To compare the occurrence of different structural elements in dextran samples, the oligosaccharides liberated by endo-dextranase were analyzed by HPAEC-PAD (Katina et al., 2009; Xu et al., 2017). Dextran samples (1 mg/mL) were hydrolyzed with an endo-dextranase from *Chaetomium erraticum* (EC 3.2.1.11, Sigma Aldrich) (1 µl enzyme solution/mg sample) at 30 °C for 24 h. The enzyme was inactivated by heating to 100 °C for 5 min and the diluted hydrolysates were analyzed by HPAEC-PAD on an ICS-5000 system (Thermo Scientific Dionex) equipped with a CarboPac PA-200 column (250 mm x 3 mm i.d., 5.5 µm particle size, Thermo Scientific Dionex). A flow rate of 0.4 mL/min and a gradient

composed of the following eluents was used at 25 °C: (A) bidistilled water, (B) 0.1 M sodium hydroxide, (C) 0.1 M sodium hydroxide + 0.5 M sodium acetate. Before every run, the column was flushed with 100% C for 10 min and equilibrated with 90% A and 10% B for 20 min. After injection, the following gradient was applied: 0-10 min, isocratic 90% A and 10% B; 10-20 min, linear from 90% A and 10% B linear to 100% B; 20-90 min, linear from 100% B to 100% C.

3.3.6. Quantification of dextrans in liquid solutions

Prior to quantification, the liquid solutions containing the dextrans were dialyzed as described in 3.2.1. Dextrans in liquid solutions (buffer or culture supernatant) were quantified using the phenol sulfuric acid method as described by Dubois et al. (1956) (Dubois et al., 1956) with some modifications: 50 µl of an aqueous phenol solution (4% w/v) were added to 50 µl sample volume in 96 well plates and mixed with 250 µl concentrated H_2SO_4 (98%). After incubation at room temperature for up to 30 min, the absorbance of appropriate dilutions was measured at 490 nm using the microplate reader. Calibration curves were created with concentration series of glucose (0.01-0.2 mg/mL) for each single microtest plate, and each sample was analyzed at least in triplicate. The amount of dextran was expressed in mg/mL glucose equivalents (Mende et al., 2013). As the sample volume of dextran solutions increased during dialysis due to its osmotic properties, the original concentration of dextran (c_0) in the samples was calculated according to $c_0 = c_1 \ x \ \left(\frac{V_1}{V_0}\right)$, with c_1 being the concentration calculated with the phenol sulfuric acid method and V_0 and V_1 representing the volumes before (5 mL) and after the dialysis, respectively. As negative control, pure buffer or non-inoculated medium was treated in the same way and used as blank value.

3.3.7. Quantification of sugars and organic acids in liquid cultures

Culture supernatants were prepared by centrifugation (5000 x g, 10 min, 4 °C) and subsequently stored at -20 °C until metabolite quantification. Sugars and organic acid concentrations were determined with a HPLC system (Dionex Ultimate 3000, Thermo Fisher Scientific, USA) coupled to Shodex refractive index (RI) detector (Showa Denko Shodex, Germany), whereas 20 µL were injected from prepared samples. For sample preparation, supernatants were either filtered (0.2 µm nylon filters, Phenomenex, Germany) and diluted (analysis of sugars) or treated as follows (analysis of organic acids): 50 µL perchloric acid (70%) were added to 1 mL of supernatant, mixed and incubated overnight (4 °C). Afterwards, the samples were centrifuged (13000 x g, 30 min, 4 °C) and filtered (0.2 µm). The sugars were measured with a Rezex™ RPM Pb^{2+} column at a flow-rate of 0.6 mL/min (85 °C) using

filtered (0.2 μm) deionized water as eluent, whereas organic acids were measured with a Rezex™ ROA H$^+$ column (both Phenomenex, Germany) at a flow-rate of 0.7 mL/min (85 °C) with 2.5 mM H_2SO_4 (prepared with filtered, deionized water). Metabolites were identified and quantified by means of appropriate standard solutions with the Chromeleon™ software (v. 6.8; Dionex, Germany).

3.4. Molecular biological methods

3.4.1. Isolation of genomic DNA and quality control

High-molecular-weight DNA was isolated and purified from liquid cultures in mMRS in the late exponential growth phase using the Genomic-tip 100/G kit (Qiagen, Hilden, Germany). The quality and quantity of isolated genomic DNA were checked by NanoDrop (Thermo Fisher, USA) and agarose gel electrophoresis: 1 μl of genomic DNA were loaded on a 0.8% agarose gel in TAE buffer and subsequently analyzed to exclude any fragmentation (120V, 45 min).

3.4.2. Protein quantification by the Bradford assay

Protein impurities in EPS were estimated with a Coomassie (Bradford) Protein Assay Kit (Thermo Scientific, USA) following the manufacturers protocol.

3.5. Genomics

3.5.1. Genome sequencing, assembly and annotation

3.5.1.1. *Lactobacillus plantarum* TMW 1.1478

High-molecular-weight DNA was isolated, purified and subjected to a quality control as described in 3.4.1. Afterwards, the DNA sequencing was carried out at GATC Biotech (Constance, Germany) using the single-molecule real-time sequencing (PacBio RSII) technology (Eid et al., 2009). For library creation, an insert size of 8-12 kb was selected, which resulted in at least 200 Mb raw data from 1-2 SMART cells (1 x 120 min movies), applying P4-C2 chemistry. SMRT Analysis version 2.2.0.p2 was applied to assemble the genome, which was finally completed by manual curation as described in (https://www.github.com/ PacificBiosciences/Bioinformatics-Training/wiki/Finishing-Bacterial-Genomes) (Chin et al., 2013). Finally, the genomes were annotated using the NCBI Prokaryotic Genome Annotation Pipeline (PGAP) and Rapid Annotation using Subsystem Technology (RAST) (Aziz et al., 2008; Tatusova et al., 2016). In addition to automatic annotation, manual BLASTp research was used to find enzymatic homologues (unless stated otherwise: >95% query coverage, >95% identity) to assist in the prediction of enzyme/protein putative functions. The prediction of transmembrane domains was carried out with the TMHMM server v. 2.0 (http://www.cbs.dtu.dk/services/TMHMM/).

3.5.1.2. *Lactobacillus sakei* TMW 1.411

High molecular weight DNA was isolated, purified and quality checked as described in 3.5.1.2. However, a different sequencing technology was applied: In contrast to *L. plantarum* TMW 1.1478, the whole genome shotgun sequence (WGS) of *L. sakei* TMW 1.411 was obtained by employing the Illumina MiSeq® sequencing technology in combination with the SPAdes 3.9 assembly algorithm. The annotation (NCBI/RAST) was carried out as described for *L. plantarum* TMW 1.1478.

3.5.2. Acquisition of published genomes

Both sequenced genomes were deposited in the GenBank database. For *L. plantarum* TMW 1.1478 (BioProject: PRJNA390483), the genomic sequences of chromosome and plasmid can be accessed via the accession numbers CP021932 and CP021933, respectively. The versions described in the present work are CP021932.1 and CP021933.1.

The WGS project of *L. sakei* TMW 1.411 can be accessed via the accession number QOSE00000000 (BioProject: PRJNA480830). The version described in this work is version QOSE01000000.

3.6. Proteomics

Several experimental steps (3.6.2, 3.6.3) of the quantitative proteomics approach were carried out in cooperation by Dr. Jürgen Behr and Dr. Christina Ludwig at the Bavarian Center for Biomolecular Mass Spectrometry (BayBioMS, Freising, Germany).

3.6.1. Experimental setup

To investigate the proteomic shift in response to sucrose as sole carbon source, 4x 15 ml precultures (four biol. replicates) of *L. sakei* TMW 1.411 were prepared in mMRS as described above (3.1.1) and used to inoculate 4 x 100 ml cultures in mMRS (20 g/L glucose) with a final OD_{600} of 0.1. The cultures were grown to the mid-exponential growth phase (pH~5.0, determined in preliminary experiments), which had given good results in previous experiments (Schott et al., 2017), and subsequently distributed to 50 ml sealed tubes each (eight tubes in total). Afterwards, the cultures were pelletized (5000 x g, 10 min) and washed once in fresh mMRS. Next, the suspensions were pelletized again and resuspended in an equal volume of mMRS supplemented with either glucose or sucrose (20 g/L each), followed by incubation at 30 °C for 2 h. Subsequently, 2.5 mL of cooled trichloroacetic acid (100%) were added to 40 mL of glucose/sucrose treated cultures (6.25% w/v final concentration) and the suspensions were immediately transferred to pre-cooled 50 ml tubes and incubated on ice for 10 min. After centrifugation (5000 x rpm, 10 min, 4 °C), the pellets were washed twice with 10 mL cold acetone (-20 °C) (2000 rpm, 10 min, 4 °C), whereas the supernatants were discarded carefully. Finally, the pellets were frozen in liquid nitrogen and stored at -80 °C until protein isolation and peptide preparation (3.6.2). In addition, aliquots were taken from each of the four precultures, as well as the eight batches after 2 h incubation to determine pH values and the viable cell count in CFU/mL on agar plates.

3.6.2. Peptide preparation, separation and mass spectrometry

Cell pellets were resuspended in lysis buffer (8 M urea, 5 mM EDTA disodium salt, 100 mM NH_4HCO_3, 1 mM Dithiothreitol (DTT) in water, pH=8.0) and disrupted mechanically using glass beads (G8772, 425-600 um, Sigma, Germany), whereas a Bradford assay (Bio-Rad Protein Assay, Bio-Rad Laboratories GmbH, Munich, Germany) was performed to determine

the total protein concentration in the lysate. Afterwards, 100 μg protein extract of each sample were used for in-solution digestion: After reduction (10 mM DTT, 30 °C, 30 min) and carbamidomethylation (55 mM chloroacetamide, 60 min in the dark), trypsin was added to the samples, and the solutions were incubated overnight at 37 °C. Next, the digested protein samples were desalted using C18 solid phase extraction with Sep-Pak columns (Waters, WAT054960) following the manufacturer's protocol. Finally, the purified peptide samples were dried with a SpeedVac device and dissolved in an aqueous solution of acetonitrile (2%) and formic acid (0.1%) at a final concentration of 0.25 μg/μL.

Peptide analysis was performed on a Dionex Ultimate 3000 nano LC system, which was coupled to a Q-Exactive HF mass spectrometer (Thermo Scientific, Germany). At first, the peptides were loaded on a trap column (75 μm x 2 cm, self-packed, Reprosil-Pur C18 ODS-3 5 μm resin, Dr. Maisch, Ammerbuch) at a flow rate of 5 μL/min in solvent A_0 (0.1% formic acid in water). Next, the separation was performed on an analytical column (75 μm x 40 cm, self-packed, Reprosil-Gold C18, 3 μm resin, Dr. Maisch, Ammerbuch) at a flow-rate of 300 nL/min applying a 120 min linear gradient (4-32%) of solvent B (0.1% formic acid, 5% DMSO in acetonitrile) and solvent A_1 (0.1% formic acid, 5% DMSO in water).

The mass spectrometer was operated in the data dependent mode to automatically switch between MS and MS/MS acquisition. The MS1 spectra were obtained in a mass-to-charge (m/z) range of 360-1300 m/z using a maximum injection time of 50 ms, whereas the AGC target value was 3e6. Up to 20 peptide ion precursors were isolated with an isolation window of 1.7 m/z (max. injection time 25 ms, AGC value 1e5), fragmented by higher-energy collisional dissociation (HCD) applying 25% normalized collision energy (NCE) and finally analyzed at a resolution of 15,000 in a scan range from 200-2000 m/z. Singly-charged and unassigned precursor ions as well as charge states >6+ were excluded.

3.6.3. Protein identification and quantification

Both identification and quantification of peptides and proteins were performed with the software MaxQuant (v. 1.5.7.4) by searching the MS2 data against all protein sequences predicted for the reference genome of *L. sakei* TMW 1.411 by the RAST annotation pipeline (3.5.1.2; GenBank QOSE0100000) using the embedded search engine Andromeda (Cox et al., 2011). While the carbamidomethylation of cysteine was a fixed modification, the oxidation of methionine as well as the N-terminal protein acetylation were variable modifications. Up to two missed Trypsin/P cleavage sites were allowed and precursor and fragment ion tolerances were set 10 ppm and 20 ppm, respectively. The label-free quantification (Jürgen Cox, 2014) and data matching were enabled within the MaxQuant software between

consecutive analyses, whereas filtering of the search results was performed with a minimum peptide length of 7 amino acids as well as 1% peptide and protein false discovery rate (FDR) plus common contaminants and reverese identifications.

3.6.4. Proteomic data deposition

A data file containing the protein sequences with corresponding FIG identifiers (from RAST annotation), as well as relevant proteome tables with assigned SEED categories and the results of the t-Test evaluation (3.6.5) are deposited online as supplementary data (Prechtl et al., 2018a, supplementary tables). The mass spectrometry proteomics data have been deposited to the ProteomeXchange Consortium via the PRIDE partner repository with the dataset identifier PXD011417 (http://proteomecentral.proteomexchange.org).

3.6.5. Data processing and statistical analysis

The Perseus software (version 1.6.0.7) was used to process the MaxQuant output file (proteinGroups.txt) and conduct statistical analyses (Tyanova et al., 2016). After filtering the protein groups (removal of identified by site hits, reverse identifications, contaminants), the LFQ intensity data were $\log_2$ transformed, whereas the IBAQ intensities were $\log_{10}$ transformed. To improve the validity of statistical analysis, only proteins which had been identified (i) by at least two unique peptides and (ii) in all four replicates of at least one group (glucose/sucrose treated cells) were considered, whereas missing values after log-transformation were imputed from a normal distribution (width: 0.2; down shift: 1.8). The $\log_2$-transformed LFQ data were used for a stringent t-Test analysis, using a Benjamini-Hochberg FDR of 0.01 for truncation, whereas proteins with an absolute $\log_2$ fold change (FC) of ≥ 1 were further discussed in the present study. To estimate absolute protein abundancies at a certain condition, the transformed IBAQ intensities were averaged ranked descending for each group.

4. RESULTS

4.1. Selection of EPS forming meat starter cultures

To identify potential starter cultures suitable for an *in situ* EPS production in fermented meat products, 77 LAB strains were selected from the in-house strain collection and submitted to various experiments, including screening for EPS formation, growth experiments and a safety assessment. All strains had been originally isolated from either meat-based or cold-stored, salt containing food products (e.g. raw-fermented sausage, sauerkraut) to increase the chance of finding promising candidate strains capable of asserting themselves in meat fermentation processes. All strains belonged to the species of *L. sakei*, *L. curvatus*, *L. plantarum*, *Lc. piscium* and *Ln. gelidum*.

The experimental results of this chapter are partly published in Hilbig et al. (2019).

4.1.1. EPS screening

The capability of EPS formation was investigated on mMRS and RSM agar plates as described in 3.1.4. The visual screening on mMRS agar revealed 23 positive strains, and the EPS formation of the EPS-positive strains was also confirmed at mild stress conditions on RSM agar (Table 8). Twelve strains displayed a sucrose dependent EPS production, thereby suggesting the formation of HoPS, i.e. glucans or fructans (Monsan et al., 2001). While these EPS displayed a mucoid character (Figure 3 A), the sucrose independent EPS formation was accompanied by a ropy phenotype with all strains and mainly occurred among the species of *L. plantarum* (Figure 3 B). While some strains of *Ln. gelidum* were capable of sucrose dependent EPS production as well, their growth on RSM agar was very weak. Among *Lactococcus spp.*, no EPS positive strains could be detected and above that, these strains did not show bacterial growth on RSM agar.
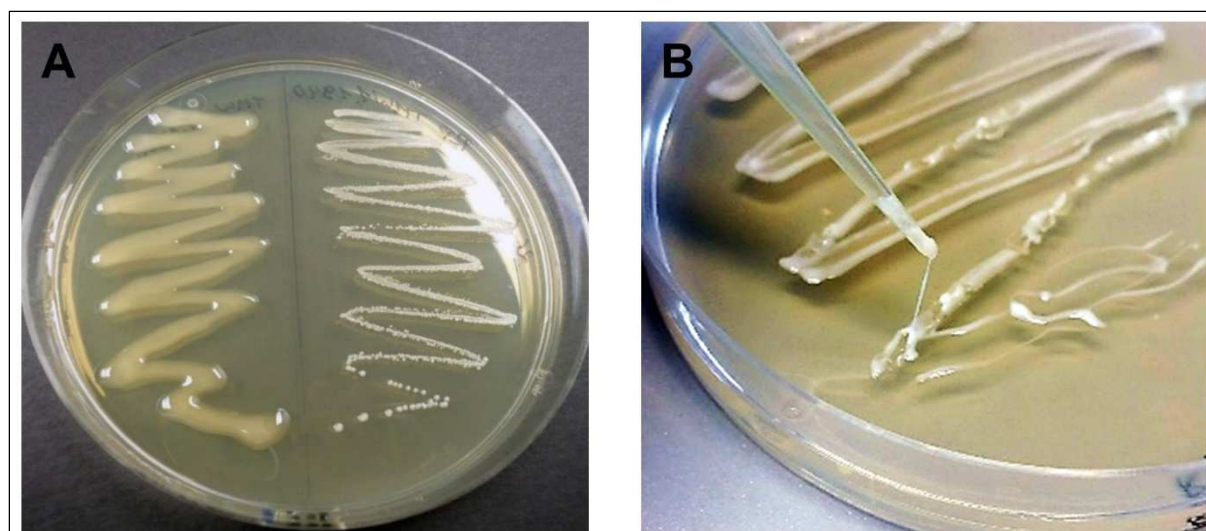
Figure 3 (A) Mucoid character of sucrose dependent EPS formation of *L. curvatus* TMW 1.1928 (left half) in comparison to the non-EPS forming strain *L. curvatus* TMW 1.1940 (right half). (B) Ropy character of the sucrose-independent EPS formation of *L. plantarum* TMW 1.1308. The composition of the screening agars is described in 3.1.4.

Table 8 Sucrose dependent (left) and independent (right) EPS formation of screened LAB isolates with assessed EPS amounts according to mucoid (sucrose dependent) and ropy (sucrose independent) phenotypes on mMRS and RSM based selection agar. (+++) strong, (++) medium, (+) weak EPS formation.

Sucrose dependent EPS formation [a]				Sucrose independent EPS formation [b]			
Strain	Species	EPS on mMRS	EPS on RSM	Strain	Species	EPS on mMRS	EPS on RSM
1.411	*L. sakei*	++	++	1.1930	*L. sakei*	++	+
1.578	*L. sakei*	+	+	1.1931	*L. sakei*	+	+
1.1936	*L. sakei*	+++	++	1.4	*L. sakei*	+	+
1.1937	*L. sakei*	++	++	1.416	*L. plantarum*	++	+
1.440	*L. curvatus*	++	++	1.1308	*L. plantarum*	++	++
1.624	*L. curvatus*	+++	+++	1.1478	*L. plantarum*	+++	++
1.50	*L. curvatus*	+++	+	1.64	*L. plantarum*	++	++
1.51	*L. curvatus*	+++	+	1.708	*L. plantarum*	+	+
1.1928	*L. curvatus*	+++	+++	1.1879	*L. plantarum*	++	+
2.1616	*Ln. gelidum*	++	+ [c]	1.1953	*L. plantarum*	+	+
2.1619	*Ln. gelidum*	+	+ [c]	1.2022	*L. plantarum*	+	+
2.1620	*Ln. gelidum*	++	+ [c]				

[a] to screen for sucrose dependent EPS formation, mMRS and RSM were supplemented with sucrose (3.1.4).

[b] to screen for sucrose independent EPS formation, mMRS and RSM were supplemented with a mix of glucose, galactose and lactose (3.1.4).

[c] for *Leuconostoc* spp., the growth on RSM agar was very slow.

4.1.2. Determination of EPS types and contained sugar monomers

The sucrose dependent EPS production of 12 LAB isolates (Table 8) had suggested the formation of glucans or fructans (4.1.1). To determine the present HoPS type, the EPS were produced in 50 ml cultures (mMRS medium), whereas sucrose (80 g/L) was applied as sole carbon source. After 48 h, the EPS were harvested, purified and hydrolyzed as described (3.2, 3.3.1.1), whereas the produced amounts lay between 1-3 g/L. HPLC analysis of the samples revealed that all 12 strains had exclusively produced glucans, as glucose was the only detectable sugar monomer in the HPLC chromatograms, even at mild hydrolysis conditions (data not shown).

To determine the sugar monomers in EPS whose production had occurred independently of sucrose (i.e. putative HePS), 200 mL cultures were prepared from the four *L. plantarum* strains TMW 1.1308, 1.1478, 1.1879 and 1.64, as these had shown promising results regarding EPS formation on both mMRS and RSM based selection agar. To avoid a potential contamination with polymers contained in yeast extract, a basal medium with peptone, but without yeast extract (MBp) was used for the cultivation. Production, purification and hydrolysis were performed as described (3.2.2.1, 3.3.1.2) and non-inoculated MBp medium was precipitated and dialyzed in the same way as the culture supernatants to serve as negative control for monomer analysis.

Contrary to the produced HoPS amounts, which had been in the range of grams per liter, only 50-120 mg/L EPS could be isolated from the put. HePS producing strains, whereas ca. 15 g/L dry matter were isolated from non-inoculated MBp medium. The HPLC chromatograms (Figure 4 A-D) suggested varying amounts of glucose, galactose and/or rhamnose in all produced EPS (due to the applied column, no discrimination between galactose and rhamnose was possible at this point). In addition, mannose was detected in the chromatograms of all HePS hydrolysates (Figure 4 A-D). Surprisingly, the mannose peak was also present in the chromatogram of the negative control (hydrolyzed matter obtained from precipitated, non-inoculated MBp medium) and the same applied for traces of glucose and galactose/rhamnose, respectively, though to a far lesser extent (Figure 4 E). Thus, it is likely that the mannose was not part of the produced EPS, but rather originated from a yet unknown contaminant contained in peptone, such as co-precipitated mannoproteins from yeast (Cohen and Ballou, 1981). Moreover, up to two minor peaks appeared in the chromatograms of the EPS hydrolysates (Figure 4 A-D), the retention times (t_R) of which (~20 min) nicely fitted to glycerol and ribitol. These sugar alcohols are the main components of teichoic acids, which represent extracellular polymers that may be linked to the gram-positive cell wall. Apart from that, all EPS except the one produced by *L. plantarum* TMW

1.1879 seemed to contain a putative sugar monomer displaying a similar t_R as mannose. However, this compound could not be identified at this point. Although a clear statement regarding the precise monomer was not possible at this stage, the chromatograms still suggested some variations between the analyzed EPS and confirmed them to be HePS.
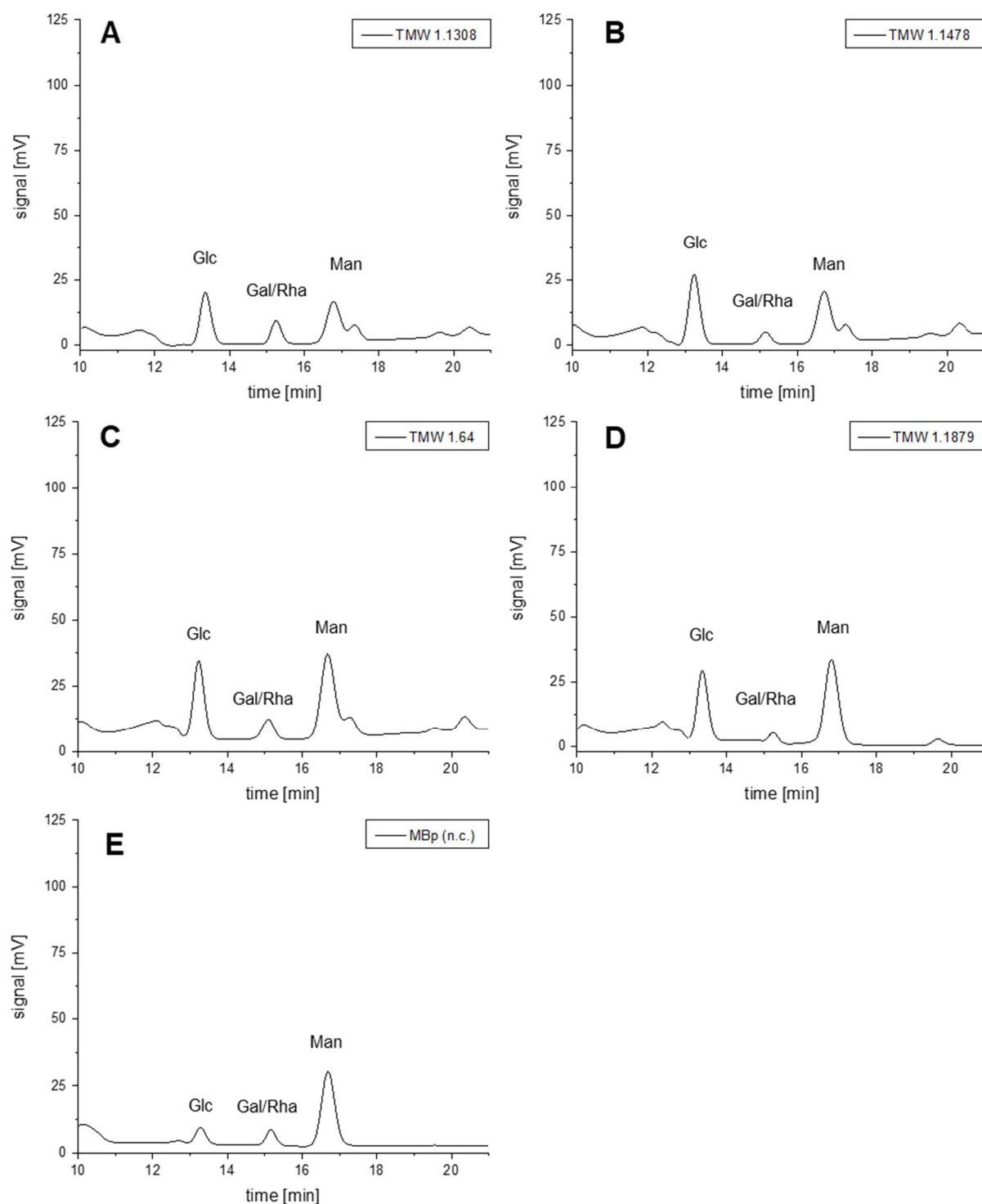
Figure 4 (A-D): HPLC-RI chromatograms of hydrolysates prepared from EPS samples of four different _L. plantarum_ strains which had been cultivated in MBp medium. (E): Hydrolysate of isolated dry matter obtained from non-inoculated MBp medium (negative control).

4.1.3. Evaluation of bacterial growth in a simulation medium for raw-fermented sausages

Based on the results of the EPS screening and the identified EPS types, nine strains (Table 9) comprising the species *L. sakei*, *L. curvatus* and *L. plantarum* were selected to be investigated for their growth behavior in RSM, which imitated the mild stress conditions during the fermentation of raw-fermented sausages (e.g. presence of nitrite curing salt, limited nutrients). Although several *Ln. gelidum* spp. had shown EPS production as well (Table 8), these strains were neglected for the growth experiments, since their growth on RSM agar had been strongly inhibited (4.1.1).

Prior to performing these experiments, the identity of each of these strains was successfully verified on the species level by MALDI-TOF MS.

Table 9 Candidate strains selected for growth experiments in RSM.

Strain	Species	EPS type
TMW 1.411	*L. sakei*	Glucan
TMW 1.440	*L. curvatus*	Glucan
TMW 1.1928	*L. curvatus*	Glucan
TMW 1.51	*L. curvatus*	Glucan
TMW 1.624	*L. curvatus*	Glucan
TMW 1.1308	*L. plantarum*	HePS
TMW 1.1478	*L. plantarum*	HePS
TMW 1.64	*L. plantarum*	HePS
TMW 1.1879	*L. plantarum*	HePS

To assess the growth behavior of the chosen candidate strains in RSM, both maximum growth rate μ_{max} and the lag-phase λ were determined for three different incubation temperatures (25 °C, 20 °C, 15 °C; Figure 5). Apart from that, the optical density (OD_{600}) was monitored over a period of up to 6 d to determine the maximum turbidity as a measure for the general adaption of a strain to the mild stress conditions (Figure 6).
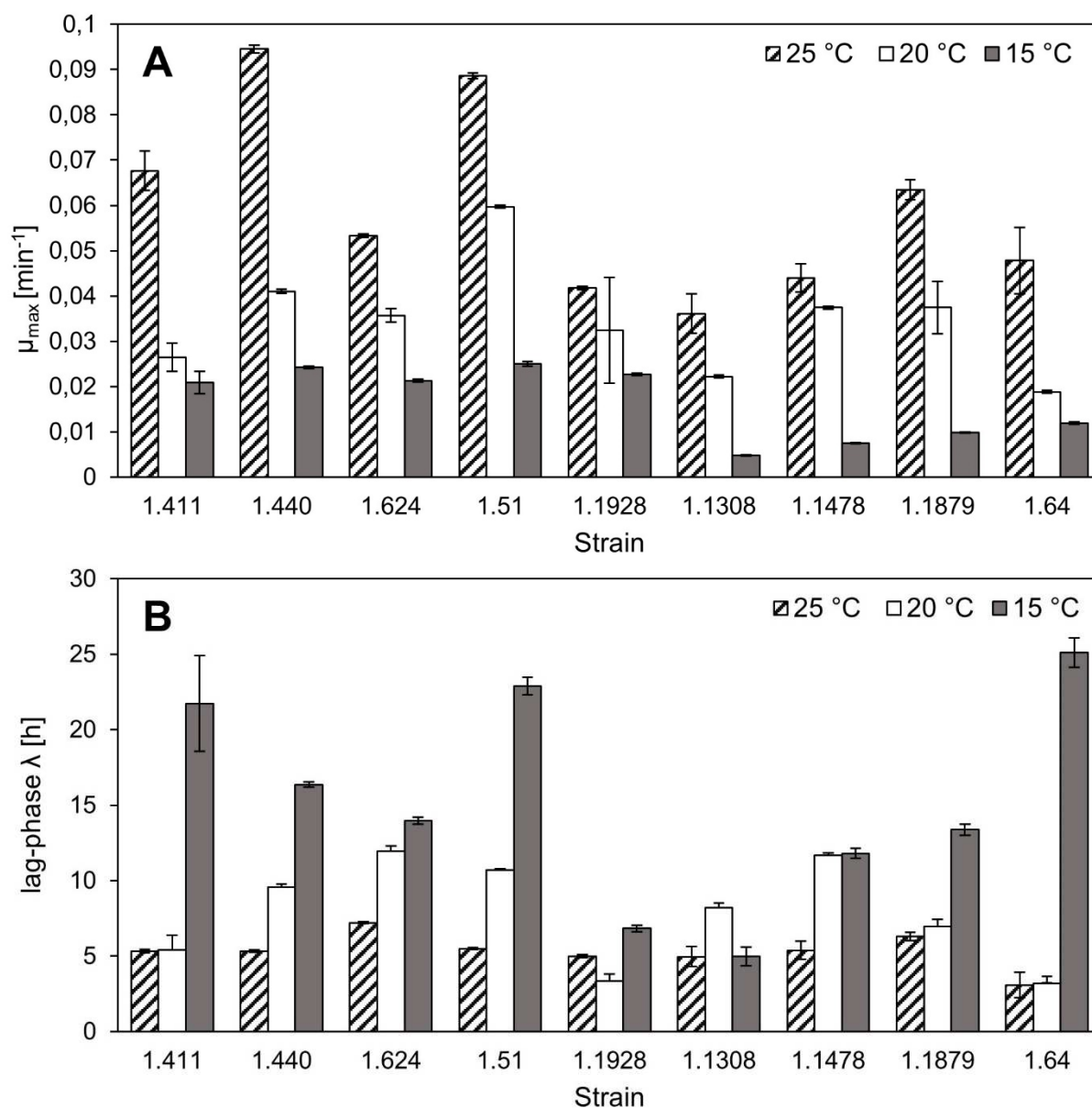
Figure 5 Characteristic growth parameters of nine candidate strains in RSM. (A) Maximum growth rates μ_{max}. (B) Lag-phase λ. All values are expressed as mean ± standard deviation of three replicates. Species: *L. sakei* (TMW 1.411); *L. curvatus* (TMW 1.440, 1.624, 1.51, 1.1928); *L. plantarum* (TMW 1.1308, 1.1478, 1.1879, 1.64).

While the maximum growth rate of all strains decreased at lower temperatures (Figure 5 A), the strength of the decrease as well as the absolute values differentiated between the strains. As for the growth at 25 °C, the strains TMW 1.440 and TMW 1.411 showed the highest growth rates among the species *L. curvatus* and *L. sakei*, respectively, whereas the μ_{max} of TMW 1.1928 was lowest. It is noteworthy that the growth of this strain seemed to be less affected by the incubation temperature, as the calculated μ_{max} values showed only minor differences and lay in an interval of 0.02-0.04 h^{-1}. In general, the growth rates of the species *L. plantarum* were markedly lower at 15 °C than those of *L. curvatus* and *L. sakei*, which pointed to a less pronounced adaption of this species to cold temperatures.

As for the lag phases (Figure 5 B), an inverse correlation of incubation temperature and λ was observed for most strains. The strains *L. curvatus* TMW 1.1928 and *L. plantarum* TMW 1.1308 formed an exception from this trend in that their lag-phases were quite similar for each temperature and surprisingly short, even at 15 °C.
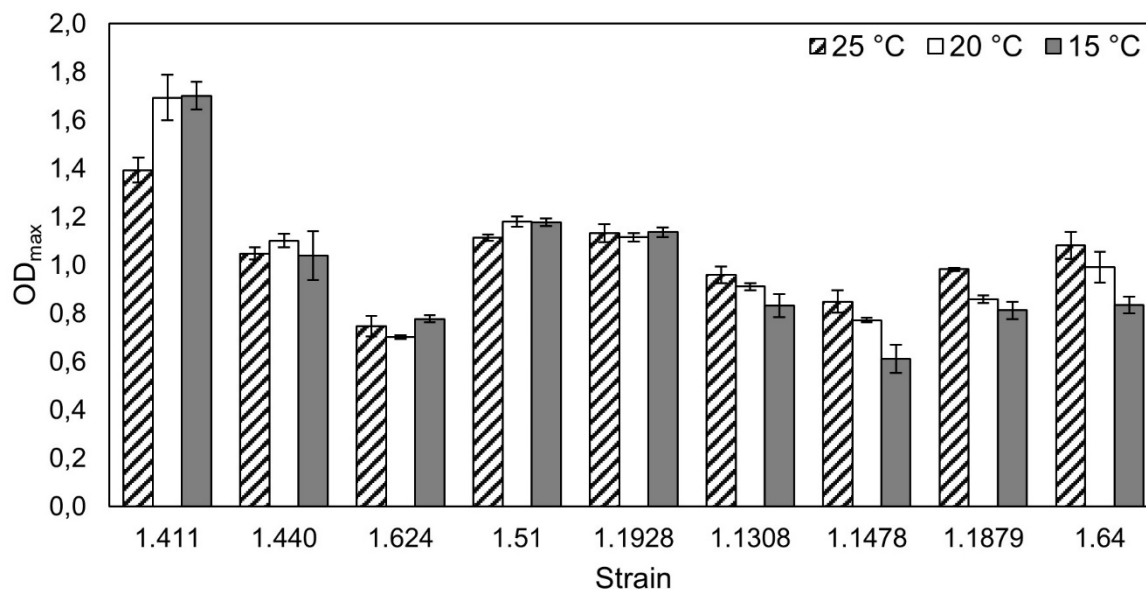
Figure 6 Maximum turbidity (OD$_{600}$) of selected candidate strains in RSM. All values are expressed as mean ± standard deviation. Species: *L. sakei* (TMW 1.411); *L. curvatus* (TMW 1.440, 1.624, 1.51, 1.1928); *L. plantarum* (TMW 1.1308, 1.1478, 1.1879, 1.64).

With respect to the maximum turbidity reached in RSM (Figure 6), the strain *L. sakei* TMW 1.411 showed the most promising results, since its OD$_{600}$ values suggested the highest cell densities. Moreover, the values suggested even higher cell densities at lower temperatures, which seemed not the case for the investigated *L. curvatus* species, whose maximum turbidity was equal for all temperatures. As for the *L. plantarum* strains, however, the lower temperatures seemed to exhibit a slight negative influence on the maximum cell density.

4.1.4. Safety assessment

Despite their generally recognized as safe (GRAS) status (Klaenhammer et al., 2005), LAB used in food and dairy fermentations may constitute a health risk factor due to transferable antibiotic resistances, which is why the nature of present antibiotic resistance determinants has to be determined prior to an application of LAB in food fermentations (Gueimonde et al., 2013). Apart from that, the formation of biogenic amines such as histamine and tyramine by some LAB may cause toxicological effects as well. Thus, the nine selected candidate strains were subjected to an antimicrobial susceptibility testing (AST, 3.1.7) on agar plates with 15

clinically relevant antibiotics (Table 10), while the formation of biogenic amines from six amino acids was investigated on decarboxylation agar (3.1.6).

Table 10 Antibiotics used for AST with corresponding pharmacological classifications.

Antibiotic	Pharmacological classification
Apramycin	Aminoglycoside antibiotics
Gentamycin	Aminoglycoside antibiotics
Kanamycin	Aminoglycoside antibiotics
Streptomycin	Aminoglycoside antibiotics
Chloramphenicol	Amphenicols
Rifampicin	Ansamycins
Ampicillin	β-Lactam antibiotics
Oxacillin	β-Lactam antibiotics
Trimethoprim	Diaminopyrimidine antibiotics
Nalidixic acid	Gyrase inhibitors
Norfloxacin	Gyrase inhibitors
Clindamycin	Lincosamide and Macrolide antibiotics
Erythromycin	Lincosamide and Macrolide antibiotics
Sulfonamide	Sulfonamide antibiotics
Tetracycline	Tetracycline antibiotics

To ensure the validity of the performed AST, the inhibition zone diameters for the control strain *Staphylococcus aureus* ATCC 25923 were measured for each antibiotic (Figure A 1), while the reference diameters were derived from the document M100-S22, which had been published by the Clinical and Laboratory Standards Institute (CLSI) (CLSI, 2012). With the exception of oxacilline, which resulted in higher inhibition zone diameters than the suggested control range, all determined zone diameters lay within the reported intervalls (Figure A 1).

The AST revealed that all of the nine strains were resistant against oxacillin, nalidixic acid and, with the exception of *L. sakei* TMW 1.411, norfloxacin. These resistances could be explained by known intrinsic resistance mechanisms and are therefore not transferable (Danielsen and Wind, 2003). For sulfonamide and trimethoprim, a species dependent clustering could be observed, as all *L. plantarum* strains were susceptible for both antibiotics, whereas most of the *L. sakei* and *L. curvatus* strains showed resistances for either one or

both antibiotics (Figure 7). All other antibiotics resulted in clear inhibition zones with strain-dependent diameters, whereupon the smallest inhibition zones of all species (10-30 mm, Figure A 2, Figure A 3) were observed for the aminoglycoside antibiotics. A reduced susceptibility of *Lactobacillus* and *Leuconostoc* spp. towards these antibiotics has been described (Franz et al., 2010).
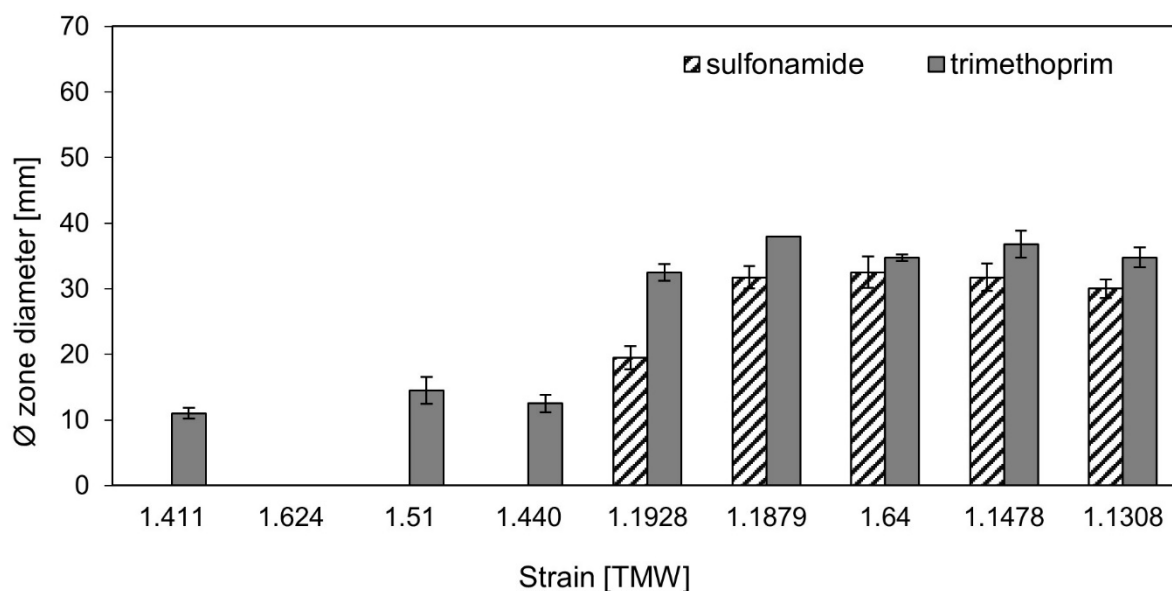
Figure 7: Inhibition zone diameters for the antibiotics sulfonamide and trimethoprim. The error bars indicate standard deviations calculated from duplicates of two biological replicates. Species: *L. sakei* (TMW 1.411); *L. curvatus* (TMW 1.440, 1.624, 1.51, 1.1928); *L. plantarum* (TMW 1.1308, 1.1478, 1.1879, 1.64).

The formation of biogenic amines was investigated for the amino acid precursors histidine, tyrosine, phenylalanine, lysine, ornithine and arginine. However, none of the selected candidate strains was able to decarboxylate any of the supplied amino acids, which would have resulted in a blue staining of the selection agar according to the applied screening method (3.1.6). Thus, the formation of biogenic amines could be excluded for each strain.

4.1.5. Strain selection

Based on the obtained results on formed EPS types, growth behavior in RSM and the safety assessment, the strains *L. plantarum* TMW 1.1478 and *L. sakei* TMW 1.411 were selected for more in-depth experiments on their EPS formation.

4.2. Formation and structure of the HePS produced by *L. plantarum* TMW 1.1478

The EPS screening experiments on agar plates had suggested a sucrose-independent EPS formation by *L. plantarum* TMW 1.1478 (4.1.1), which already pointed to the presence of a HePS. This was confirmed by a preliminary monomer analysis of hydrolyzed samples, which revealed a complex monomer composition involving more than one sugar monomer (4.1.2). To further investigate the HePS formation of *L. plantarum* TMW 1.1478, it was produced in a chemically defined medium (CDM) and various analytical techniques were applied to elucidate the structure of the HePS repeating unit and measure macromolecular parameters of the polymer. Above that, the genetic basis of HePS formation should be investigated by identifying the associated biosynthesis cluster through a comparative genomics approach.

The experimental results of this chapter were published in the journal "*Carbohydrate Polymers*" (Prechtl et al., 2018c).

4.2.1. Kinetics of HePS formation in chemically defined medium

Prior to detailed structural analyses of the HePS, the produced amount was investigated in dependence of the culturing time to determine the optimum harvest time for later experiments and to gain knowledge about both changes in its composition and a possible degradation during the stationary phase. Since preliminary experiments on agar plates had suggested slightly increased EPS amounts upon growth at 20 °C compared with growth at 30 °C (data not shown), the lower temperature was chosen for preparative HePS production despite the reduced growth rates at these conditions.

While only low amounts of HePS were obtained after 12 h, significant amounts of HePS (ca. 50 mg/L) were harvested after 24 h (Figure 8 A). The HePS formation continued during the stationary phase and a maximum HePS amount of 134 mg/L was reached after 72 h. Finally, the EPS amount decreased to approximately 75 mg/L after 96 h, which pointed at a possible degradation of the polysaccharide. To check for a contamination of the HePS with co-precipitated proteins, the protein content was determined for each isolate. This was of particular importance, since the heat incubation during HePS detachment might have led to a damage of the cells and thus an increased protein content in the HePS samples. Although the results suggested only a low contamination (0.08-0.78% w/w, Figure 8 B), it was striking that the content in the 96 h sample (0.78%) was markedly higher than in the preceding HePS isolates (< 0.3%). This might indeed be an evidence for a degradation of the HePS by extracellular glycoside hydrolases, which were co-precipitated during EPS isolation.
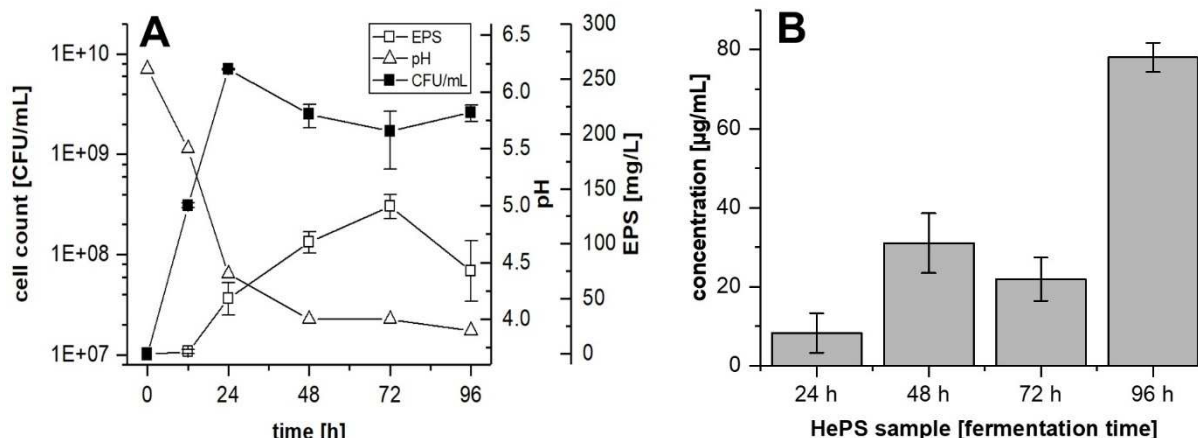
Figure 8 (A) Monitoring of cell count (■), pH (Δ) and HePS formation (□) during growth of *L. plantarum* TMW 1.1478 over 96 h in CDM (Glc, Gal, Lac, 10 g/L each) at 20 °C. Values are expressed as mean ±SD of three replicates. (B) Protein concentration in HePS samples (10 mg/mL solutions) harvested after varying culturing times as determined by the Bradford method. Error bars indicate standard deviations of three replicates.

4.2.2. Detailed analysis of the monomer composition of the HePS

Since monomer analysis with HPLC-RI did not allow for a distinction between galactose and rhamnose due to limitations of the equipped column, another system (high performance anionic exchange chromatography, HPAEC) was used for detailed monomer analysis in combination with pulsed amperometric detection (PAD), which allowed for both highly sensitive detection as well as reliable identification of present monosaccharides.

The evaluation of the monomer composition of the HePS revealed glucose (49 ± 3%), rhamnose (35 ± 3%) and galactose (ca. 16 ± 1%) as main compounds (Figure 9 A, B). The relative amounts of the monomers remained constant during the first 72 h, however, after 96 h the HePS composition was slightly modified in that an increased amount of glucose (ca. 59%) as well as reduced amounts of rhamnose (ca. 28%) and galactose (ca. 13%) were measured in the hydrolysates. Statistical analysis of the monosaccharide compositions revealed the glucose and rhamnose contents in the 96 h isolate to be significantly different from those in the 24 h and 48 h isolates (p=0.05). The slightly reduced amount of galactose in the 96 h sample, however, only showed a significant difference from the 24 h isolate. Considering the possible degradation of the HePS in the late stationary phase (Figure 8 A), this might have given rise to altered monomer ratios in the corresponding isolates as well.
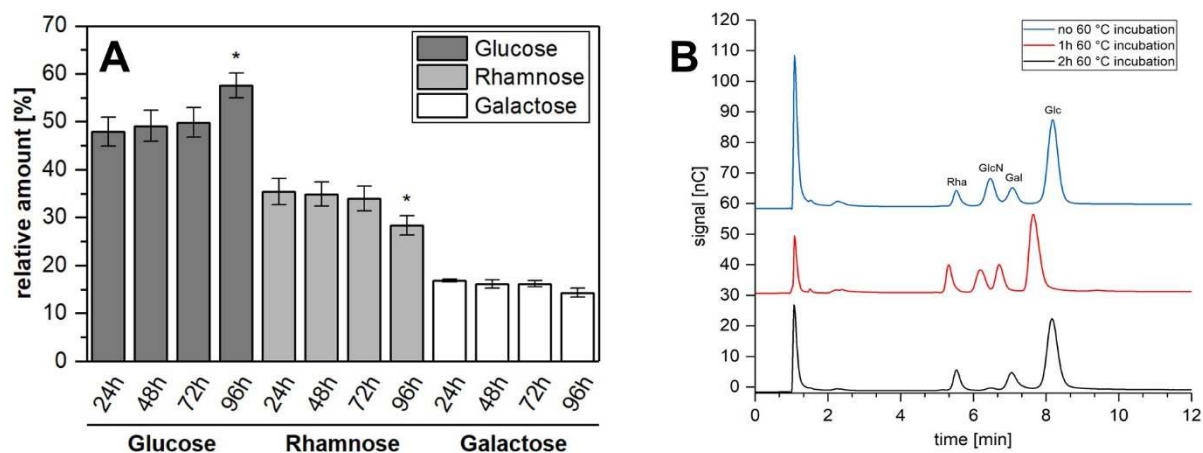
Figure 9 (A) Relative amounts [%] of sugar monomers in TFA hydrolysates prepared from HePS samples which were isolated after 24 h, 48 h, 72 h and 96 h cultivation. Relative amounts of monosaccharides which differed significantly (p=0.05) from at least two others within a particular monosaccharide group are marked with an asterisk. (B) HPAEC-PAD chromatograms of hydrolyzed HePS samples (72 h culturing time), which had been isolated from culture broths with and without heat-incubation at 60°C (0 h, blue line; 1 h, red line; 2 h, black line).

Apart from glucose, rhamnose and galactose, traces of the amino sugar glucosamine (GlcN) were detected in all samples. This monomer most likely originated from a de-acetylation of the cell wall constituent N-acetylglucosamine (GlcNAc) during acid hydrolysis (25 µM GlcNAc were completely de-acetylated at the applied conditions, Figure A 4). Accordingly, improved detachment of the HePS through prolonged heat incubation (up to two hours at 60 °C) reduced the contamination with cellular residuals (proved by microscopy, data not shown) as well as the intensity of the GlcN peak (Figure 9 B).

4.2.3. Macromolecular structure of the HePS

Since detailed structural analyses such as determination of particle radii with AF4-MALS required increased amounts of HePS, the culture volume was increased to 1 L and the HePS were harvested after 72 h at 20 °C. These conditions were chosen because monitoring of HePS formation throughout cultivation had suggested the highest amount at this point (Figure 8 A). To further increase the purity of the isolated HePS, a protein precipitation step with TCA (10%) was performed prior to dialysis of the re-dissolved polysaccharides.

The macromolecular HePS structure was assayed with AF4-MALS analysis, which revealed a minor peak after 7 min and a main peak after 20 min (Figure 10). However, the UV chromatogram (dashed blue line) unveiled a high absorbance of the first peak (t_R=7 min) at 280 nm, which suggested a contamination of the HePS solution with low molecular mass proteins/polypeptides that had probably been too small to be precipitated by TCA (Dent and Sun, 1982). Despite the high light scattering intensity, the second peak (t_R=20 min) did not show any UV absorption or extinction as shown for high molecular mass levans and dextrans

at 400 nm (for these polymers, measurement of an UV absorption is based on turbidity) (Ua-Arak et al., 2016; Prechtl et al., 2018b). By means of a commercial dextran standard, the apparent molecular mass of the second polymer fraction could be estimated about $M_r= 2 \times 10^6$, and evaluation of the corresponding MALS data resulted in a weight average RMS radius (R_w) of R_w=60 nm (Figure 10, red line).
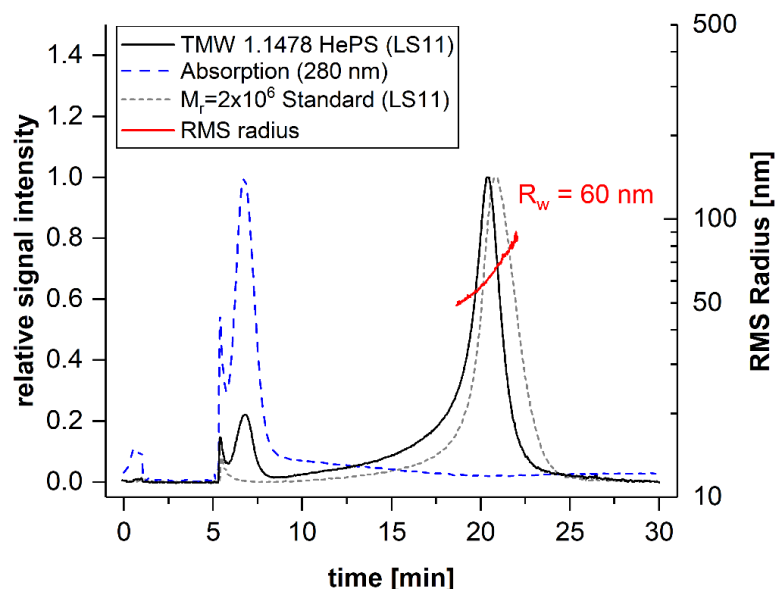
Figure 10 AF4-MALS chromatograms (relative signals of the 90 °light scattering detector LS11) of TMW 1.1478 HePS (black line) and a commercial dextran standard ($M_r= 2 \times 10^6$; dashed grey line). The UV absorption at λ= 280 nm is indicated in dashed blue (relative signal) and the particle sizes (RMS radii) of the HePS fraction (second peak) are depicted in red. This figure was published as Fig. 2 in Prechtl et al. (2018c).

4.2.4. Analysis of the chemical structure of the HePS repeating unit

To resolve the chemical structure of the repeating unit of the HePS produced by *L. plantarum* TMW 1.1478, comprehensive chemical analyses were conducted, including GLC-MS and methylation analysis, as well as various NMR techniques. These experiments were performed by Dr. Daniel Wefers, a cooperation partner at the Department of Food Chemistry and Phytochemistry, which is affiliated to the Institute of Applied Biosciences of the Karlsruhe Institute of Technology (KIT).

The glycosidic linkages present in the HePS were investigated by means of a methylation analysis, while NMR spectroscopy was applied for more detailed structural analysis. As expected for a complex HePS, a complex proton spectrum with several (partially) overlapping signals was obtained. Therefore, various two-dimensional NMR experiments were applied for signal assignment and for determination of the inter-glycosidic linkages,

namely HSQC, HSQC-TOCSY, COSY, HMBC and HSQC-NOESY experiments. The detailed results of the methylation analysis are presented in Figure A 1, while NMR data and recorded spectra are depicted in Table A 2 and Figure A 5-7.

Evaluation of the results of the performed analytical experiments revealed a branched heptameric repeating unit, which comprised an additional acetyl moiety (Figure 11). A detailed interpretation of the generated NMR data which led to the proposed structure of the repeating unit is given in the associated publication (Prechtl et al., 2018c).

Figure 11 Proposed structure of the repeating unit of the HePS produced by *L. plantarum* TMW 1.1478. The start of the repeating unit (descriptor A) was derived from genetic cluster analysis, and the suggested enzymes responsible for the transfer of the particular units are indicated in red according to Table 11. This figure is based on Fig. 4, which was created by Dr. Daniel Wefers and published in Prechtl et al. (2018c).

4.2.5. Comparative genomic analysis of EPS clusters in *L. plantarum* TMW 1.1478, TMW 1.25 and WCFS1

In order to identify and investigate EPS clusters encoded in the genome of *L. plantarum* TMW 1.1478, the genomic DNA of this strain was isolated, sequenced and annotated as described in 3.5.1. As stated in 3.5.2, the sequence data was deposited in the NCBI database with the accession number CP021932.

The analysis of the annotated genome revealed three putative EPS biosynthesis clusters encoded on the chromosomal DNA harboring numerous characteristic enzymes of a Wzy-dependent pathway such as regulatory enzymes, glycosyltransferases (GTs) and a flippase (Remus et al., 2012; Schmid et al., 2015; Zeidan et al., 2017). While the first two clusters (designated as *eps1* and *eps2)* were located close to each other and shared the same orientation, the third cluster (*eps3*) was located in another region, distant to the previous ones and encoded on the complementary strand (Figure 12). A comparison with the described, rather capsular polysaccharide clusters of *L. plantarum* WCFS1 (Remus et al., 2012) revealed a high sequence similarity between cluster *eps2* of TMW 1.1478 and *cps3* of WCFS1, which also applied for the 7.4 kb region downstream of both clusters (Figure 12). Apart from that, cluster *eps3* of TMW 1.1478 proved to be identical to cluster *cps4* of

WCFS1. Interestingly, this cluster also exists in *L. plantarum* TMW 1.25, which was sequenced previously (Kafka et al., 2017) and is *not* capable of EPS production under the conditions used (data not shown), and its conservation in other *L. plantarum* strains was described (Remus et al., 2012). Considering the conservation of the cluster *eps3/cps4* (even in non EPS forming strains), as well as the findings of Remus et al. (2012) that a deletion of *cps3* (*eps2* homologue) in *L. plantarum* WCFS1 did not affect the composition of the surface polysaccharide of this strain, the crucial role of cluster *eps1* for HePS formation in *L. plantarum* TMW 1.1478 became apparent (5.2.2).
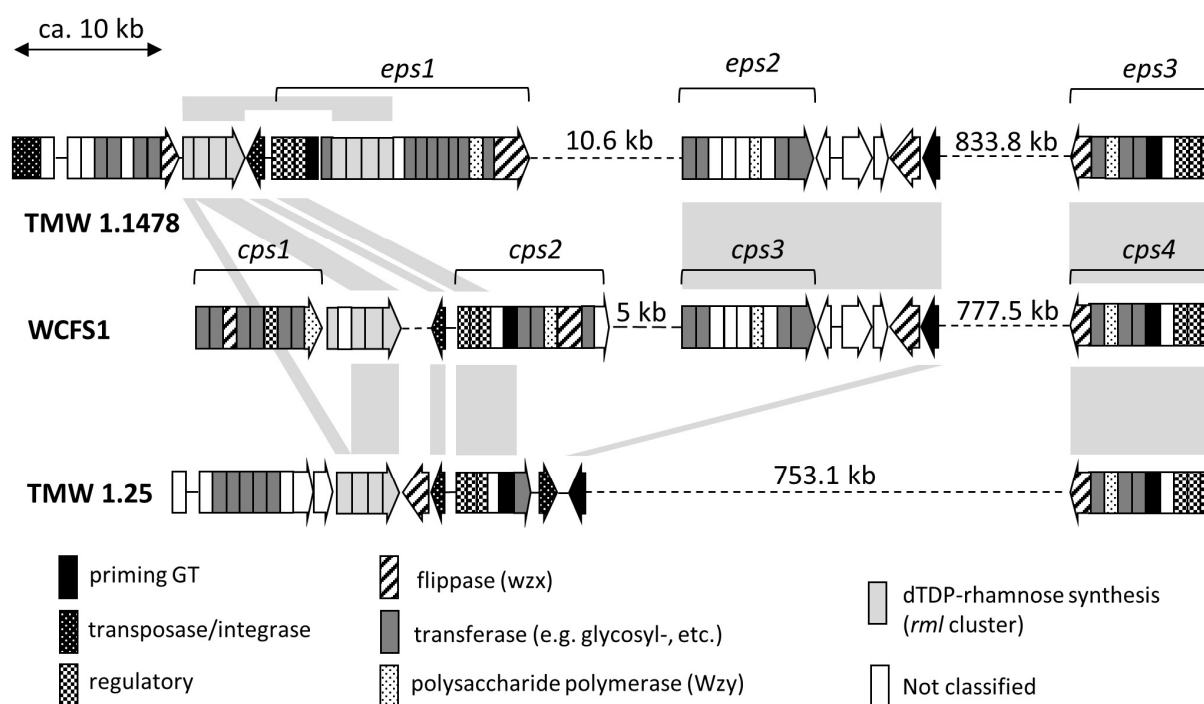
Figure 12 Comparative genetic organization of polysaccharide biosynthesis clusters in *L. plantarum* TMW 1.1478 (CP021932), *L. plantarum* WCFS1 (NC_004567) and *L. plantarum* TMW 1.25 (CP017354) chromosomal DNA. The presented sequence areas refer to locus tags CEB41_05075-09530 (TMW 1.1478), lp_1176-2108 (WCFS1) and BIZ31_04810-08525 (TMW 1.25). Light grey boxes indicate regions with high nucleotide sequence homology (>90% nucleotide identity upon >95% coverage) and dashed lines represent omitted segments (no open reading frames (ORFs) indicated).

The sequences covering the first three genes of *eps1* (TMW 1.1478) and *cps2* (WCFS1) were highly homologous (94%), whereas the remainder of *eps1* was markedly larger than its corresponding region in WCFS1, which arose from an increased number of predicted (glycosyl) transferases (Figure 12). Moreover, the entire cluster *eps1* turned out to be identical to a putative polysaccharide cluster in *L. plantarum* ATCC 14917 (GenBank accession no. NZ_AZEJ01000020; locus tags FC76_RS13330 through FC76_RS13420), the exopolysaccharide formation of which has not yet been investigated.

4.2.6. Analysis and modular organization of cluster *eps1*

A detailed scheme of the modular organization of cluster *eps1* is presented in Figure 13 and additional information about the particular genes of the cluster is provided in Table 11.
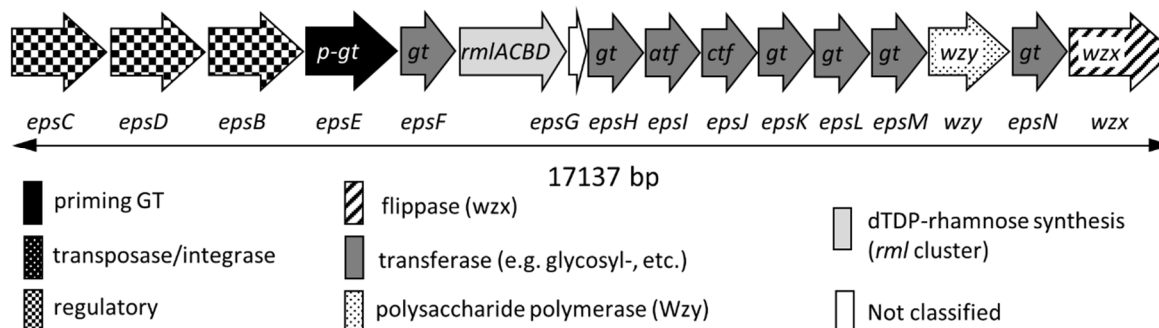

Figure 13 Modular organization of *L. plantarum* TMW 1.1478 HePS cluster *eps1*. Abbreviations: p-GT= priming glycosyltransferase, GT=glycosyltransferase; atf=acetyltransferase; ctf=cholinephosphotrans-ferase.

Table 11 Locus tags (GenBank ac. no. CP021932) and assigned genes in the putative HePS cluster *eps1* of *L. plantarum* TMW 1.1478. The annotations/predicted functions were derived from RAST annotation or enzyme homologues identified by BLASTp search (unless stated otherwise: >95% query coverage, >95% identity). The designated gene names are based on the nomenclature applied in *S. thermophilus* as proposed (Zeidan et al., 2017)and the putatively transferred monomers were deduced from the structure of the repeating unit, assuming sequential synthesis (Peant et al., 2005). This table was published as Table 3 in Prechtl et al. (2018c).

Locus tag	Designated gene	Annotation/Predicted function [a]	Put. Transferred monomer	Size (kDa) [c]
CEB41_05155	*epsC (wzd)*	Tyrosine-protein kinase transmembrane modulator		28.2
CEB41_05160	*epsD (wze)*	Tyrosine-protein kinase		26.4
CEB41_05165	*epsB (wzh)*	Tyrosine protein phosphatase		28.7
CEB41_05170	*epsE*	Priming GT	Glucose	25.7
CEB41_05175	*epsF*	GT family 1, put. Rhamnosyltransferase	Rhamnose	45.7
CEB41_05180-05195	*rmlACBD*	dTDP-rhamnose biosynthesis cluster		n.a.
CEB41_05200	*epsG*	Polysaccharide biosynthesis protein/ RelB superfamily		7.9
CEB41_05205	*epsH*	GT	Galactose	37.1
CEB41_05210	*epsI*	Acetyltransferase	Acetate	25.3
CEB41_05215	*epsJ*	LPS-cholinephosphotransferase LicD1		31.5
CEB41_05220	*epsK*	GT family 2 [d]	Rhamnose	34.1
CEB41_05225	*epsL*	GT family 2	Glucose	39.9

Locus tag	Designated gene	Annotation/Predicted function [a]	Put. Transferred monomer	Size (kDa) [c]
CEB41_05230	*epsM*	GT family 1	Rhamnose	42.6
CEB41_05235	*wzy*	Hypothetical protein/put. Polysaccharide polymerase (Wzy) [b]		47.1
CEB41_05240	*epsN*	GT family 2	Glucose	35.8
CEB41_05245	*wzx*	O-antigen flippase Wzx / repeat unit transporter		58.0

[a] based on manual BLASTp search for homologues and RAST annotation.

[b] ca. 25% amino acid identity (70% coverage) with O-antigen ligase domain containing protein; contains ten transmembrane helices according to a prediction derived by the TMHMM server (v. 2.0) (Figure 14).

[c] according to ExPASy/ProtParam (https://web.expasy.org/protparam/).

[d] 38% amino acid identity (97% coverage) with rhamnosyltransferase wchQ of *S. pneumoniae.*

Regarding the biosynthesis of activated sugar precursors required for the assembly the HePS repeating unit, only the genes required for dTDP-rhamnose biosynthesis were contained in the cluster *eps1* (Table 11), whereas glucose-1-phosphate uridylyltransferase (EC: 2.7.7.9; locus tag CEB41_03245) and UDP-glucose-4-epimerase (EC: 5.1.3.2; locus tag CEB41_03045), which are required for the synthesis of UDP-glucose and UDP-galactose, respectively, were located elsewhere in the genome. The open reading frame (ORF) downstream of the *rml* cluster encoded a small 7.9 kDa polysaccharide biosynthesis protein (epsG, Table 11), which shared homology with cps2K from *L. plantarum* WCFS1 and is the predicted antitoxin of a type II toxin-antitoxin (TA) system of the RelB/DinJ family, as suggested by manual BLASTp search.

While the repeat unit transporter Wzx (flippase) is encoded by the large ORF at the 3' end of the cluster (Figure 13), no gene could be identified as polysaccharide polymerase (Wzy homologue) in the first place. However, the hypothetical protein encoded at locus CEB41_05235 displays distant similarity to proteins containing an O-antigen ligase domain, and bioinformatic analysis for transmembrane domains revealed ten putative transmembrane helices displaying a similar arrangement as those in the Wzy homologue cps1 of strain WCFS1 (Figure 14). The high number of transmembrane domains (9-14) is typical for Wzy homologues (Jolly and Stingele, 2001), and despite the lack of a clear homology it can thus be assumed that it serves as polysaccharide polymerase, thereby belonging to a yet unknown family of Wzy homologues.
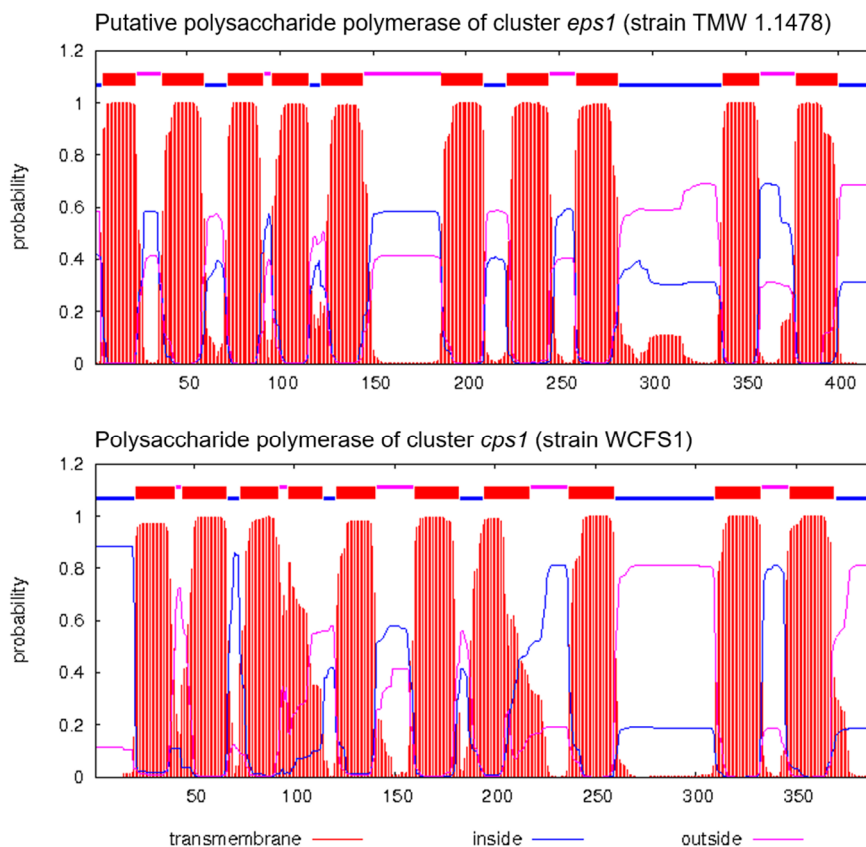
Figure 14 Comparison of predicted transmembrane topologies of the putative polysaccharide polymerase in cluster *eps1* of *L. plantarum* TMW 1.1478 (locus CEB41_05235, GenBank accession no. CP021932) and the annotated polysaccharide polymerase cps1l in cluster *cps1* of strain *L. plantarum* WCFS1 (locus lp_1185, GenBank accession no. NC_004567). The prediction was derived from the TMHMM server v. 2.0 (http://www.cbs.dtu.dk/services/TMHMM/). This figure was published as Figure S6 in Prechtl et al. (2018c).

4.3. Investigation of glucan formation by *L. sakei* TMW 1.411

In contrast to *L. plantarum* TMW 1.1478, which had demonstrated a sucrose-independent EPS formation, the EPS formation of *L. sakei* TMW 1.411 only occurred if sucrose was available in the medium, thereby suggesting a HoPS (4.1.1). HPLC analysis of monomer hydrolysates confirmed this hypothesis and revealed the HoPS to be a glucan (4.1.2). In the following experiments, the glucan formation of *L. sakei* TMW 1.411 should be examined in more detail, including production kinetics and macromolecular structural parameters. Apart from that, the glucan type should be determined, and genome sequencing was applied to discover the genetic basis of HoPS formation by identifying the responsible glucansucrase gene.

Several experimental results of this chapter were published in the journals *"Food Hydrocolloids"* (Prechtl et al., 2018b), and *"Frontiers in Microbiology"* (Prechtl et al., 2018a).

4.3.1. Glucan production and macromolecular structure analyses

The glucan formation of *L. sakei* TMW 1.411 was investigated in 50 mL batches at 30 °C (mMRS, 50 g/L sucrose, fin. OD_{600}=0.1) as described in 3.2.1. Bacterial growth (OD_{600}) and pH were monitored over 48 h, and the produced glucan was isolated, purified and gravimetrically quantified at various time points (Figure 15).
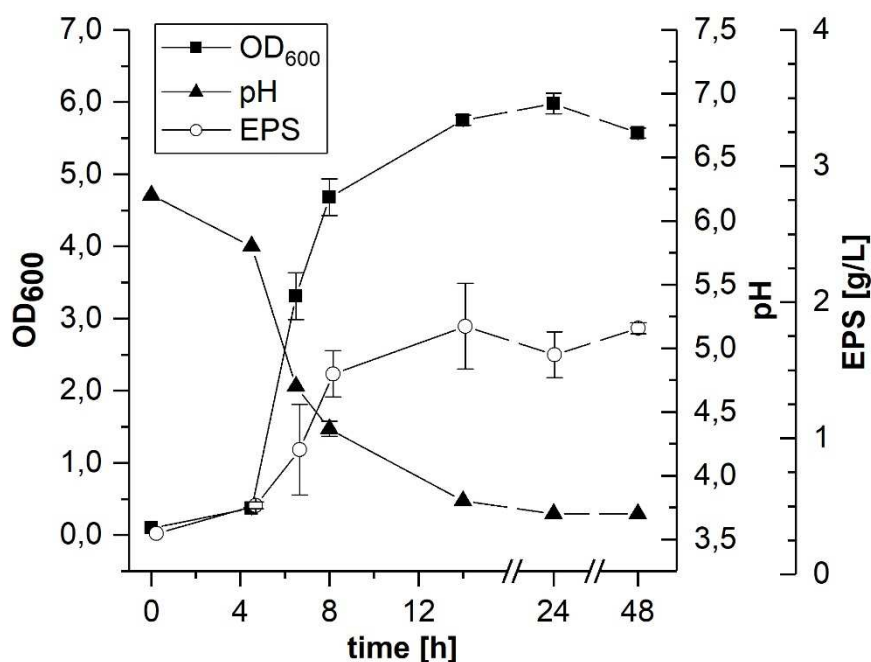
Figure 15 Monitoring of growth (■, OD_{600}), pH (▲) and EPS/glucan (○) formation by *L. sakei* TMW 1.411 in mMRS medium supplemented with sucrose (50 g/L) as sole carbon source over 48 h. Error bars indicate standard deviations of triplicates.

The glucan formation occurred mainly during the exponential growth phase (4-8 h) and stayed more or less constant (1.5-1.8 g/L) during the stationary phase, while no degradation could be observed within 48 h. As inferred from the 0 h sample, about 15 mg (~0.3 g/L) dry matter could be isolated from (more or less) pure mMRS medium, which probably resulted from yeast cell wall polymers contained in yeast extract as suggested by characteristic NMR signals (data not shown). However, since these polymers are unlikely to be co-precipitated with the glucans at constant ratios throughout the cultivation, a subtraction as blank value was not suitable at this point.

With respect to the macromolecular structure of the glucan, its average molecular weight and particle size should be determined with AF4-MALS. As determination of the molecular weight required the calculation of UV extinction coefficients and was thus much more elaborative than measuring the particle sizes, which were determined from the MALS signals only, this parameter should be determined of only one glucan sample. However, since the

macromolecular structure of the glucan might be influenced by the cultivation time, it was important to obtain information about possible changes in the macromolecular structure of the glucan throughout the cultivation. Thus, the particle sizes of selected glucan isolates were determined in dependence of the cultivation time by measuring the average geometric radii of these samples (Figure 16).
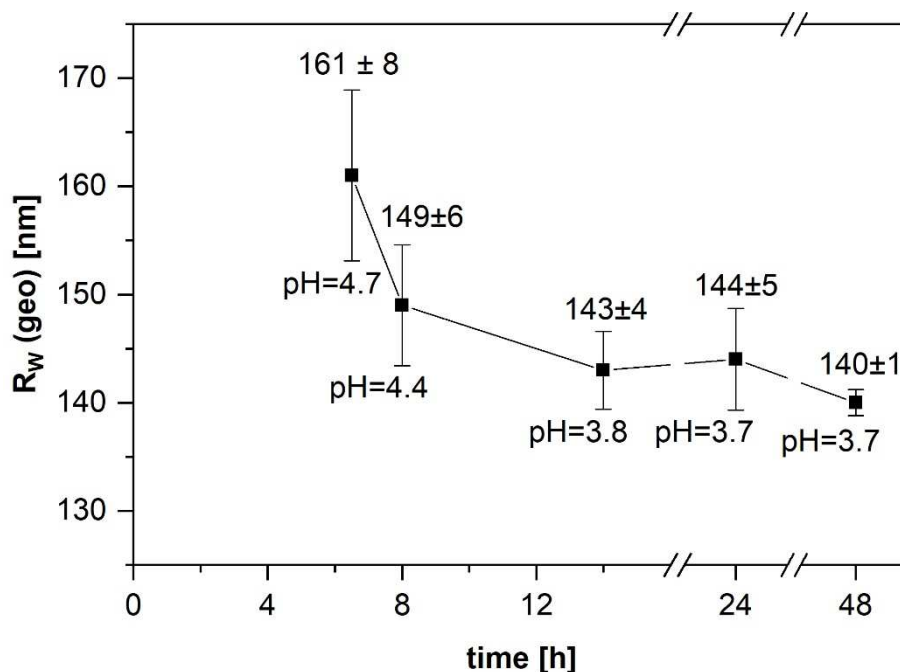
Figure 16 Development of the weight average geometric radius ($R_{w\,(geo)}$) of glucan polymers during growth in mMRS medium at 30 °C upon ongoing acidification. Values are expressed as mean·±SD from three replicates. This figure was published as Fig. S4 in Prechtl et al. (2018b).

The glucan polymers were largest in the late exponential growth phase (6.5 h, pH=4.7) as clarified by a weight average geometric radius ($R_{w\,(geo)}$) of ~160±8 nm. During the next 42 h, the radii continuously decreased until they finally reached a value of 140±1 nm. However, the strongest decrease in the geometric radii occurred between 6.5 h and 14 h, while only minor changes could be observed thereafter. Interestingly, this coincided with the point of time at which the acidification of the medium had reached its maximum and the pH stayed constant.

The decreasing particle sizes also became apparent from the retention times of the corresponding glucan samples in the AF4 chromatograms (Figure 17): While the glucan harvested after an incubation time of 6.5 h (pH=4.7) showed the highest retention time of ca. 27.5 min (according to the peak maximum), the later isolated glucans demonstrated continuously decreasing retention times, and the relative signal of the 24 h sample completely overlapped with the 48 h sample (not shown in the figure for clarity reasons).
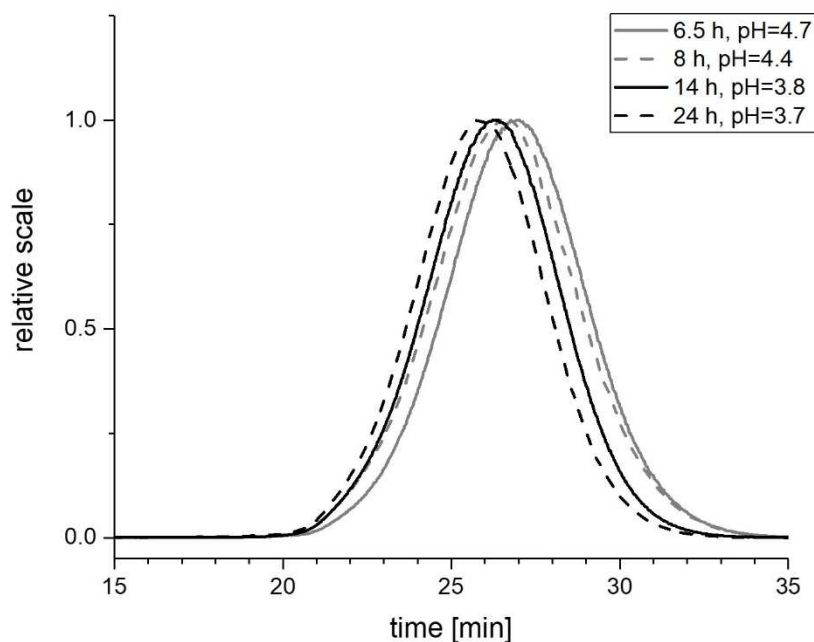
Figure 17 AF4-Chromatograms (light scattering signal 90°) of glucan samples produced by _L. sakei_ TMW 1.411, which had been isolated after varying cultivation times. For clarity reasons, the 48 h sample was not included in the figure, as its its relative signal was identical to the 24 h sample.

Since no significant changes in the particle size could be observed after 24 h, this glucan isolate was regarded as reference for these conditions (30 °C, 50 g/L sucrose) and used to calculate the weight average molecular weight (M_w) of the polymer. The result pointed to a high molecular weight glucan of $1.8\pm0.2 \times 10^8$ Da (Figure 18), while the polydispersity index (PDI) of 1.08 ± 0.02 suggested a rather uniform mass distribution. A detailed list of the measured values is given in Table 16.
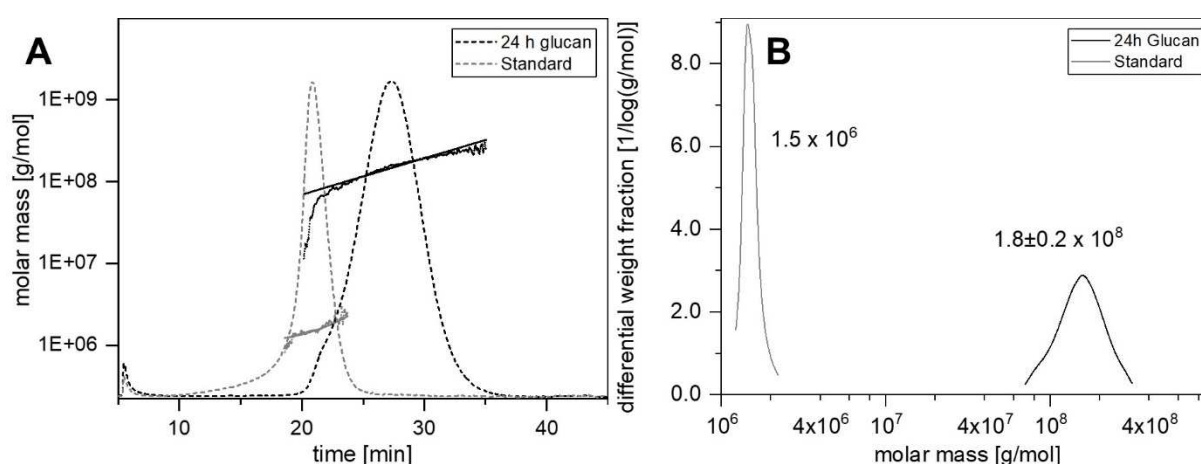
Figure 18 (A) AF4 chromatograms (light scattering signal 90°, dashed) and corresponding (fitted) molar masses (solid lines) of the 24 h glucan and a commercial dextran standard (M_r=2 MDa, grey). Dots indicate the raw data of molecular weights without fitting. (B) Differential weight fractions of the calculated molar masses of the dextran standard (grey line) and the 24 h glucan (black line). Values are expressed as ±SD from three biological replicates. For clarity reasons, only one replicate is shown.

4.3.2. Analysis of the chemical structure of the glucan

To reveal the chemical structure of the glucan, namely the present linkages and thus the type of the glucan, the 24 h sample was investigated with NMR analysis by a cooperating research institute as described in 3.3.5.3. The ^{1}H and ^{13}C chemical shifts in the proton and HSQC spectra revealed that the glucan was a dextran with an α-1,6-linked backbone and branches at position *O*3. The assignments were made based on standard compounds and literature data (Maina et al., 2011).

4.3.3. Genome sequencing and identification of the dextransucrase gene

The genome of *L. sakei* TMW 1.411 was sequenced and subsequently annotated as described in the materials and methods section 3.5.1.2.

The obtained WGS of *L. sakei* TMW 1.411 comprised 41 contigs, while a genome size of ca. 1.9 Mb with a GC content of 41.0 % was predicted, which is in the usual range of different genome-sequenced strains of *L. sakei*. Additional information including the genome coverage, the number of predicted coding sequences (CDS) and RNAs is presented in Table 12.

The contigs seq28, seq32 and seq36 could be circularized due to sequence overlaps, and manual BLASTn analysis of the processed sequences confirmed a high nucleotide sequence identity (90-99%) with known plasmids of *L. sakei* and *L. curvatus* species (Table 13).

Table 12 General features of the sequenced genome of *L. sakei* TMW 1.411. This table was published as Table 1 in Prechtl et al. (2018a).

Parameter	Value
Coverage	200x
Number of contigs	41
Genome size (bp)	1,944,239
GC content (%)	41.0
Number of CDS	1912
Number of RNAs	63
Number of put. plasmids	3
Origin	Sauerkraut
GenBank ac. no.	QOSE00000000

Table 13 WGS contigs of *L. sakei* TMW 1.411 with assigned plasmid names, identified homologues and related information. This table was published as Table 2 in Prechtl et al. (2018a).

Contig/ Plasmid	Hmlg. plasmids	Size (bp)	Strain	Isolation source	Identity/ Coverage	GenBank ac. number
Contig: seq28 Plasmid: p-1.411_1 Size: 11,246 bp Ac. No. QOSE01000028	pMN1	11,126	*L. sakei* MN1	Fermented meat product	99%/100%	MF590088.1
	plasmid 4	11,068	*L. sakei* FLEC01	Human feces	99%/100%	LT960780.1
	plasmid 4	11,156	*L. sakei* MFPB19	Beef carpaccio	99%/100%	LT960787.1
	pJ112C	10,871	*L. sakei* J112	French dry-type Pork sausage	99%/100%	OBHN01000041.1
	pJ156C	10,871	*L. sakei* J156	French dry-type Pork sausage	99%/100%	OBHL01000056.1
	p-1.1928_3	11,381	*L. curvatus* TMW 1.1928	Raw-fermented sausage	99%/100%	CP031006
Contig: seq32 Plasmid: p-1.411_2 Size: 6,593 bp Ac. no. QOSE01000041	pKCA15	14,826	*L. sakei* KCA311	n.a.	91%/58%	KF559313.1
Contig: seq36 Plasmid: p-1.411_3 Size: 2,499 bp Ac. no. QOSE01000040	pLC2	2,489	*L. curvatus* LTH683	Raw-fermented sausage	99%/100%	Z14234.1
	p-1.1928_4	2,627	*L. curvatus* TMW 1.1928	Raw-fermented sausage	99%/100%	CP031007

Among the plasmids, seq28 (denoted as plasmid p-1.411_1) harbored a 5.3 kb ORF, which encoded a 1807 aa comprising predicted glucansucrase of the glycoside hydrolase (GH) family 70 (gene locus DT321_09485, ac. no. RFN55776.1). The corresponding amino-acid sequence was almost identical (> 95% identity and > 95% coverage) to those of known dextransucrases (Dsr) in *L. sakei* and *L. curvatus* species, such as DsrLS (*L. sakei* MN1, ac. no. ATN28243) and GtfKg15 *(L. sakei* Kg15, ac. no. AAU08011.1), or Gtf1624 (*L. curvatus* TMW 1.624, ac. no. CCK33643) and Dsr11928 (*L. curvatus* TMW 1.1928, ac. no. AXN36915.1), respectively. The main difference between the amino-acid sequences was the length of an alanine-rich amino acid repeat, which formed a putative linker segment between the GH70 domain and the C-terminal, LPxTG cell-wall anchor motif (Figure 19).
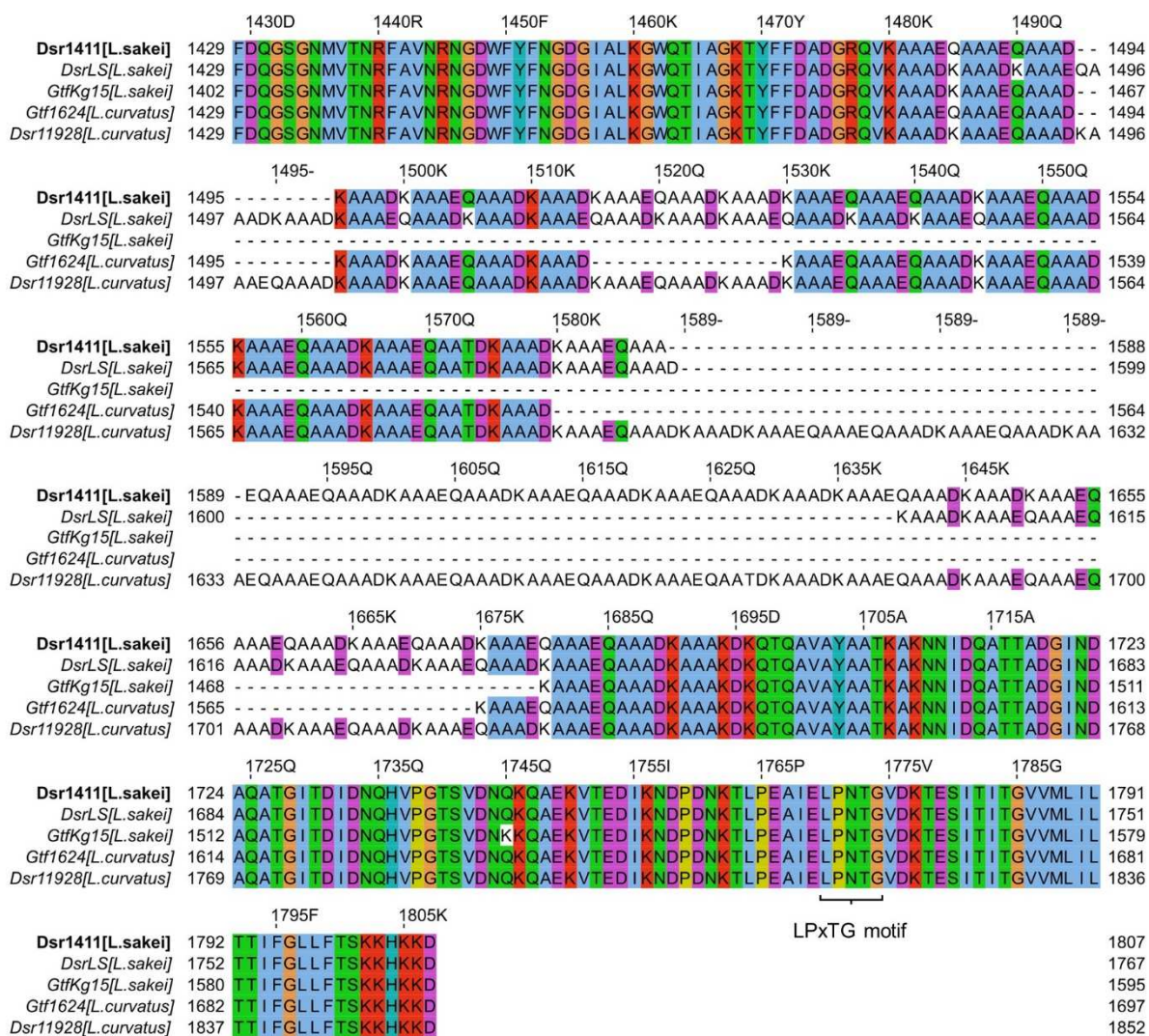
Figure 19 Multiple sequence alignment (ClustalW) of *L. sakei* and *L. curvatus* dextransucrases. The sequence Dsr1411 (bold) served as reference for numeration (above the sequences). For clarity reasons, only a part of the entire alignment is shown.

4.4. Carbohydrate utilization of *L. sakei* TMW 1.411 during dextran formation and sucrose-induced proteomic response

With respect to the application of *L. sakei* TMW 1.411 and *L. plantarum* TMW 1.1478 as EPS forming starter cultures for the manufacturing of spreadable raw fermented sausages with reduced fat content, the former strain had shown the most promising results, as it could significantly reduce the hardness of the product (Hilbig et al., 2019). Because such applications require the use of sucrose as carbon source, it is beneficial to understand the metabolism of this carbohydrate. However, the general physiological response of *L. sakei* spp. to sucrose as sole carbohydrate source has not been investigated yet, especially upon simultaneous dextran formation. Hence, the sucrose-induced changes in the proteomic profile of this strain should be investigated in comparison to its response to glucose by means of a combined genomic and quantitative proteomics approach. Furthermore, dextran formation and carbohydrate utilization should be monitored throughout the cultivation.

The generation of the proteomic dataset was carried out by the Bavarian Center for Biomolecular Mass Spectrometry (BayBioMS, Freising, Germany). The experimental results of this chapter were published in the journal *"Frontiers in Microbiology"* (Prechtl et al., 2018a).

4.4.1. Genetic adaption of *L. sakei* TMW 1.411 to sucrose and fructose utilization

The genomic sequence of *L. sakei* TMW 1.411 had already been obtained in the frame of another experiment, namely the identification of the dextransucrase gene (4.3.3), and was analyzed in more detail regarding its sucrose metabolism upon simultaneous dextran formation. Since fructose is constantly released from sucrose during dextran synthesis, this did not only include genes required for sucrose utilization, but also those required for fructose utilization.

Ca. 14% of all SEED category assignments accounted for the metabolism of carbohydrates, including mono-, di- and oligosaccharides, as well as amino-sugars and sugar alcohols (Prechtl et al., 2018a, Table S1). Among these, the genes associated with sucrose and fructose metabolism were considered to be most relevant for a growth of *L. sakei* TMW 1.411 on sucrose as sole carbon source as stated above. In both cases, the corresponding genes were arranged in an operon (Table 14).

Manual BLASTn analysis revealed, that among all currently 38 genome-sequenced *L. sakei* strains solely *L. sakei* LK-145 lacks the sucrose operon (Prechtl et al., 2018a, Table S2),

while each deposited *L. sakei* genome contains the fructose operon. On the contrary, only four of these strains comprised a dextransucrase gene (*L. sakei* FLEC01, MFPB19, J112, J156). As described in 4.3.3, the dextransucrase genes were encoded on plasmids in all of these strains, while the nucleotide sequences were nearly identical (Table 13).

Table 14 Sucrose and fructose operons of *L. sakei* TMW 1.411 with associated genes and predicted functions according to RAST annotation. The gene names were assigned according to the strain *L. sakei* ssp. *sakei* 23K. The gene loci refer to the deposited WGS (GenBank ac. no. QOSE00000000), whereas the FIG identifiers refer to the RAST annotation which was used for the evaluation of proteomic data (Prechtl et al., 2018a, Table S4). This table was published as Table 3 in Prechtl et al. (2018a).

Operon	Gene	Function	Contig	FIG identifier	Gene locus
Sucrose	*scrR*	Sucrose operon repressor	seq5	fig|1664.9.peg.1584	DT321_04270
	scrB	Sucrose-6-phosphate hydrolase	seq5	fig|1664.9.peg.1585	DT321_04275
	scrA	PTS beta-glucoside transporter subunit IIBCA	seq5	fig|1664.9.peg.1586	DT321_04280
	dexB	Glucan 1,6-alpha-glucosidase	seq5	fig|1664.9.peg.1587	DT321_04285
	scrK	Fructokinase	seq5	fig|1664.9.peg.1588	DT321_04290
Fructose	*fruA*	PTS fructose transporter subunit IIABC	seq3	fig|1664.9.peg.1236	DT321_02745
	fruK	1-phosphofructokinase	seq3	fig|1664.9.peg.1237	DT321_02750
	fruR	Fructose operon repressor	seq3	fig|1664.9.peg.1238	DT321_02755

4.4.2. Generation and evaluation of the proteomic dataset

The proteomic data were generated as described in the materials and methods section (3.6). As indicated in that section, a part of this experiment was carried out at the Bavarian Center for Biomolecular Mass Spectrometry by Dr. Jürgen Behr and Dr. Christina Ludwig.

A scheme of the chosen approach, which describes the performed experimental steps to investigate the proteomic changes of L. sakei TMW 1.411 after a switch to sucrose as sole carbon source, is presented in Figure 20.
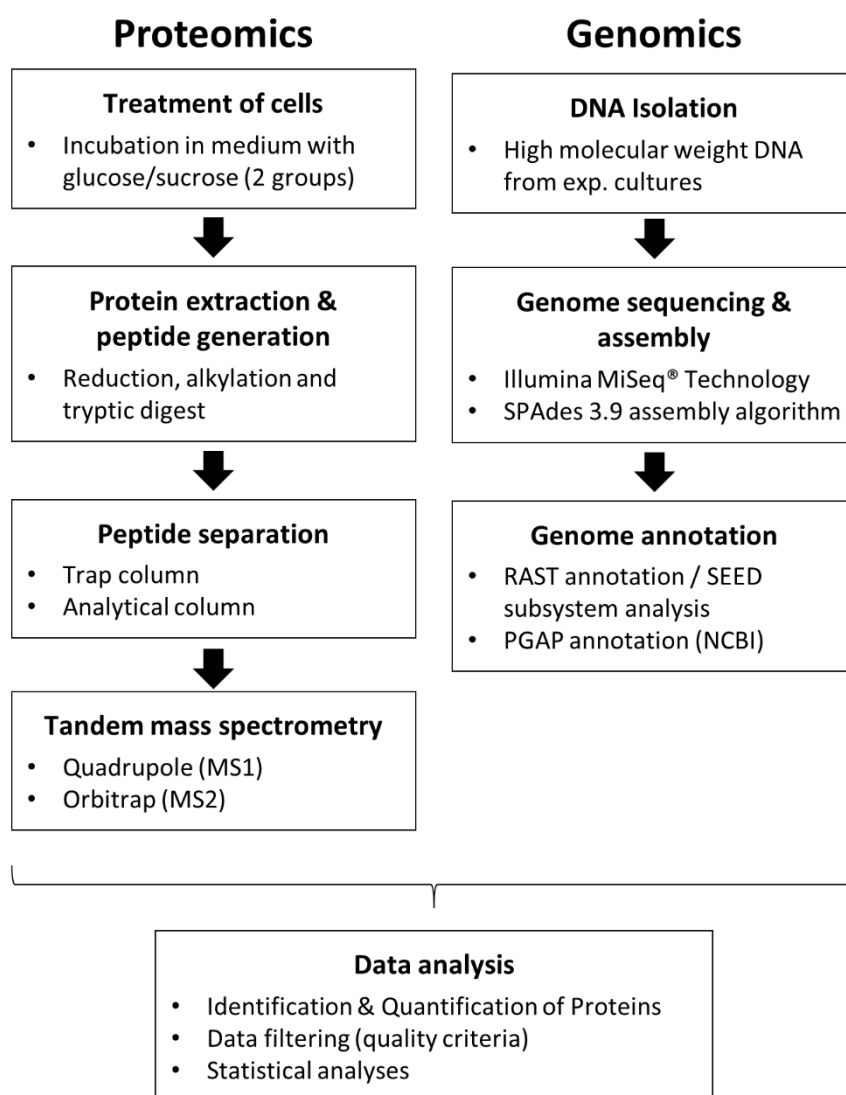

Figure 20 Overview of the experimental steps for the analysis of sucrose-induced changes in the proteomic profile of *L. sakei* TMW 1.411. The genomic part of this experiment had been performed in 4.3.3. This figure is partly based on Figure 1 of Schott et al. (2017) and was published as Figure S1 in Prechtl et al. (2018a).

To evaluate the plausibility of the generated data set and exclude a bias for distinct protein categories during the sequential data filtering steps, the *in silico* proteome of *L. sakei* TMW 1.411 was compared with the protein sub-groups created during data filtering with respect to protein numbers and corresponding SEED categories, which had been derived from RAST annotation (Figure 21).
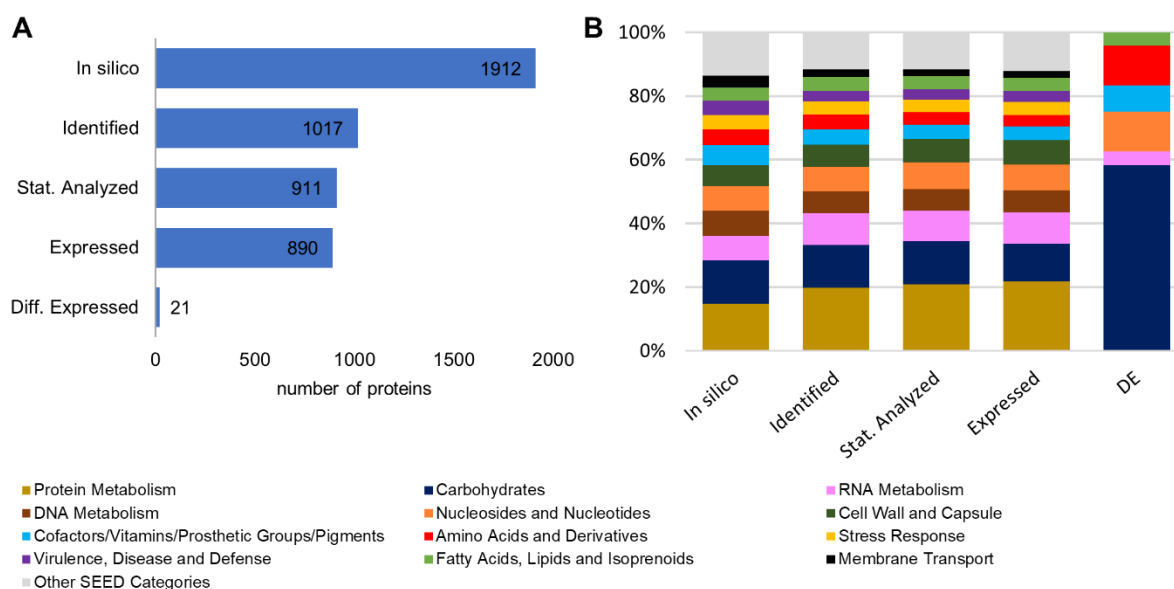
Figure 21 Comparison of the *in silico* proteome with the protein sub-groups generated by data filtering steps. (A): Total protein numbers of *in silico* predicted proteins, identified proteins (according to quality criteria described in 3.6.5), statistically analyzed proteins (detected in all four replicates of at least one group), expressed proteins, differentially expressed proteins (B): Corresponding SEED category distributions. The SEED subsystem proteome coverage was ca. 50%. This figure was published as Figure 1 in Prechtl et al. (2018a).

Compared to the *in silico* proteome of *L. sakei* TMW 1.411, which comprised 1912 putative proteins according to the number of coding sequences (CDS) predicted by RAST annotation, 1017 proteins could be identified based on the applied quality criteria described in 3.6.5. This resulted in a proteome coverage of ~ 53%, which is in the typical range of label-free quantitative proteomics approaches (Liu et al., 2014). To further increase the accuracy of statistical evaluation, only proteins detected in all four replicates of a group (glucose or sucrose) were considered for statistical analysis (3.6.5), which amounted to a subset of 911 proteins, whose expression levels were compared between both groups by statistical analysis. The SEED category distributions were similar for all protein sub-groups (except for the differentially expressed proteins being addressed in 4.4.3). Therefore, a potential bias for any protein category during the data filtering steps could be excluded (Figure 21 B).

Another important measure to ensure the validity of the proteomic experiment was to confirm equal viable cell counts and pH values in both groups (glucose and sucrose) prior to protein isolation, as any variation could have been the result of non-uniform cell growth/death or

acidification during the 2 h of incubation, which might have influenced the proteomic profiles as well. Thus, the average viable cell count was determined in both batch groups and the values (glucose: 1.3 ± 0.2 x 10^8 CFU/mL; sucrose: 1.6 ± 0.5 x 10^8 CFU/mL) were demonstrated to be statistically not different (t-Test, p=0.05). As for the pH values, the cells incubated in sucrose containing mMRS medium (pH=4.17$\pm$0.02) showed a slightly weaker acidification compared to the reference batch in glucose containing mMRS medium (pH=4.10$\pm$0.01). Although the mean difference was only 0.07 pH units, statistical analysis (two sample t-test, Table A 3) revealed it to be significant (p=0.01).

4.4.3. Comparison of the proteomic states associated with growth in glucose and sucrose

To compare the proteomic profiles of the cultures incubated in glucose and sucrose, respectively, the $\log_2$ transformed LFQ intensities of 911 proteins (Figure 21) were compared between both groups applying a stringent statistical analysis (t-Test with Benjamini-Hochberg FDR ≤ 0.01, 3.6.5). The results are visualized in a volcano-plot (Figure 22).

At the applied statistical criteria (3.6.5), 21 proteins were found to be differentially expressed in cells incubated with glucose or sucrose as sole carbon source, whereas 16 displayed an absolute $\log_2$ FC of > 1 and will be further discussed in this study. As reflected by the SEED category distribution of the differentially expressed proteins (Figure 21 B), approximately 60% of the assigned categories were associated with the metabolism of carbohydrates. This included the genes of the sucrose and fructose operon, respectively, which were up-regulated in sucrose incubated cells, whereas the highest $\log_2$ FC (7.1 and 5.8) were observed for the characteristic enzymes of the sucrose metabolic pathway, namely the PTS sucrose transporter subunit and the sucrose-6-phosphate hydrolase (Figure 22; Table A 4). Interestingly, although being significantly upregulated in the sucrose treated cells, the proteins of the fructose operon showed a relatively high abundance in the glucose treated cells as well, as suggested by the IBAQ intensities (Figure 23), which can be used to estimate absolute proteome-wide protein abundances (Schwanhausser et al., 2011; Ahrne et al., 2013).
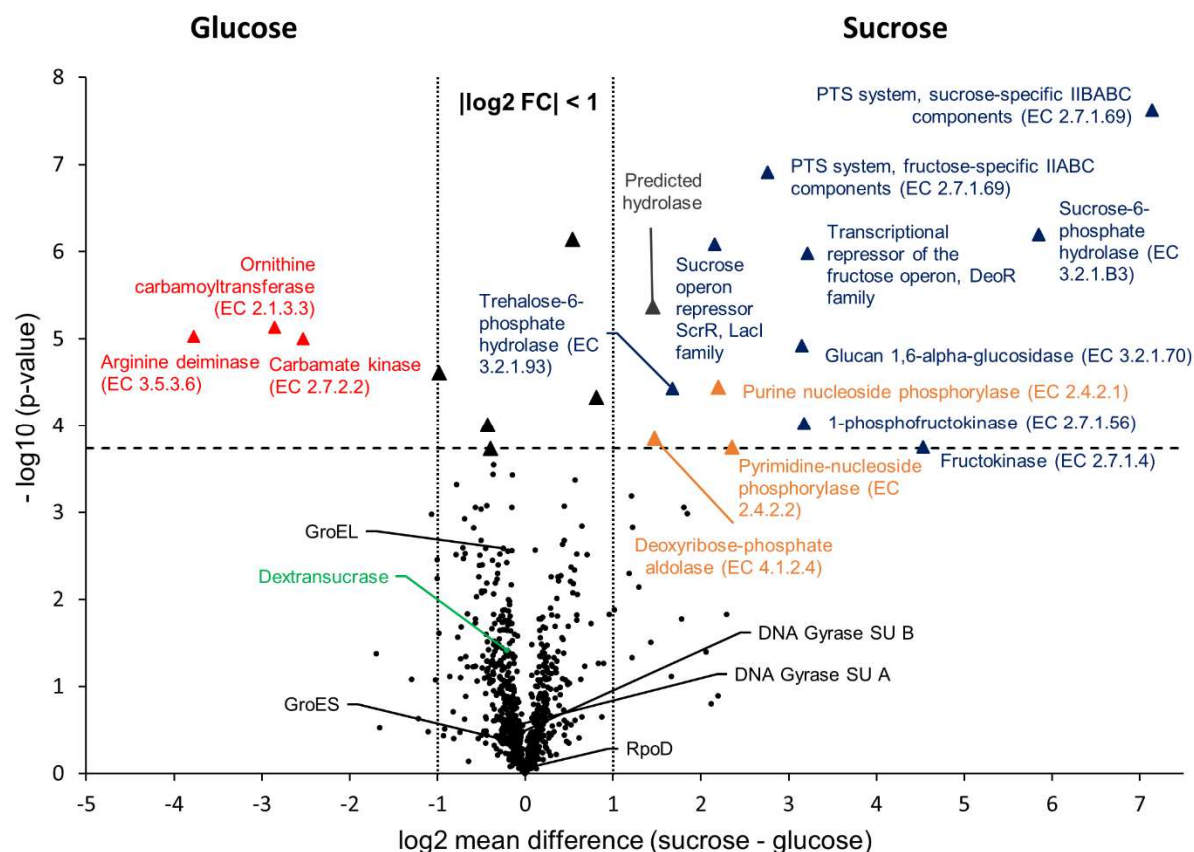
Figure 22 Volcano-Plot of the -Test comparison of 911 quantified proteins, which had been isolated from cultures incubated in mMRS with glucose and sucrose as sole carbon sources, respectively. The dashed horizontal line indicates the FDR threshold of 0.01, whereas dotted vertical lines enclose an area with a log$_2$ fold change of -1 ≤ x ≤ 1. Black dots below the FDR threshold indicate non-differentially expressed proteins with a selection of common house-keeping proteins (GroEL, GroES, DNA Gyrase subunits A, B, RpoD) and the dextransucrase, being marked in black and green, respectively. Triangles indicate statistically differentially expressed proteins, whereas different colors were used to group the proteins: red= Amino acids and derivatives (SEED category); blue= Carbohydrates (SEED category); orange= Nucleosides and nucleotides (SEED category); black: absolute log2 FC < 1 (not addressed in this study); grey: predicted hydrolase (no SEED category assigned). This figure was published as Figure 2 in Prechtl et al. (2018a). Further information about differentially expressed proteins are provided in Table A 4 and Prechtl et al., 2018a, Table S3.

Three enzymes associated with the catabolism of deoxynucleosides (Figure 22, orange), as well as the trehalose-phosphate hydrolase and a predicted hydrolase also showed an increased expression in sucrose treated cells. The enzymes of the arginine-deiminase pathway were found to be more abundant in glucose treated cells, which either suggested a sucrose-induced downregulation or a glucose mediated upregulation (Figure 22, red).

To demonstrate the validity of the experiment, the t-Test results for the expression of five common housekeeping proteins (GroEL/ES, RpoD, DNA Gyrase Subunits A/B), which was expected to be independent of the present carbon source, were highlighted in the Volcano-Plot (Figure 22, black descriptors). Additional supplementary information about the differentially expressed proteins and a detailed summary of the t-Test evaluation are provided in Table S3 (Prechtl et al., 2018a), and Table A 3.

4.4.4. Dextransucrase expression

Since sucrose is the natural substrate of dextransucrases and could thus have a positive impact on their expression, the expression levels of the dextransucrase Dsr1411 were compared for both carbon sources (i.e. glucose and sucrose). However, this enzyme was not differentially expressed (Figure 22, green). Moreover, an evaluation of the IBAQ intensities pointed at relatively high amounts of this enzyme within the cellular proteome - irrespective of the present carbon source (Figure 23, green).
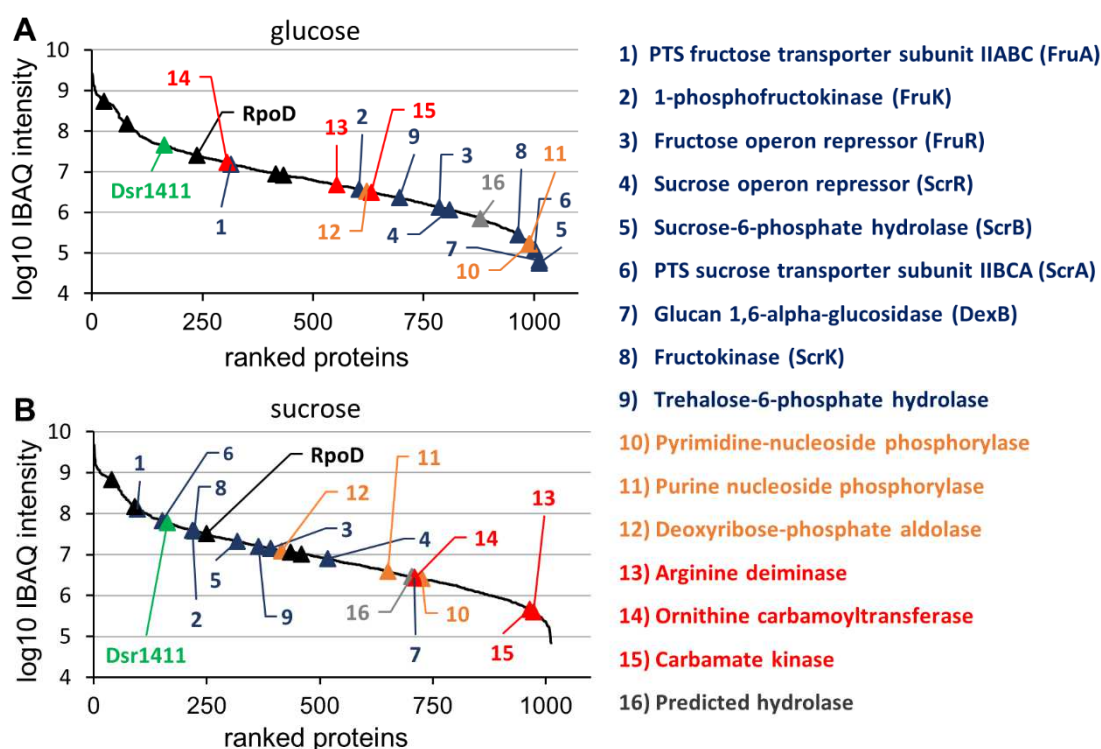
Figure 23 Log$_{10}$ transformed IBAQ intensities of identified proteins, which had been isolated from cultures incubated in glucose (A) and sucrose (B). The colors were used according to Figure 22, except for the housekeeping proteins, which were marked with black triangles. This figure was published as Figure 3 in Prechtl et al. (2018a). Further information (e.g. IBAQ values, FIG identifiers) are presented in Table A 4.

4.4.5. Monitoring of sugar consumption as well as lactate and dextran formation during growth on sucrose

The proteomic experiment (0-4.4.4) gave insights into the basic response of *L. sakei* TMW 1.411 to sucrose at an early stage of growth (after 2 h incubation in sucrose containing mMRS). In this way, the differential expression of sucrose-metabolizing pathways could be detected. To further investigate sucrose utilization under common EPS production conditions (Prechtl et al., 2018b), metabolite and dextran concentrations were monitored during growth in mMRS medium (15 mL sealed tubes) over 48 h (Figure 24).
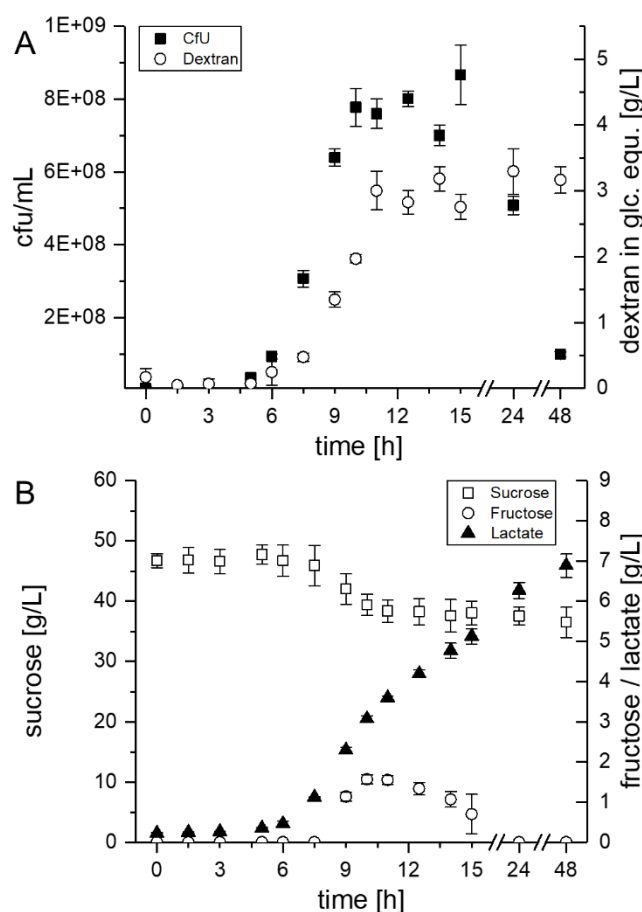
Figure 24 EPS and metabolite concentrations during growth of *L. sakei* TMW 1.411 in mMRS medium (15 mL sealed tubes) supplemented with 50 g/L sucrose. (A) Viable cell count (■) and dextran concentration (○) in glucose equivalents (glc. equ.). (B) Sucrose (□), fructose (○) and lactate (▲) concentrations. Error bars are standard deviations of triplicate measurements from two biological replicates (n=6). This figure was published as Figure 4 in Prechtl et al. (2018a).

The CFU of *L. sakei* TMW 1.411 increased after ca. 6 h, which was accompanied by dextran synthesis, sucrose consumption and lactate formation during the exponential growth phase (Figure 24 A + B). Fructose was detectable for the first time after 9 h of cultivation and

reached a maximum after 10 h (ca. 1.6 g/L; Figure 24 B). Afterwards, the fructose concentration decreased until it was depleted after 24 h, whereas the sucrose concentration stayed more or less constant at 39 g/L between 10 h and 24 h, and finally showed another slight decrease to 37 g/L after 48 h. The fructose concentrations lay always below the dextran concentrations, although the amount of fructose released during dextran synthesis and the produced amount of dextran in glucose equivalents (glc. equ.) should be stoichiometrically identical, if released fructose reflected the total dextransucrase activity. In total, ca. 10 g/L sucrose were consumed during the 48 h of fermentation, whereas about 3 g/L dextran were produced. Considering the theoretical maximum possible amount of ~ 5 g/L dextran (<. 50% of the consumed sucrose due to one released fructose + water molecule per transferase reaction), this resulted in a dextran yield of roughly 60%. Glucose, which could possibly be released by the hydrolysis activity of dextransucrases, as well as fermentation products such as acetate or ethanol could not be detected in the culture supernatant.

4.5. Dextran production of *L. sakei* TMW 1.411 during cold and salt stress

Due to the close structure-function relationship of hydrocolloids, the knowledge of any impact on their macromolecular structure, which might be exerted by environmental parameters such as cold temperatures and high salt concentrations, is of particular importance. This applies in particular to *in situ* applications, where production conditions are commonly defined by technological aspects, as hydrocolloids structure and thus functionality *in situ* may differ from that one determined upon production under optimal laboratory conditions. Since *L. sakei* TMW 1.411 had shown the most promising result in experiments aimed at the manufacturing of spreadable raw-fermented sausages with reduced fat content (Hilbig et al., 2019), formation and structural properties of the dextran produced by this strain should be investigated in dependence of common stress parameters applying during the manufacturing of processed meat products, namely cold and salt stress.

The experimental results of this chapter were published in the journal *"Food Hydrocolloids"* (Prechtl et al., 2018b).

4.5.1. Determination of stress parameters

The growth of *L. sakei* TMW 1.411 was studied at increasing cold and salt stress conditions, whereas parameters leading to a relative μmax of approximately 10% compared to standard conditions (30 °C/0% NaCl) were defined as uniform stress parameters for the following experiments. For this purpose, the maximum growth rates were determined for decreasing temperatures (30-10 °C) as well as increasing salt concentrations (0-10% NaCl) and related to standard conditions (30 °C/0% NaCl; Figure A 10). Based on the calculated values presented in Figure A 10, these parameters were estimated as T=10 °C and c (NaCl)=9.5%, respectively. In addition, a combination of both stress parameters was applied (10 °C/9.5% NaCl), however, no bacterial growth could be observed at these conditions within 96 h.

4.5.2. Production of dextrans during growth at stress conditions

The dextrans were produced at the predefined stress conditions (4.5.1) and subsequently purified as described in the methods section (3.2.1), while the 24 h dextran samples produced at 30 °C/0% NaCl (defined as standard condition) in the previous experiment (4.3.1) served for comparison. Since the geometric radii of dextrans had been demonstrated to decrease throughout the cultivation until a constant pH value was reached (4.3.1), this

condition served as criterion for the isolation of dextrans produced at different conditions. The quantified amounts and other growth-related parameters are presented in Table 15.

While only 1.6 g/L dextran were produced at 30 °C/0% NaCl, the amount increased more than four-fold to 6.7 g/L when the cells were cultivated at cold stress (10 °C/0% NaCl). In contrast, the EPS produced in cultures growing under salt stress conditions (30 °C/9.5% NaCl) were strongly decreased, yielding only about 0.5 g/L. The corresponding pH values varied between the different batches, whereas the lowest acidification (pH=4.3) was determined at salt stress conditions. The lower acidification rate in these cultures also correlated with lower cell counts, however, this could not be observed for the cultures grown at cold stress. In these batches, the cell count increased to 1.5×10^9 CFU/mL, despite the pH being higher than in the cultures grown at standard conditions (30 °C/0% NaCl).

Table 15 Parameters determined for cultures grown at different (stress-) conditions in mMRS medium (50 g/L sucrose) at the time of EPS harvest (stationary phase). All values are expressed as mean ±SD of three biological replicates. This table was published as Table 1 in Prechtl et al. (2018b).

Growth conditions	CFU/mL (t=0)	Growth time	CFU/mL (harvest)	pH (harvest)	$C_{(dextran)}$ [g/L]
30 °C/0% NaCl	1.0×10^7	24 h	$5.1 \pm 0.3 \times 10^8$	3.7±0.0	1.6±0.2
10 °C/0% NaCl	1.0×10^7	88 h	$1.5 \pm 0.6 \times 10^9$	4.1±0.0	6.7±0.7
30 °C/9.5% NaCl	1.0×10^7	100 h	$0.9 \pm 0.8 \times 10^8$	4.3±0.0	0.5±0.1
10 °C/9.5% NaCl	1.0×10^7	no growth observed			

4.5.3. Determination of molar mass and particle size distributions of the dextran variants

Characteristic structural parameters for the isolated dextran variants were determined by AF4-MALS analysis as described in 3.3.4.1, while the 24 h dextran samples of the experiment described in 4.3.1 (30 °C/0% NaCl) again served for comparison. The results are presented in Figure 25 and Table 16.
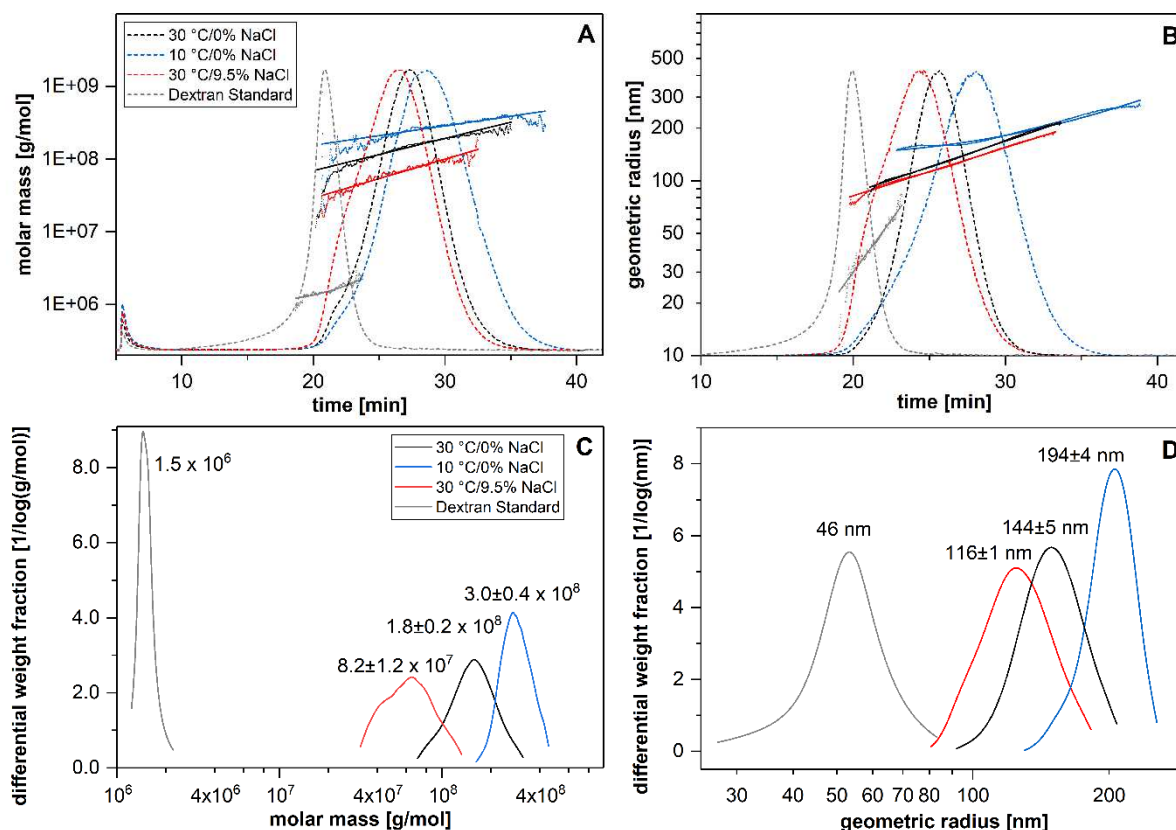
Figure 25 (A) AF4 chromatograms (light scattering signal 90°, dashed) and corresponding molar masses (solid lines) of dextran variants (30 °C/0% NaCl, 30 °C/9.5% NaCl, 10 °C/0% NaCl) and a commercial dextran standard (2 MDa, grey). Dots indicate the raw data of molecular weights without fitting. **(B)** AF4 chromatograms (light scattering signal 90°, dashed lines) and corresponding geometrical radii (solid lines; for the dextran standard (grey), the RMS radii calculated from model "berry", fit degree 2 are depicted). Dots indicate the raw data of geometric/RMS radii without fitting. **(C)** Differential weight fractions of the calculated molar masses with indicated M_w ±SD from three biological replicates. **(D)** Differential weight fractions of geometrical radii of isolated dextran variants (RMS radii for dextran standard) with corresponding R_w ±SD from three biological replicates. For clarity reasons, only one replicate of each variant is shown. This figure was published as Fig. 3 in Prechtl et al. (2018b).

The largest dextran molecules had been produced upon cold stress (10 °C/0% NaCl), as demonstrated by an M_w of 3 x 10^8 Da and an $R_{w(geo)}$ of 194.3 nm (Figure 25 C+D, blue), respectively. According to a slightly shortened retention time of the corresponding polymer fraction in the AF4 chromatogram, the dextran produced at 30 °C/0% NaCl were notably smaller and showed a decreased molecular weight of 1.8 x 10^8 Da (Figure 25, black). The salt stressed cultures (30 °C/9.5% NaCl) had produced the smallest dextran, displaying an M_w of 8.2 x 10^7 Da and an $R_{w\ (geo)}$ of 116 nm (Figure 25 C+D, red), which agreed with the shortest retention time in the chromatogram. Evaluation of the polydispersity indices (PDI) of the different polysaccharide variants demonstrated that the dextran produced at 10 °C/0% NaCl was more monodisperse than the dextran obtained from salt stressed cultures, and the same trend was observed for the distribution of the geometrical radii (Table 16).

Table 16 Determined parameters describing the macromolecular structures of the dextran variants and a commercial standard (M$_r$=2 MDa). To evaluate the dextran standard, the "berry" model was used (fit degree 2) and RMS radii are indicated instead of geometric radii. Values are expressed as mean ±SD of three biological replicates. This table was published as Table 2 in Prechtl et al. (2018b).

Variant	M$_w$ [Da]	M$_n$ [Da]	PDI[a] M$_w$/M$_n$	R$_w$ [nm]	R$_n$ [nm]	R$_w$/R$_n$	ε$_{400nm}$[b]
30 °C/0% NaCl	$1.8\pm0.2 \times 10^8$	$1.7\pm0.2 \times 10^8$	1.08±0.02	144±5	135±8	1.07±0.03	0.1003±0.0089
10 °C/0% NaCl	$3.0\pm0.4 \times 10^8$	$2.9\pm0.4 \times 10^8$	1.03±0.02	194±4	188±7	1.03±0.02	0.1135±0.0136
30 °C/9.5% NaCl	$8.2\pm1.2 \times 10^7$	$7.4\pm1.6 \times 10^8$	1.11±0.03	116±1	107±1	1.09±0.01	0.0696±0.0179
2 MDa Standard	1.5×10^6	1.5×10^6	1.01	46	n.a.	n.a.	0.0040

[a] Polydispersity index.

[b] Specific UV extinction coefficient at λ=400 nm (in [mL mg-1 cm-1]).

Apart from that, the difference of the UV extinction coefficients of the three dextran variants were nicely reflected by standardized (5 mg/mL) aqueous solutions in terms of clearly diverging turbidity (Figure 26).
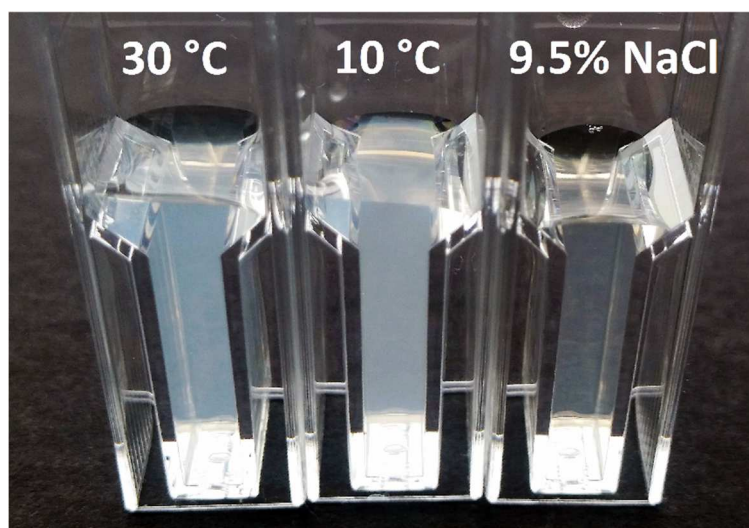
Figure 26 Solutions (5 mg/mL) of dextran produced at standard (30 °C/0% NaCl), cold (10 °C/0% NaCl) and salt stress conditions (30 °C/9.5% NaCl). The varying turbidity reflects the corresponding UV extinction coefficients (Table 16). This figure was published as Fig. S3 in Prechtl et al. (2018b).

4.5.4. Analysis of the degree of branching of the dextran variants

Because NMR spectroscopy of the intact dextran macromolecules cannot reveal their complete structural complexity, the samples were additionally analyzed by an enzymatic fingerprinting approach: Incubation of the dextran samples with endo-dextranase leads to a random hydrolysis of the linear, 1,6-linked backbone. Finally, isomaltose is produced as the end product, while the occurrence of branched backbone residues results in the formation of

branched oligosaccharides, which elute later in the chromatogram. NMR analyses and the enzymatic fingerprinting approach were carried out as part of a cooperation by Dr. Daniel Wefers at the Department of Food Chemistry and Phytochemistry, which is affiliated to the Institute of Applied Biosciences of the Karlsruhe Institute of Technology (KIT).

The chromatographic analyses of the hydrolysates demonstrated that the same branched oligosaccharides are enzymatically liberated from the dextrans (Figure 27 A). The dextrans produced with and without NaCl addition at 30 °C showed largely comparable oligosaccharide patterns, which indicates that these polysaccharides show a comparable structural composition.
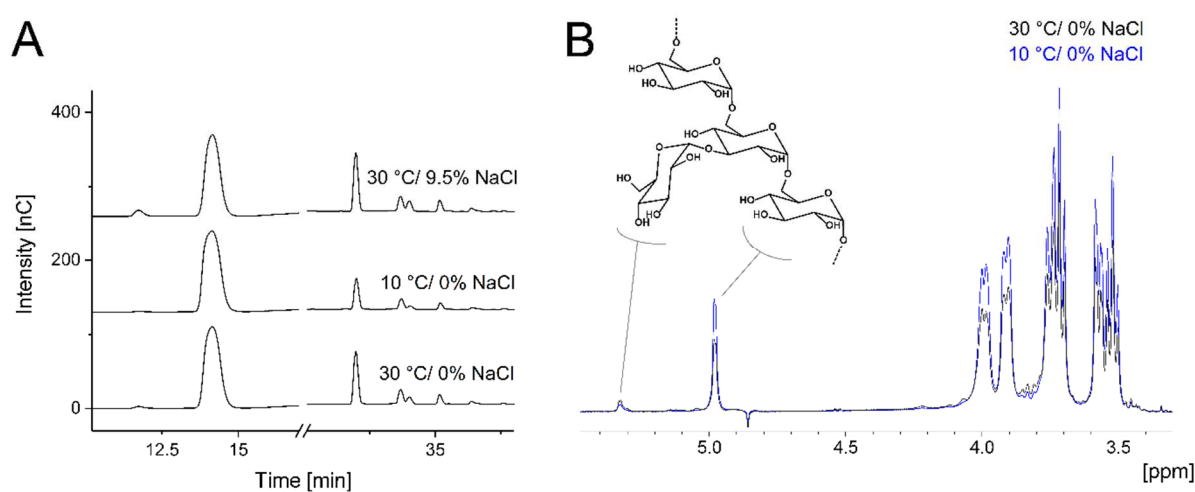
Figure 27 HPAEC-PAD chromatograms of the endo-dextranase hydrolysates of the dextrans produced at different conditions (30 °C/0% NaCl, 30 °C/9.5% NaCl, 10 °C/0% NaCl). For a better visualisation, the intensities of the chromatograms were adjusted to give a comparable intensity of the isomaltose peak at 14 min. (B) Comparison of the proton spectra of the dextrans produced at 30 °C/0% NaCl (black line) and 10 °C/0% NaCl (blue line). This figure was created by Dr. Daniel Wefers and published as Fig. 2 in Prechtl et al. (2018b).

However, a clearly different ratio between isomaltose (eluting at about 14 min) and the branched oligosaccharides (eluting after 32 min) was observed in the hydrolysate of the dextrans produced at 10 °C/0% NaCl. The higher relative abundance of isomaltose in this sample suggested that these dextrans were less branched than the dextrans produced at 30 °C.

This finding was also confirmed by comparing the NMR proton spectra of the dextran variants produced at 30 °C/0% NaCl and 10 °C/0% NaCl (Figure 27 B), since the corresponding ratios between the signals derived from the anomeric protons of the dextran side chains (5.33 ppm) and the dextran backbone (4.98 ppm) demonstrated the same trend.

While the dextrans obtained from the fermentation without NaCl addition (30 °C/0% NaCl and 10 °C/0% NaCl) were clearly dominated by dextran-derived signals, the dextrans produced with 9.5% NaCl contained several other, potentially carbohydrate-derived signals (Figure A 12). By using a blank sample (precipitated mMRS medium), it was possible to assign these signals to components, which were present in the growth medium and probably originated from yeast cell wall fragments.

4.5.5. Verification of cold and salt stress related effects in cell-buffer solutions

Although the formation of dextran at stress conditions by growing cells was closer to the conditions of an *in situ* production, it was difficult to clearly assign the observed structural changes in the dextrans to the applied (stress) conditions, due to varying pHs, cell-counts and fermentation times in the cultures (Table 15). Thus, an additional experimental approach was chosen, which allowed for an analysis of the dextran formation by native, cell-bound dextransucrases at more comparable conditions in buffer solutions (3.2.3).

Liquid cultures were harvested in the mid-exponential growth phase (pH=5) and subsequently resuspended in an equal volume of buffer for EPS production, which was analyzed at the same conditions as described in 4.5.2. Additionally, dextran production was investigated at a combination of cold and salt stress parameters (10 °C/9.5% NaCl), to test whether EPS could also be produced at conditions that had been shown to inhibit growth in mMRS medium in previous experiments (4.5.1). As the purification and gravimetric quantification of dextrans according to the standard protocol (3.2.1) was not suitable for this experimental approach due to low sample volumes and increased sample numbers, the phenol sulfuric acid method was applied to quantify dextrans produced in cell-buffer solutions (3.3.6). To validate the method and ensure a reliable hydrolysis of the polysaccharides, dextran solutions of known concentration were quantified, thereby demonstrating the applicability of the method (Figure A 9). The amount of produced dextrans in cell-buffer solutions and the corresponding particle size distributions are depicted in Figure 28.
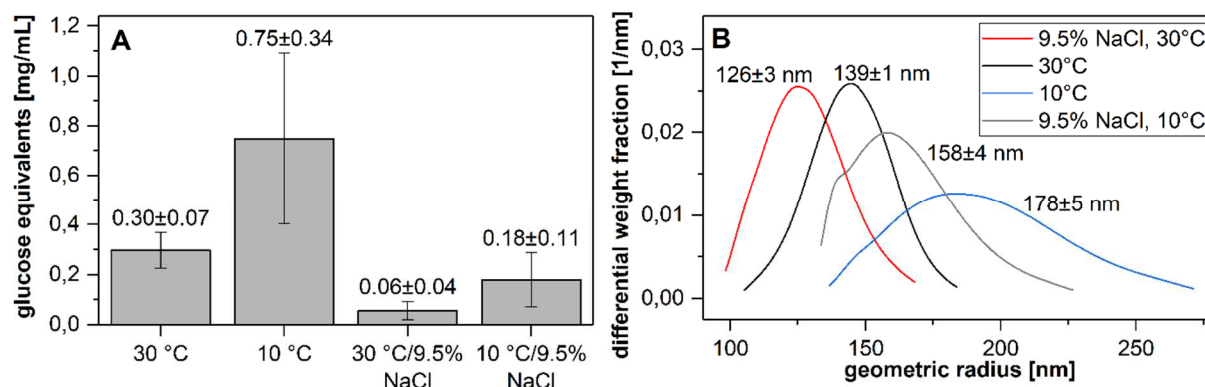
Figure 28 Amounts of dextran (glucose equivalents) produced in cell-buffer suspensions within 20 h of incubation at different conditions (30 °C/0% NaCl, 30 °C/9.5% NaCl, 10 °C/0% NaCl, 10 °C/9.5% NaCl). Values are expressed as mean ±SD from six biological replicates. No significant amounts (<0.02 mg/mL) could be detected in the negative controls (cell-buffer suspensions without sucrose and sucrose containing buffer without cells). (B) Distributions of geometrical radii for dextran variants produced in cell-buffer suspensions with average $R_{w(geo)}$ values ±SD from three biological replicates. As only small amounts of EPS had been produced in the cell-buffer suspensions, no M_w could be determined for the variants. For clarity reasons, only one replicate of each variant is shown. This figure was published as Fig. 4 in Prechtl et al. (2018b).

The highest yields, namely 0.75 g/L, were reached at 10 °C/0% NaCl and the geometrical radii of these particles were the largest, while the lowest amounts and smallest particle sizes were measured at salt stress conditions. The geometrical radii of the 30 °C/0% NaCl dextrans lay between the variants obtained at cold and salt stress conditions, and the same was observed for the produced amounts. When the cells were subjected to both cold and salt stress conditions simultaneously (10 °C/9.5% NaCl), dextran production could be observed as well, and the amount of produced dextran was even slightly increased compared to the batch where only salt stress had been applied (Figure 28 A), which also applied for the particle size (Figure 28 B). The pHs in the buffer solutions were somewhat decreased after 20 h of incubation, to final values of 4.1±0.1 (30 °C/0% NaCl), 4.3±0.1 (10 °C/0% NaCl), 4.6±0.2 (30 °C/9.5% NaCl) and 4.7±0.1 (10 °C/9.5% NaCl), whereas the pHs in the negative controls (cell-buffer solutions without sucrose) were decreased as well, to 4.7±0.1.

5. DISCUSSION

The main results of the presented work can be summarized in the following theses:

- Several LAB isolates from meat based or cold stored, salt containing foods produce EPS and belong to the species *L. sakei*, *L. curvatus*, *L. plantarum* and *Ln. gelidum*.
- The EPS forming isolates are able to grow and produce EPS at mild stress conditions, which reflect the conditions of meat fermentation processes.
- The studied EPS forming cultures do neither harbor transferable antibiotic resistances nor form biogenic amines, which is why their use as starter cultures is uncritical for health.
- The strain *L. plantarum* TMW 1.1478 produces a complex HePS, which is composed of a branched, acetylated repeating unit containing glucose, rhamnose and galactose in a ratio of 3:3:1.
- HePS synthesis in *L. plantarum* TMW 1.1478 follows the Wzx/Wzy dependent pathway and involves a chromosomally encoded biosynthesis cluster, the composition of which supports the structure of the repeating unit.
- The strain *L. sakei* TMW 1.411 produces a high molecular weight dextran with an α-1,6 linked backbone and α-1,3 linked branchings.
- Dextran synthesis is catalyzed by an extracellular dextransucrase, which is encoded on a stably inherited plasmid and expressed constitutively, irrespective of the carbon source.
- This plasmid is conserved in several other *L. sakei* and *L. curvatus* strains, which had been isolated from similar habitats. Since sucrose is already used as carbohydrate by some butchers, it can be supposed that *in situ* dextran formation by respective starter strains is already ongoing in any butchers product empirically employing sucrose for a better result.
- Dextran synthesis at cold stress results in increased yields and particle sizes upon a decreased degree of branching, whereas dextran synthesis at salt stress results in reduced yields and particle sizes without affecting the degree of branching.
- The presence of sucrose induces both sucrose and fructose operons in *L. sakei* TMW 1.411, while fructose is preferentially metabolized during dextran synthesis.

5.1. Selection of EPS forming meat starter cultures

After having investigated EPS types, growth behavior at mild stress conditions and potential safety risks of EPS positive LAB, two strains should be selected for more detailed experiments on their EPS formation (4.1.5).

Since the performed safety assessment had proven all strains as harmless in regard to both a potential transfer of antibiotic resistances and the formation of biogenic amines, only EPS formation on agar plates and the determined growth parameters were considered in the decision-making process.

Due to a close structure-function relationship of hydrocolloids, the type of EPS (i.e. HoPS or HePS) may have a vital effect on their functionality conditioned by differences in their physicochemical properties or localization. While HoPS produced from sucrose usually reach high molecular weights and are typically secreted into the extracellular space, for example, HePS are commonly smaller and may be attached to the cell wall/membrane of bacteria. This might also explain the clear differences in the according phenotypes: While glucan formation from sucrose was accompanied by a mucoid but non-ropy phenotype (Figure 3 A), the putative HePS forming strains displayed a clear ropy phenotype (Figure 3 B), which was most likely the result of cell aggregates enabled by cell-wall attached HePS. Hence, in order to ensure a high degree of physicochemical diversity, one HoPS and one HePS forming strain should be selected.

Among the HoPS forming strains, *L. sakei* TMW 1.411 had reached the highest turbidity in RSM, which suggested an improved biomass formation under these conditions compared to the other strains (Figure 6). Furthermore, the strain demonstrated relatively short lag-phases at 25 °C and 20 °C (Figure 5 B), which marks a temperature range being commonly used at the beginning of raw-fermented sausage production (Feiner, 2006). Hence, *L. sakei* TMW 1.411 was selected for further in-depth experiments. As for the HePS forming *L. plantarum* strains, the growth parameters were less varying than those of the HoPS forming *L. sakei* and *L. curvatus* strains (Figure 5, Figure 6). However, the visual estimation of EPS formation on mMRS and RSM agar had suggested distinct differences in respect of the quantity of formed EPS (Table 8). As detailed structural analyses require sufficient amounts of sample material, the strain *L. plantarum* TMW 1.1478 was chosen for more detailed experiments on EPS formation, as this strain had displayed the strongest EPS formation on mMRS and RSM agar.

5.2. HePS formation by *L. plantarum* TMW 1.1478

5.2.1. Formation and structure of the HePS

Although the growth rate was reduced at 20 °C compared to 30 °C, preliminary experiments on agar plates had pointed to a possibly increased HePS production at this condition, which is why HePS formation in CDM was monitored at this temperature. Such an inverse correlation of growth rate and HePS formation has already been described in the literature and was assigned to increased concentrations of lipid carriers and activated sugar precursors as a result of reduced cell-wall biosynthesis at lower temperatures (Vandenberg et al., 1995).

Eventually, gravimetric analysis of isolated HePS yielded a maximum amount of ca. 130 mg/L. Although being more than a magnitude less than the quantified amount of HoPS produced by *L. sakei* TMW 1.411 (4.3.1), similar amounts were reported for HePS forming LAB that had been grown at non-optimized culture conditions (De Vuyst and Degeest, 1999). Another important difference to the HoPS formation by *L. sakei* TMW 1.411 became apparent in the production kinetic of the HePS. In contrast to dextran biosynthesis by *L. sakei* TMW 1.411, HePS biosynthesis did not only occur in the exponential growth phase, but also during the first 48 h of the stationary phase, where the pH had dropped below 4.5 and the living cell count was even decreasing (Figure 8 A). Similar findings have also been reported for other HePS forming strains (Peant et al., 2005; Arskold et al., 2007). The marked decrease of the HePS concentration after 96 h by more than 40% was striking and a breakdown of the polymer after prolonged incubation was reported for several other strains as well (De Vuyst et al., 1998; Pham et al., 2000; Degeest et al., 2001), however, it is generally believed that EPS do not serve as an energy reserve for the host strains, which usually lack the enzymes required for the degradation of the biopolymers they synthesize (Cerning, 1990). Nonetheless, it cannot be generally excluded at this point and the increased protein content of the respective HePS isolates (Figure 8 B) would support the hypothesis of a HePS degradation by extracellular enzymes such as glycoside hydrolases, which could indeed be detected in the extracellular fraction of a HePS producing *L. rhamnosus* strain (Pham et al., 2000). However, this hypothesis cannot be proven for *L. plantarum* TMW 1.1478 by the available data and more in-depth experiments would have been necessary, which were beyond the scope of the present work.

With respect to the chemical structure of the HePS, an acetylated, branched heptameric repeat unit could be established based on the results of the structural analyses (Figure 11). The use of a chemically defined medium (CDM) for HePS production was of special

importance for the detailed structural characterization of the HePS, as the complex ingredients contained in MRS, namely yeast extract, meat extract and peptone, contain compounds that interfere with EPS analysis (Kimmel and Roberts, 1998). This also appeared in the present study, since even the HPLC chromatogram of a hydrolyzed sample prepared from a non-inoculated, minimal medium (MBp) lacking yeast and meat extract showed clear monomer peaks for glucose, galactose/rhamnose and mannose (Figure 4 E). Thus, an exact structural characterization of complex HePS is only possible, if those ingredients are omitted in the medium.

The identified monomers glucose, rhamnose and galactose (Figure 9 A) are very common for LAB derived HePS, and the same applies for the derivatization with an acetyl group, which was discovered only in NMR experiments (Figure A 5-8) and is a known modification in HePS (De Vuyst and Degeest, 1999). As to the number of monomers contained in the repeating unit, varying sizes have been reported for LAB derived HePS, while *L. delbrueckii* ssp. *bulgaricus* Lfi5 and *L. rhamnosus* RW-9595M were constituted of a heptameric repeating unit as well. Although the presence of N-acetyl-aminosugars (e.g. GlcN and GlcNAc) has been described for several LAB derived HePS as well (De Vuyst and Degeest, 1999; Mozzi et al., 2006), it could be demonstrated in the present work that these monosaccharides were not part of the HePS, but rather originated from a contamination of the HePS with cellular residuals. As a consequence, improved detachment of the HePS through prolonged heat incubation (up to two hours at 60 °C) reduced the contamination with cellular residuals (proven by microscopy, data not shown) as well as the intensity of the GlcN peak (Fig. S3).

As to the macromolecular structure of the HePS, the applied dextran standard suggested an apparent molar mass of approximately 2×10^6 Da (Figure 10), which is a typical magnitude for LAB derived HePS (Cerning et al., 1992; Marshall et al., 1995; De Vuyst and Degeest, 1999; Degeest and de Vuyst, 1999).

5.2.2. Identification and modular organization of the putative HePS cluster

The bioinformatic analysis of the genomic sequence of *L. plantarum* TMW 1.1478 revealed three putative HePS biosynthesis clusters encoded on the chromosomal DNA (*eps1, eps2, eps3*), which partly shared a high sequence homology with EPS biosynthesis clusters of the well characterized *L. plantarum* strain WCFS1 (Figure 12). The cluster *eps3* in *L. plantarum* TMW 1.1478 seems to be conserved among *L. plantarum* spp., as it is not only present in *L. plantarum* WCFS1 (denoted as *cps4*) and *L. plantarum* TMW 1.25, but also in many other strains including those, which are *not* capable of EPS production as described by Remus et

al. (Remus et al., 2012). Thus, cluster *eps3* is unlikely to be responsible for HePS formation by *L. plantarum* TMW 1.1478, which is further supported by the fact, that a deletion of the corresponding cluster (*cps4*) in *L. plantarum* WCFS1 did neither affect the monosaccharide composition of the produced glycan nor its molecular mass, and the same was observed upon deletion of cluster *cps3* (eps2 homologue) (Remus et al., 2012). However, a deletion of these clusters was associated with reduced polysaccharide production, thereby suggesting a sort of stimulating function of both gene clusters. The only clusters affecting monomer composition and/or molecular mass of the polysaccharides formed by WCFS1 were *cps1* and *cps2,* which emphasizes their crucial role in synthesis and polymerization of the polysaccharide repeating units (Remus et al., 2012). Since TMW 1.1478 does not contain a complete equivalent to *cps1* of WCFS1 except a few predicted GTs and a flippase in the corresponding area, only *eps1* can be responsible for both synthesis and polymerization of the repeating unit in *L. plantarum* TMW 1.1478. However, clusters *eps2* and *eps3* might still exhibit stimulating effects on its production as discussed above.

In comparison with the cluster *cps2* (strain WCFS1), only the first three genes of cluster *eps1* (strain TMW 1.1478) showed a high nucleotide sequence homology. These genes were designated as chain-length modulator genes *wzd*, *wze* and *wzh* (Figure 12, Figure 13), which are important elements of the Wzy dependent pathway and involved in the modulation of capsule synthesis by forming a tyrosine phosphoregulatory circuit (Groot and Kleerebezem, 2007; Yother, 2011; Remus et al., 2012; Zeidan et al., 2017). The remaining genetic composition of cluster *eps1* is in good agreement with the chemical structure of the HePS (Figure 11), since (i) the number of GTs (epsE, F, H, K, L, M, N) complies with the heptameric repeating unit of the polysaccharide, (ii) the acetylation of unit B can be explained by a predicted acetyltransferase (epsI), and (iii) the cluster contains all enzymes required for the biosynthesis of dTDP-rhamnose (rmlACBD), which was shown to be a major compound of the HePS. Although several strains were shown to harbor the genes for NDP-sugar synthesis (e.g. the *rml* cluster) at the 3' end of the polysaccharide biosynthesis cluster (Zeidan et al., 2017), this does not seem to be conserved among LAB, as other arrangements have been reported as well. In *L. plantarum* WCFS1, for example, the *rml* genes were located even outside of the cluster, while *L. plantarum* ATCC 14917 showed the same arrangement as *L. plantarum* TMW 1.1478, in that the *rml* genes are located in the center of the eps cluster (Remus et al., 2012). The synthesis of the remaining activated sugar precursors UDP-glucose and UDP-galactose does often not require unique enzymes, as they can be obtained from cellular pools originating from other cellular pathways (Yother, 2011). Nevertheless, the presence of glucose-1-phosphate uridylyltransferase (EC: 2.7.7.9; locus tag CEB41_03245) and UDP-glucose-4-epimerase (EC: 5.1.3.2; locus tag

CEB41_03045) required for the synthesis of UDP-glucose and UDP-galactose, respectively, could be proved.

With respect to the predicted antitoxin gene epsG (Figure 13, Table 11), it is tempting to speculate that this gene and its homologue cps2K in *L. plantarum* WCFS1 might contribute to the genetic stability of associated polysaccharide clusters, if a corresponding toxin gene is present. However, a toxin counterpart, which is usually located close to the antitoxin in type II TA systems (Fraunhofer et al., 2018), could not be identified yet and further bioinformatic analyses are required to confirm this hypothesis, which was beyond the scope of this work.

Apart from an acetylation, the composition of the cluster would also point to a derivatization of the repeating unit with phosphocholine (P-Cho), as suggested by the presence of a choline-phosphotransferase (epsJ, Table 11). However, with respect to the NMR results, no evidence was found for the presence of a P-Cho moiety, which is a known modification in *S. pneumoniae* type IV lipoteichoic acids (LTA) (Denapaite et al., 2012). Thus, it remains unclear at this stage whether the predicted phosphocholine transferase epsJ is inactive or indeed functionally expressed but fails to transfer the P-Cho moiety due to the lack of other essential enzymes (e.g. LicA, etc.).

It is worth noticing at this point that the entire cluster *eps1* is identical to a yet uncharacterized polysaccharide cluster in *L. plantarum* ATCC 14917, thereby suggesting this strain to produce the same HePS as *L. plantarum* TMW 1.1478.

5.2.3. Mapping of glycosyltransferases to the structure of the repeating unit

Although a reliable mapping of the GTs encoded in the cluster to the corresponding sugar units of the oligosaccharide is difficult at this stage and will require in-depth experiments with recombinant enzymes, the initial step in repeat unit synthesis can be inferred from the predicted enzyme functions, as the order of glycosyl transferases in a HePS cluster has been supposed to reflect the sequential synthesis of its repeat unit (Peant et al., 2005). Therefore, the second sugar monomer of the repeating unit can be assumed to be a rhamnose monomer, because epsF (the second GT) is a predicted rhamnosyltransferase. The two following genes (*epsH* and *epsI*) encode a glycosyl- and an acetyltransferase and thus indicate attachment of another glycosyl residue and acetylation. Because unit B (ʟ-rhamnose, Figure 11) contains a galactosyl side chain and an acetyl residue, it can be assumed that epsF, epsH, and epsI are responsible for the synthesis and decoration of unit B. Consequently, the putative starting point of the repeating unit synthesis which is catalyzed by epsE can be assigned to unit A (Figure 11). Hence, the putative substrate of the priming

GT (epsE) is UDP-glucose, which has already been demonstrated for several other priming GTs of HePS forming LAB, the amino acid sequences of which share significant homology with epsE of *L. plantarum* TMW 1.1478 (61-65% identity upon 89% coverage) (Lamothe et al., 2002; Peant et al., 2005). Despite the indefinite annotation of the remaining GTs, which only allows for the classification into GT family 1 or 2, the putatively transferred monomers can be assigned according to their sequence in the repeating unit and are presented in Table 11. Interestingly, epsK did indeed show a distant similarity with the putative rhamnosyltransferase wchQ of *S. pneumoniae* (38% identity upon 97% coverage). Apart from that, the predicted GT families 1 and 2 almost exclusively contain hexosyltransferases (EC 2.4.1.X) transferring hexoses or deoxyhexoses (www.cazy.org), which agrees with the sugar types contained in the repeating unit.

The poor annotation of the GTs results from their high diversity in LAB, which has already been described (Zeidan et al., 2017) and is emphasized by our results as well: None of the GTs encoded in cluster *eps1* of *L. plantarum* TMW 1.1478 (except the priming GT) displays a significant homology with any GT contained in the HePS clusters of *L. rhamnosus* ATCC 9595 (accession no. AY659976) and *L. delbrueckii* Lfi5 (accession no. AF267127), although their HePS are composed of just the same sugar monomers (i.e. glucose, galactose, rhamnose; data not shown) (Lamothe et al., 2002; Peant et al., 2005).

Once the repeating unit synthesis is completed, it is flipped across the membrane by the flippase Wzx, and eventually linked with other repeating units by the putative polysaccharide polymerase Wzy. Based on the HePS structure and the putatively transferred monosaccharide by the priming glycosyltransferase EpsE, this would occur via the formation of a β-1,3 glycosidic bond between the terminal units A and E.

5.3. Dextran formation by *L. sakei* TMW 1.411

5.3.1. Formation and macromolecular structure of the dextran

As indicated in 5.2.1, several differences occurred between HePS formation by *L. plantarum* TMW 1.1478 and dextran formation by *L. sakei* TMW 1.411. As presented in Figure 15, dextran synthesis only occurred during the exponential growth phase and the dextran concentration remained more or less constant during the stationary phase, while no degradation of the EPS could be observed within 48 h. This coincides with the results published for other HoPS forming LAB species, since the expression of responsible glycosyl hydrolases and the HoPS production itself have been reported to occur mainly during the exponential growth phase (van Geel-Schutten et al., 1998; Arskold et al., 2007; Rühmkorf et al., 2013). The maximum amount of dextran in the 50 mL batches was determined as ca. 1.8 g/L, which is indeed a magnitude higher than the maximum amount of quantified HePS produced by *L. plantarum* TMW 1.1478 (ca. 130 mg/L, Figure 8), but relatively low as compared to the amounts of other glucan/dextran forming LAB species, which have been demonstrated to produce several grams per litre and even more (Korakli et al., 2003; Badel et al., 2011; Rühmkorf et al., 2013).

Interestingly, the capability to produce increased amounts of dextran seems to be not necessarily dependent on the dextransucrase enzyme itself, as the amino-acid sequences of the dextransucrases of *L. curvatus* TMW 1.624 and *L. sakei* TMW 1.411 were found to be highly similar (4.3.3), although the former strain was reported to produce up to 5 g/L dextran at comparable conditions (50 g/L sucrose, 30 °C) (Rühmkorf et al., 2013). Strikingly, *L. curvatus* TMW 1.624 exhibited a markedly less acidification of the growth medium (end pH=4.5) as compared to *L. sakei* TMW 1.411 (end pH=3.75) and above that, the exponential growth phase was longer for TMW 1.624 (10 h) compared to TMW 1.411 (ca. 5 h) (Fig. 1 in (Rühmkorf et al., 2013)). Since the enzymatic activity of dextransucrases was reported to be strongly pH dependent in that markedly decreased at pH values of 4.0 and below (Fig. 5 in (Rühmkorf et al., 2013)), this might offer an explanation for the relatively small amounts of dextran produced by *L. sakei* TMW 1.411: Due to its fast growth and strong acidification, the dwell time of the extracellular dextransucrases in a tolerable pH range was relatively short, thereby resulting in decreased dextran amounts. This hypothesis is further supported by the observation that up to 3 g/L dextran could be produced by *L. sakei* TMW 1.411 if it was not cultivated in 50 mL batches but in 15 mL batches, where the exponential growth phase was slightly prolonged (ca. 6 h; comparable acidification) (Figure 24 A).

In any case, the limitation of dextran formation by acidification of the medium could explain the altered kinetic of HePS formation, which takes place in the cytoplasm and even occurred at a pH below 4.5, where the dextran synthesis by *L. sakei* TMW 1.411 was nearly aborted.

As to the macromolecular structure of dextran, which had a molecular weight of ca. 1.8×10^8 Da (24 h sample), very similar values were described for dextrans produced by other LAB, including *L. sakei* MN1 (1.7×10^8 Da) and *L. curvatus* TMW 1.624 ($1.2\text{-}2.4 \times 10^8$ Da) (Rühmkorf et al., 2012; Zarour et al., 2017). However, the conditions at which these dextrans had been produced slightly differed from those used in the present study: While a sucrose concentration of 50 g/L had been used in this study, 20 g/L and 80 g/L had been applied to produce dextrans with *L. sakei* MN1 and *L. curvatus* TMW 1.624, respectively (Rühmkorf, 2012; Zarour et al., 2017). Since the sucrose concentration was demonstrated to exhibit an impact on the molecular weight of the produced dextrans, these values are not directly comparable. Nevertheless, however, they are in the same magnitude. The same applied for the average particle radius and the polydispersity index (PDI) of the TMW 1.624 dextran, which were determined as $R_w = 148\text{-}192$ nm (RMS radius) and PDI = 1.10 (TMW 1.411 dextran: $R_{w\,(geo)} = 144$ nm, PDI = 1.08). It is worth to stress out here, that the dextransucrases of *L. sakei* MN1 and *L. curvatus* TMW 1.624 were almost identical to the one of *L. sakei* TMW 1.411 in terms of their amino-acid sequence (4.3.3), which is post probably the reason for their highly similar polymer products.

The decrease of the average radii (and possibly the molecular weight, which was not determined in the present work) of the dextran macromolecules (Figure 16) with ongoing cultivation has not been published so far, however, it was reported for levan polymers synthesized by *Gluconobacter albidus* (Ua-Arak et al., 2017a). In this work, it was demonstrated that the decreasing pH accounted for both reduction of the particle radius and the molecular weight, which was associated with several factors including altered enzymatic activity and acid hydrolysis. However, as no significant changes in the dextran radii could be observed after 14 h (Figure 16), it is unlikely that the decrease of the particle radii was the result of acid hydrolysis since this would have implied a further decrease during the next hours. Thus, it is more likely that the acidification of the medium affected the activity of the extracellular dextransucrases in that it shifted its activity from transferase activity towards hydrolysis activity, which is an inherent function of both dextran- and levansucrases (Monsan et al., 2001; Ua-Arak et al., 2017a).

5.3.2. Identification of the dextransucrase gene and sucrose independent expression

Genome analysis had revealed the dextransucrase gene *dsr1411* to be located on a ~11 kb plasmid (p-1.411_1, Table 13), which seems to be highly conserved among several strains of *L. sakei* and *L. curvatus*, including the aforementioned strain *L. sakei* MN1. The corresponding plasmid in *L. sakei* MN1 (pMN1) was shown to be a stably inherited low-copy number plasmid, which was attributed to its *repA/B* based replication mechanism and a possible toxin-antitoxin system. The dextransucrase gene has been proposed to have integrated through a transposition process (Nacher-Vazquez et al., 2017b). As dextran formation is responsible for biofilm formation in diverse LAB species (Leathers and Cote, 2008; Walter et al., 2008; Zhu et al., 2009; Leathers and Bischoff, 2011; Nacher-Vazquez et al., 2017a; Fels et al., 2018; Xu et al., 2018), its production could protect *L. sakei* against desiccation and could enable surface adhesion, providing an advantage in the colonialization of plants (Cerning, 1990; Badel et al., 2011; Zannini et al., 2016) or provide another selective advantage in habitats, where sucrose is the predominant carbon source, such as in plant sap sucking insects. In a meat-based environment, however, the expression of dextransucrases is unlikely to provide any advantages, since sucrose is not available in this environment.

The same sequence homology as observed for the whole plasmid also applied for the dextransucrase genes encoded on these plasmids, which only showed significant differences in the length of an alanine-rich amino acid repeat forming a putative linker segment between the GH70 domain and the C-terminal cell-wall anchor motif (LPxTG) (Figure 19). One possible explanation for this variation could be the underlying nucleotide sequence: Just as the amino-acids, the nucleotide sequence also displayed many repetitive segments (tandem repeats) in the corresponding region (see associated GenBank entries listed in 4.3.3). Thus, the variation in the length of the linker sequence could be the result of errors during the replication of the plasmid by replication slippage during strain diversification (Lovett et al., 1993).

As to the regulation of dextransucrase expression, Nácher-Vázquez et al. have already reported a constitutive gene expression, which was independent of the used carbohydrate and associated with replication and maintenance functions of the plasmid (Nacher-Vazquez et al., 2017b). This was confirmed in this study, as a comparison of the proteomic states of L. sakei TMW 1.411 in the presence of glucose and sucrose, respectively, did not reveal any significant differences in the quantified amounts of dextransucrase enzymes (Figure 22). Moreover, dextran synthesis with resuspended cells in a buffer solution (4.5.5) also supported a sucrose-independent dextransucrase expression, because equal amounts of dextran were quantified irrespective of the carbon source which was available in the

precultures before resuspending the cells (transcription/translation had been inhibited in the buffer solution by the antibiotic trimethoprim). Thus, the sucrose-independent expression of dextransucrases in *L. sakei* and *L. curvatus* species is contrary to the mostly sucrose-induced dextransucrase expression in *Leuconostoc* spp. and *Weissella* spp.

Apart from that, the IBAQ values presented in Figure 23 did not only reflect the sucrose-independent expression of the dextransucrases, but also highlight a surprisingly high abundance of this enzyme within the cellular proteome, which was even comparable to the house-keeping protein RNAse sigma factor RpoD. This adds even more weight to the question for the benefit being conferred by the high level constitutive expression of a tremendous ~190 kDa protein. Especially in a meat based environment, where no sucrose is present and thus no dextran synthesis can occur, it is even likely to represent a metabolic burden for the host strain. However, this question cannot be answered at this stage and needs further experimental analyses, which lay beyond the scope of the present work.

5.3.3. Impact of environmental stress parameters

As discussed above, the amount of produced dextran is likely to be affected by the pH of the medium, and influences of its macromolecular structure by the pH and sucrose concentration have been described as well (5.3.2).

5.3.3.1. Impact of environmental stress parameters on dextran formation

Apart from that, a severe impact of environmental stress parameters, namely cold and salt stress, could be observed on both, produced amounts and (macro-) molecular structures of the dextrans. While cold stress had led to a strong (more than fourfold) increase of produced dextran amounts, salt stress had resulted in clearly decreased amounts (4.5.2). These trends were also reflected in the macromolecular structures of the polymers in that cold stress gave rise to increased particle radii and molecular weights, while salt stress caused the opposite.

Although a direct correlation between increased EPS production and reduced growth rates has been reported for HePS forming strains, where the polysaccharide synthesis competes with cell growth (e.g. cell wall biosynthesis) for activated sugar precursors or lipid carriers (Vandenberg et al., 1995; Fialho et al., 2008; Freitas et al., 2011; Freitas et al., 2017), this has not been described for HoPS forming strains. However, it was reported that the expression of responsible glycosyl hydrolases and the HoPS production itself occur mainly during the exponential growth phase (van Geel-Schutten et al., 1998; Arskold et al., 2007; Rühmkorf et al., 2013), which is why the increased amount of dextran produced at cold

stress could be the result of the notably prolonged growth phase in the cold stressed cultures, whereas the increased cell count might have contributed to the higher amounts (Table 15). Furthermore, the acidification of the medium was more slowly and weaker at low temperatures as indicated by a final pH of 4.1 (Table 15). As discussed in 5.3.1, this is another key factor that must be taken into account, since the enzymatic activity of *L. curvatus* dextransucrase TMW 1.624, the amino acid sequence of which is highly homologous to *L. sakei* TMW 1.411 (4.3.3), was shown to be markedly decreased at pH values of 4.0 and below, thus resulting in lower EPS yields for strongly acidifying species (Rühmkorf et al., 2013). Consequently, the increased dextran amounts in cold stressed cultures could as well have arisen from a prolonged dwell time of cell-bound or secreted dextransucrases in a tolerable pH range, which was much shorter in the cultures grown at 30 °C/0% NaCl as compared to 10 °C/0% NaCl. Apart from that, other factors such as altered enzyme folding, or aggregation must be considered as well, while decreased enzyme inactivation at low temperatures was proposed by Shamala and Prasad (1995), who described enhanced dextran production of *Leuconostoc* spp. at cold temperatures (Shamala and Prasad, 1995). An increased enzymatic activity of the TMW 1.411 dextransucrase at low temperatures can be excluded, as this was already disproved for the highly homologous dextransucrase of *L. curvatus* TMW 1.624, which rather displayed decreasing activities upon temperature reduction (Rühmkorf et al., 2013).

Contrary to the dextran production at cold stress, the amount produced upon salt stress (30 °C/9.5% NaCl) was severely reduced, as only about 0.5 g/L could be isolated in the stationary phase, even though these cultures had been incubated longest (Table 15). Bearing in mind that these EPS were slightly contaminated by co-precipitated components of the growth medium (4.5.4), the dextran yield can be considered even lower. Although the cell count was decreased compared to the 30 °C control, which had possibly influenced the EPS yield as discussed above, it was unlikely to be the only reason for the markedly reduced dextran production, as the long fermentation time should have compensated the lower cell count to a certain extent. Since dextransucrases are extracellular enzymes and thus susceptible for environmental influences such as pH or solute concentration, it is therefore probable that their activity and/or stability was impaired by the high NaCl concentration in the medium (van Geel-Schutten et al., 1999; Tieking et al., 2005; Schwab and Gänzle, 2006; van Hijum et al., 2006).

5.3.3.2. Impact of environmental stress parameters on the dextran structure

At standard conditions (30 °C/0% NaCl), *L. sakei* TMW 1.411 had produced a rather monodisperse, high molecular weight dextran (Figure 25, black; Table 16), which was similar to the compact dextran produced by *L. curvatus* TMW 1.624 in the studies of Rühmkorf et al. (2012) in terms of molar mass and polydispersity. When produced at cold and salt stress conditions, however, its macromolecular structure was changed, which became apparent in varying retention times of the polymer fractions (Figure 25 A). As the separation principle of an AF4 system relies on distinct diffusion properties of the analyte molecules, which is dependent on their hydrodynamic radius, the relative retention times pointed towards an increased particle size of the 10 °C/0% NaCl dextran variant, while the one produced under salt stress conditions (30 °C/9.5% NaCl) seemed to display a decreased particle size. This was reflected well by the UV extinction coefficients of the corresponding dextran variants (Table 16; Figure 26), as larger spherical particles result in higher extinction coefficients due to enhanced light scattering. Evaluation of the MALS data finally confirmed the different particle sizes as depicted in Figure 25 B+D, and the molecular weights of these samples were changed accordingly (Figure 25 A+C). Even though the pH values differed between the cultures (Table 15) and possibly influenced the macromolecular structure of the dextran polymers as formerly reported for levan polymers (Ua-Arak et al., 2017a), it was unlikely to have solely caused the observed differences in particle sizes, as the previous experiment which had addressed the development of geometric radii during ongoing acidification in cultures without pH control only suggested variations of ±20 nm (Figure 16).

Only slight differences could be observed regarding the polydispersity of the dextrans, whereas the variant obtained from 30 C/9.5% NaCl had displayed the highest PDI of 1.11 (Table 16). The co-precipitated components of the growth medium had probably contributed to the increased polydispersity, which also became apparent in an increased peak asymmetry in the corresponding AF4 chromatogram (Figure 25 A+B, red). Interestingly, the dextrans produced by *Leuconostoc* spp. in the studies of Shamala et al. (1995) were also supposed to have increased molecular weights, which was derived from apparently higher viscosities in aqueous solutions (Shamala and Prasad, 1995). Although strains and medium composition were different in their experiments compared to this study, the enlargement of the polymers at low temperatures might be based on the same effect and it is tempting to speculate, if it also applies for the synthesis of other HoPS.

Apart from increased particle size and molecular weight, enzymatic fingerprinting and comparison of NMR spectra suggested that the dextrans produced at 10 °C/0% NaCl were less branched at position *O*3 than the dextrans from 30 °C/0% NaCl. The same effect has

been reported by Kim et al. (2003), who analyzed the influence of temperature on the degree of branching in a dextran produced by a purified dextransucrase from *Leuconostoc mesenteroides* and ascribed their observations to elevated diffusion rates at higher temperatures (Kim et al., 2003). This observation might explain why the M_w of the dextran at 10 °C/0% NaCl was only increased ca. 1.7-fold compared to the 30 °C/0% NaCl variant, whereas the $R_{w\,(geo)}$ was enlarged roughly 1.4-fold (Table 16). Due to the cubic relation between radius and sphere volume, a much higher increase of M_w ($1.35^3 = 2.5$-fold) would have been expected at similar packing densities of the spherical dextran polymers. Comparing the dextrans from 30 °C/9.5% NaCl and 30 °C/0% NaCl, however, the expected increment of M_w based on the enlargement of the geometric radii ($1.24^3 = 1.9$-fold) was quite similar to the one observed (ca. 2.2-fold), which accords with their comparable structural composition (4.5.4, Figure 27).

5.3.3.3. Stress-mediated effects on EPS formation and structure by resting cells

The quantification and structural analysis of the formed polysaccharides revealed that both quantity and particle size of the dextran polymers produced in cell-buffer suspensions followed the same trend as observed in the fermentation experiments performed previously (4.5.3). Although the molecular weights of the polymers formed in the buffer solution were not determined in this experiment due to the low yields, it can be assumed that they were changed according to their geometrical radii. While the $R_{w\,(geo)}$ of the polymers were quite similar in both experiments (Figure 25 D and Figure 28 B), the polydispersity of the 10 °C/0% NaCl dextran was markedly higher in the buffer experiment, which cannot be explained at this point and might be investigated in enzymatic studies.

Interestingly, the formation of dextran was even possible at a combination of both stress parameters (10 °C/9.5% NaCl), which demonstrated that inhibition of cell growth (Table 15) did not necessarily suppress the production of EPS by cell-bound enzymes. Furthermore, the particle size distribution of these dextrans and the corresponding amounts virtually suggested an additive effect of both environmental stress parameters, as the dextrans synthesized at a combination of both stress parameters (10 °C/9.5% NaCl) were larger than their counterparts produced at salt stress only, but smaller compared to the ones produced at cold stress, and the same trend could be observed for the produced amounts (Figure 28 A). Since cell count and incubation time had been identical in this experimental setup, any influence of these parameters on dextran amount or macromolecular structure can be ruled out at this point. Although the pH in the buffer solutions decreased during their incubation depending on the respective (stress) conditions, the differences between these setups were less than in the experiment with growing cells and unlikely constituted a major factor in these

experiments as discussed in 5.3.3.2. Moreover, the final pH in the 30 °C/0% NaCl buffer setup was the same as in the 10 °C/0% NaCl setup with growing cells (pH=4.1), whereas the geometric radii were still different and should have been similar if the pH had played a critical role.

Taken together, the results of the dextran production by resting cells clearly demonstrated that the applied (stress) conditions alone were sufficient to induce the same changes in the particle size of the dextran, which had previously been found in the fermentation experiments (4.5.3), and the same was observed for the quantities. Even though an explanation of the underlying mechanisms requires more in-depth experiments, including altered dextransucrase secretion at different conditions as recently proposed (Bechtner, J. et al., 2018, unpublished data), it can be assumed that varying enzymatic stability and/or activity at the applied (stress) conditions played a crucial role in determining both quantity and macromolecular structure of the produced polymers. Additionally, altered diffusion rates and substrate binding at low temperatures must be considered as well, and might have caused the decrease of branching. While altered diffusion rates might have less an impact in meat-based food matrices due to decreased water activity, other mechanisms affecting amount and (macromolecular) structure of produced dextran such as enzyme stability and activity should in fact be transferable to these food matrices. Since exopolysaccharides with higher molecular weight have been shown to give better results in terms of water binding than polymers with a lower molecular weight, even when smaller amounts had been used (Jakob et al., 2013), appropriate process parameters could eventually be used to optimize both molecular weight and amount of *in situ* produced EPS to obtain the best structural effects in the final food product.

5.4. Sucrose-induced proteomic response and carbohydrate utilization by *L. sakei* TMW 1.411 during dextran synthesis

After the performed switch to sucrose as sole carbon source, the upregulation of both the sucrose and the fructose operon was detected. The upregulation of the fructose operon, which contains a fructose uptake system, indicates the active uptake of extracellular fructose at an early stage of growth. This could be explained by the simultaneous secretion of active dextransucrases (5.3.2), which extracellularly release fructose. The corresponding metabolic pathways are described in Figure 29.

Furthermore, the glucan-1,6-α-glucosidase DexB was upregulated in the sucrose treated cells suggesting induced dextran degradation. Although DexB of *L. acidophilus* NCFM (60% amino acid identity) was demonstrated to be active on dextran (Moller et al., 2012), neither of the two DexB variants contains a N-terminal signal peptide targeting its secretion into the extracellular environment according to SignalP analysis (Petersen et al., 2011). This conforms with the general assumption, that high molecular weight EPS does not primarily serve as a carbon reserve for the producer strains (Zannini et al., 2016), as active uptake of such high molecular weight polymers has not been reported to our knowledge. The upregulation of this enzyme might rather be indicative for uptake and metabolization of short-chain isomaltooligosaccharides (IMO), which could be produced by dextransucrases in addition to high molecular weight dextran. However, their possible import mechanism remains unclear, while it was reported that fructooligosaccharides (FOS) are efficiently imported by the PTS sucrose transport system in *L. plantarum* (Saulnier et al., 2007).

Apart from the enzymes accounting for the intracellular utilization of sucrose and fructose, three further enzymes were upregulated upon growth on sucrose, which are involved in the catabolism of deoxyribose-nucleosides (Figure 22, orange). This pathway includes three major steps: (i) release of 2-deoxyribose-1-phosphate from purine/pyrimidine-deoxynucleosides by the corresponding phosphorylases (EC 2.4.2.1/2.4.2.2); (ii) interconversion of 2-deoxyribose-1-phosphate and 2-deoxyribose-5-phosphate by phosphopentomutase (EC 5.4.2.7); (iii) formation of acetaldehyde and the glycolysis intermediate glyceraldehyde-3-phosphate by deoxyribose-phosphate aldolase (EC 4.1.2.4) (Tozzi et al., 2006). All enzymes of this pathway were significantly upregulated after sucrose treatment (Figure 22), except for the phosphopentomutase (gene locus DT321_08540), whose upregulation ($\log_2$ FC = 1.2) was only significant at less stringent t-Test criteria (FDR ≤ 0.05; Table S3). Interestingly, the same enzymes where shown to be upregulated in some *L. sakei* strains after a switch of the carbon source from glucose to ribose by a

transcriptomic approach (McLeod et al., 2011). As the upregulation of these proteins can currently not be related to sucrose metabolism, their differential expression could be interpreted as general response to the change of the carbon source, e.g. to maintain glycolytic reactions during starvation until the organism has adapted to the new carbon source. However, further experimental analyses are necessary to confirm this hypothesis, since other factors such as glucose mediated carbon catabolite repression (CCR) might play a role as well.

Upon growth on glucose only three proteins were detected, which were more abundant in the presence of glucose (and thus downregulated after sucrose treatment). These proteins belonged to the arginine-deiminase (ADI) pathway (Figure 22, red), which involves three enzymes being encoded in the *arc* operon, namely (i) arginine deiminase (arcA, EC 3.5.3.6), (ii) ornithine carbamoyltransferase (arcB, EC 2.1.3.3) and (iii) carbamate kinase (arcC, EC 2.7.2.2). This pathway enables the synthesis of ATP from arginine upon formation of NH_3, CO_2 and ornithine, and was therefore supposed to provide a metabolic advantage in nutrient-poor, meat-based environments (Rimaux et al., 2011). Apart from that, several other physiological functions of the ADI pathway have been discussed, including *de novo* pyrimidine synthesis and the cytoplasmic alkalization by NH_3 as protection against acid stress (Arena et al., 1999; Rimaux et al., 2011).

Basically, the *arc* operon has been shown to be subjected to CcpA/HPr mediated carbon catabolite repression (CCR), which is initiated at high concentrations of ATP and fructose-1,6-bisphosphate (FBP) in the presence of a preferred carbon source (Montel and Champomier, 1987; Deutscher et al., 1995; Fernandez and Zuniga, 2006; Gorke and Stulke, 2008; Landmann et al., 2011). The mechanism involves regulatory *cre* sites in promotor regions, which are targeted by the CcpA/HPr complex, and both *cre* sites identified upstream of the *arcA* gene in *L. sakei* 23K (Zúñiga et al., 1998) are present in *L. sakei* TMW 1.411 as well (positions -124 and -44 from the start codon of *arcA*, gene locus DT321_05025). However, the ADI pathway should be downregulated in the glucose treated cultures, if glucose were the preferred carbon source of *L. sakei* TMW 1.411 for energy generation and concomitant lactate production.

With respect to the alkalizing function of the ADI pathway, the pH values measured prior to protein isolation indeed suggested a slightly stronger acidification by the cells incubated in glucose containing mMRS medium (4.4.3), which might be explained by the lack of a metabolic switch to sucrose utilization. Although the difference in the pH values of both batches was only small (0.07 pH units), it was statistically significant (p=0.01) and might point to an increased lactate formation from glucose. Hence, it is possible that the ADI pathway

was upregulated in the glucose treated cells to compensate for a faster lactate formation in the presence of this carbohydrate. However, this hypothesis cannot be proven by the available data and has to be examined in future experiments, as it is beyond the scope of the present work.
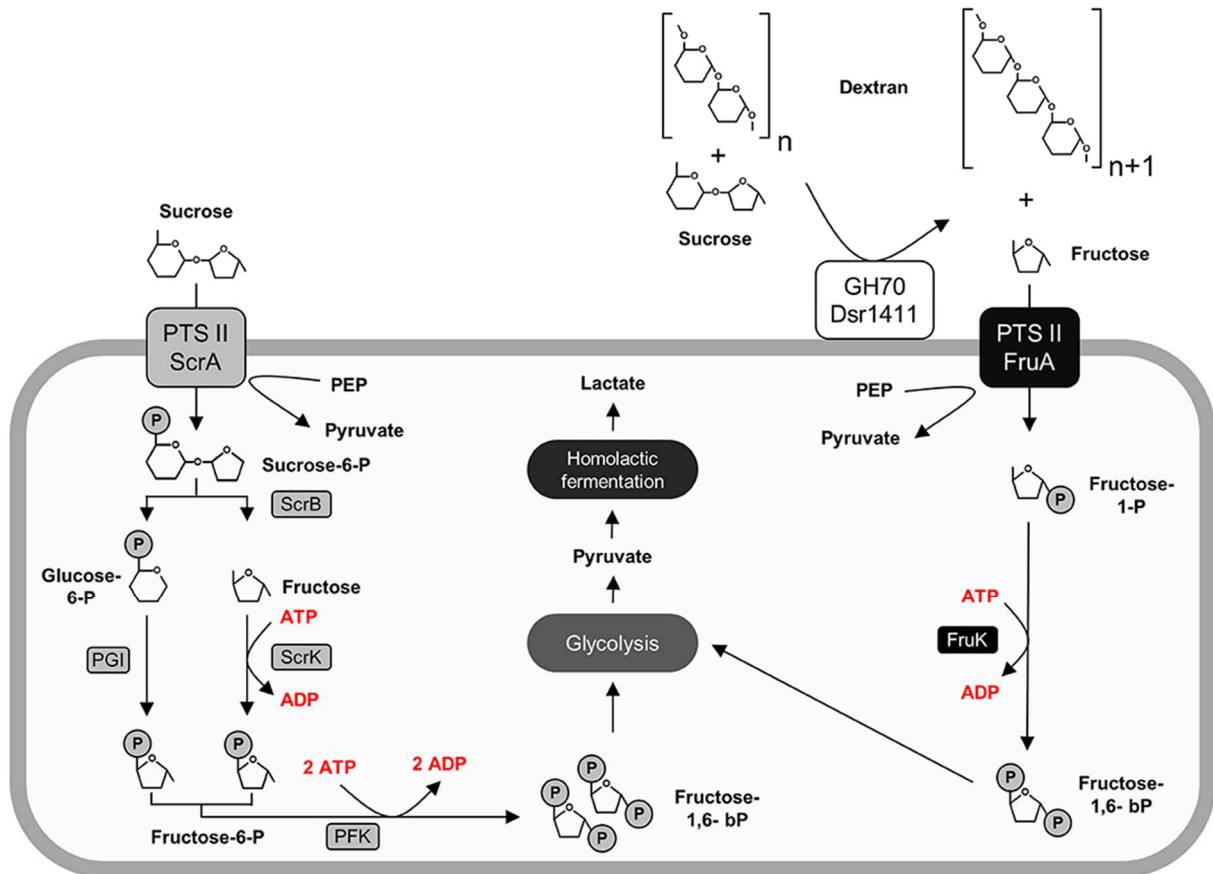

Figure 29: Active carbohydrate utilization pathways in *L. sakei* TMW 1.411 upon growth on sucrose as sole carbon source as suggested by the proteomic data (Figure 22) and metabolite analysis (Figure 24). Enzymes involved in the catabolism of sucrose (left) and fructose (right) are marked in grey and black, respectively. Protein names were used according to the gene names in Table 14. For clarity reasons, water molecules were omitted in the figure. Further abbreviations: Dsr1411 GH70: dextransucrase of *L. sakei* TMW 1.411, glycoside hydrolase 70 family; PEP: phosphoenolpyruvate; PTS II: phosphotransferase-system subunit II; PGI: phosphoglucose-isomerase; PFK: phosphofructokinase. This figure was published as Figure 6 in Prechtl et al. (2018a).

5.5. Sucrose metabolism of *L. sakei* TMW 1.411 during dextran synthesis

The evaluation of the proteomic data had revealed the upregulation of the fructose operon after 2 h of sucrose exposure, which suggested an utilization of this carbohydrate already at an early stage of growth (5.4). Monitoring of the fructose concentration during growth on sucrose containing mMRS medium confirmed this result, since fructose was detectable in the supernatant only after 9 h, whereas dextran formation and thus release of fructose had already started after 6 h of cultivation (Figure 24). If no fructose utilization had occurred, its concentration curve would have been expected to overlap with the dextran curve due to the stoichiometry of dextran synthesis. However, the concentrations of fructose were lower than the theoretically released amounts at any time. Furthermore, fructose seemed to be the only utilized carbohydrate after 10 h. Its depletion was observed after 24 h, suggesting its preferential use by *L. sakei* TMW 1.411 compared to sucrose, whose concentration was stagnating within this time period. Since the metabolic pathway for energy generation from fructose requires less enzymes to be translated than the one for sucrose (Figure 29), a preferential metabolization of fructose could indeed be energetically beneficial in that it reduces the metabolic burden. As a consequence, the constitutive production and secretion of dextransucrases might provide another advantage for a life in a sucrose-dominated environment, as it not only facilitates biofilm formation, but simultaneously provides a favorable carbon source. This is further confirmed by the results of Nàcher-Vàzquez et al., who reported an increased biomass if *L. sakei* MN1, which contained the plasmid pMN1 harboring an identical dextransucrase as *L. sakei* TMW 1.411, was cultivated in MRS containing sucrose instead of glucose (Nacher-Vazquez et al., 2017b).

The induction of the sucrose operon indicates that *L. sakei* TMW 1.411 can metabolize this carbon source intracellularly. However, solely the slight decrease of the sucrose concentration between 24 h and 48 h points towards an active utilization of sucrose after fructose depletion, as no significant increases in dextran amounts could be detected. It is thus difficult to infer the amount of intracellularly metabolized sucrose in the exponential or early stationary growth phase. Although the calculated dextran yield was only 60% compared to the consumed amount of sucrose, this might have been the result of the intrinsic hydrolysis activity of dextransucrases as well (van Hijum et al., 2006; Leemhuis et al., 2013). However, glucose was never detected throughout the cultivation, which was also observed for the dextran forming strain *L. sakei* MN1 upon growth on sucrose (Nacher-Vazquez et al., 2017a). Yet, it is most likely that any released glucose was immediately taken up into the cytoplasm and subsequently metabolized.

6. SUMMARY

The manufacturing of fermented foods dates back into prehistoric times and has given rise to a large variety of traditional products worldwide. The decisive role of microorganisms – mostly lactic acid bacteria (LAB) – for the production process, however, was only elucidated in the past century. Nowadays, starter culture preparations are systematically used in standardized industrial food fermentation processes to ensure the product's safety, taste and textural characteristics. Exopolysaccharides (EPS), which are formed by certain LAB strains, make an important contribution to these textural characteristics. Although EPS forming LAB strains are most exclusively used in the manufacturing of fermented dairy products, they might also be exploited to manufacture novel fermented meat products with improved properties. However, such meat starter cultures and their EPS have not yet been identified and investigated, respectively.

The screening of 77 LAB isolates for EPS formation yielded 23 strains, which were capable of EPS production. While twelve strains showed a sucrose-dependent glucan production, eleven strains formed putative heteropolysaccharide (HePS), which was confirmed by HPLC-RI analysis. In subsequent comparative growth experiments in a simulation medium for raw-fermented sausages, two potential candidate strains of the species *Lactobacillus plantarum* and *Lactobacillus sakei*, respectively, were identified, and their safety was ensured by means of an antibiotic susceptibility testing and a screening for biogenic amine formation.

Extensive structural analyses with HPAEC-PAD, AF4-MALS and various NMR techniques revealed the *L. plantarum* strain to produce a $\sim 2 \times 10^6$ Da HePS which was composed of a branched, acetylated heptameric repeating unit consisting of glucose, rhamnose and galactose. The associated genetic biosynthesis cluster was identified after whole genome sequencing and comparative genetic analyses, and the composition of the cluster supported the previously determined structure of the repeating unit.

The *L. sakei* strain produced a high molecular weight dextran with an average molecular weight of 1.8×10^8 Da according to AF4-MALS analysis, and dextran production at cold (10 °C) and salt stress (9.5%) conditions revealed that produced amounts and its macromolecular structure were strongly influenced by these parameters: While cold stress led to higher molecular weights, increased amounts and a reduced degree of branching, salt stress had a negative effect on both dextran synthesis and particle size, without changing the degree of branching. Comparable results regarding amounts and sizes were obtained when the dextrans were produced by resting cells in buffers under the same conditions, which

demonstrated that the stress conditions alone were sufficient to induce the observed structural changes. Furthermore, dextran synthesis by resting cells was even possible at a combination of both stress parameters, where bacterial growth was inhibited. Whole genome sequencing of the strain revealed the responsible dextransucrase gene to be encoded on a plasmid, which showed a high sequence homology to plasmids present in several other *L. sakei* and *L. curvatus* strains. By means of a label free quantitative proteomics approach, it could be demonstrated that the dextransucrase was constitutively expressed at a high level, irrespective of the present carbohydrate source.

Investigation of the physiological response of the *L. sakei* strain to sucrose as carbon source relative to glucose revealed 16 proteins to be significantly differentially expressed and enabled the prediction of the sucrose metabolism of the strain upon simultaneous dextran formation. Monitoring of dextran and metabolite formation, as well as carbohydrate utilization during growth on sucrose as sole carbon source confirmed the predicted pathways of sucrose metabolism and pointed to the preferential use of fructose, which was released during dextran synthesis.

7. ZUSAMMENFASSUNG

Die Herstellung von fermentierten Lebensmitteln reicht bis in vorgeschichtliche Zeiten zurück und hat weltweit zu einer großen Vielfalt traditioneller Lebensmittelprodukte geführt. Die entscheidende Rolle von Mikroorganismen - meist Milchsäurebakterien (LAB) - im Produktionsprozess wurde jedoch erst im vergangenen Jahrhundert aufgeklärt. Heutzutage werden Starterkulturpräparate gezielt in standardisierten industriellen Fermentations-prozessen eingesetzt, um die Sicherheit, den Geschmack und die strukturellen Eigenschaften der Lebensmittelprodukte zu gewährleisten. Exopolysaccharide (EPS), die von bestimmten Milchsäurebakterien gebildet werden, leisten einen wichtigen Beitrag zu diesen strukturellen Eigenschaften. Obwohl EPS-bildende Milchsäurebakterien-Stämme bisher fast ausschließlich zur Herstellung fermentierter Milchprodukte verwendet werden, könnten sie auch zur Herstellung neuartiger fermentierter Fleischprodukte mit verbesserten Eigenschaften genutzt werden. Solche Fleischstarterkulturen und ihre EPS wurden jedoch noch nicht identifiziert bzw. untersucht.

Durch ein Screening von 77 LAB-Isolaten auf EPS-Bildung konnten 23 EPS-bildende Stämme identifiziert werden. Während zwölf Stämme eine Saccharose-abhängige Glucan Produktion zeigten, bildeten elf Stämme mutmaßliche Heteropolysaccharide (HePS), was durch HPLC-RI-Analysen bestätigt wurde. In anschließenden vergleichenden Wachstumsexperimenten in Rohwurstsimulationsmedium wurden zwei potenzielle Kandidatenstämme der Art *Lactobacillus plantarum* bzw. *Lactobacillus sakei* identifiziert, deren Sicherheit durch eine Empfindlichkeitsprüfung gegenüber Antibiotika, sowie ein Screening auf die Bildung biogener Amine sichergestellt werden konnte.

Umfangreiche Strukturanalysen mittels HPAEC-PAD, AF4-MALS und verschiedenen NMR-Techniken zeigten, dass der *L. plantarum* Stamm ein HePS mit einer Größe von ~ 2×10^6 Da produzierte, das aus einer verzweigten, acetylierten, heptameren Wiederholungseinheit aus Glucose, Rhamnose und Galactose bestand. Das zugehörige genetische Biosynthesecluster wurde nach Genomsequenzierung und vergleichenden genetischen Analysen identifiziert, und dessen Zusammensetzung spiegelte die zuvor bestimmte Struktur der Wiederholungseinheit wider.

Der *L. sakei* Stamm bildete ein Dextran mit einem mittleren Molekulargewicht von $1{,}8 \times 10^8$ Da, und die Dextran-Produktion bei Kälte (10 °C) und Salz Stress (9,5% NaCl) zeigte, dass die produzierten Mengen und die makromolekulare Dextran-Struktur von diesen Parametern stark beeinflusst wurden: Während Kältestress zu höheren Molekulargewichten, erhöhter

Ausbeute und reduziertem Verzweigungsgrad führte, wirkte sich Salzstress negativ auf die Produktion und Größe der Dextrane aus, ohne den Verzweigungsgrad zu beeinflussen. Vergleichbare Ergebnisse hinsichtlich Ausbeute und Partikelgrößen der Dextrane wurden erhalten, wenn diese unter den gleichen Bedingungen von in Puffern resuspendierten Zellen produziert wurden, wodurch gezeigt wurde, dass die Stressparameter allein ausreichten, um die beobachteten strukturellen Veränderungen auszulösen. Darüber hinaus war die Dextransynthese durch resuspendierte Zellen sogar bei einer Kombination beider Stressparameter möglich, bei denen kein bakterielles Wachstum mehr möglich gewesen war. Die Genomsequenzierung des Stammes ergab, dass das verantwortliche Dextransucrase-Gen auf einem Plasmid kodiert ist, das eine hohe Sequenzhomologie mit Plasmiden einiger anderer *L. sakei* und *L. curvatus* Stämme besitzt. Mithilfe eines markierungsfreien, quantitativen Proteomik Ansatzes konnte außerdem gezeigt werden, dass die Dextransucrase unabhängig von der vorhandenen Kohlenhydratquelle konstitutiv und auf hohem Level exprimiert wurde.

Die Untersuchung der physiologischen Reaktion des *L. sakei*-Stamms auf Saccharose als Kohlenstoffquelle im Vergleich zu Glukose ergab, dass 16 Proteine signifikant differentiell exprimiert wurden und ermöglichte zudem die Vorhersage des Saccharose-Metabolismus des Stammes während der Dextran-Bildung. Das Monitoring von Dextran- und Metabolit-Bildung, sowie des Zuckerverbrauchs während des Wachstums auf Saccharose bestätigte die vorhergesagten Stoffwechselwege und wies auf die bevorzugte Verstoffwechselung von Fructose hin, die während der Dextransynthese freigesetzt wurde.

8. REFERENCES

Ahrne, E., Molzahn, L., Glatter, T., and Schmidt, A. (2013). Critical assessment of proteome-wide label-free absolute abundance estimation strategies. *Proteomics* 13(17)**,** 2567-2578. doi: 10.1002/pmic.201300135.

Arena, M.E., Saguir, F.M., and Manca de Nadra, M.C. (1999). Arginine dihydrolase pathway in Lactobacillus plantarum from orange. *International Journal of Food Microbiology* 47(3)**,** 203-209. doi: https://doi.org/10.1016/S0168-1605(99)00004-5.

Arskold, E., Svensson, M., Grage, H., Roos, S., Radstrom, P., and van Niel, E.W.J. (2007). Environmental influences on exopolysaccharide formation in Lactobacillus reuteri ATCC 55730. *International Journal of Food Microbiology* 116(1)**,** 159-167. doi: 10.1016/j.ijfoodmicro.2006.12.010.

Aziz, R.K., Bartels, D., Best, A.A., DeJongh, M., Disz, T., Edwards, R.A., et al. (2008). The RAST Server: rapid annotations using subsystems technology. *BMC Genomics* 9**,** 75. doi: 10.1186/1471-2164-9-75.

Badel, S., Bernardi, T., and Michaud, P. (2011). New perspectives for Lactobacilli exopolysaccharides. *Biotechnol Adv* 29(1)**,** 54-66. doi: 10.1016/j.biotechadv.2010.08.011.

Bover-Cid, S., and Holzapfel, W.H. (1999). Improved screening procedure for biogenic amine production by lactic acid bacteria. *Int J Food Microbiol* 53(1)**,** 33-41.

Buckenhüskes, H.J. (1993). Selection criteria for lactic acid bacteria to be used as starter cultures for various food commodities. *FEMS Microbiology Reviews* 12(1-3)**,** 253-271. doi: 10.1111/j.1574-6976.1993.tb00022.x.

Cerning, J. (1990). Exocellular polysaccharides produced by lactic acid bacteria. *FEMS Microbiology Letters* 87(1-2)**,** 113-130. doi: doi:10.1111/j.1574-6968.1990.tb04883.x.

Cerning, J., Bouillanne, C., Landon, M., and Desmazeaud, M. (1992). Isolation and Characterization of Exopolysaccharides from Slime-Forming Mesophilic Lactic Acid Bacteria. *Journal of Dairy Science* 75(3)**,** 692-699. doi: https://doi.org/10.3168/jds.S0022-0302(92)77805-9.

Chaillou, S., Champomier-Verges, M.C., Cornet, M., Crutz-Le Coq, A.M., Dudez, A.M., Martin, V., et al. (2005). The complete genome sequence of the meat-borne lactic acid bacterium Lactobacillus sakei 23K. *Nat Biotechnol* 23(12)**,** 1527-1533. doi: 10.1038/nbt1160.

Champomier-Verges, M.C., Chaillou, S., Cornet, M., and Zagorec, M. (2001). Lactobacillus sakei: recent developments and future prospects. *Res Microbiol* 152(10)**,** 839-848.

Chin, C.S., Alexander, D.H., Marks, P., Klammer, A.A., Drake, J., Heiner, C., et al. (2013). Nonhybrid, finished microbial genome assemblies from long-read SMRT sequencing data. *Nat Methods* 10(6)**,** 563-569. doi: 10.1038/nmeth.2474.

CLSI (2012). Performance Standards for Antimicrobial Susceptibility Testing; Twenty-Second Informational Supplement. *M100-S22* 32(3).

Cohen, R.E., and Ballou, C.E. (1981). "Mannoproteins: Structure," in *Plant Carbohydrates II: Extracellular Carbohydrates,* eds. W. Tanner & F.A. Loewus. (Berlin, Heidelberg: Springer Berlin Heidelberg), 441-458.

Cox, J., Neuhauser, N., Michalski, A., Scheltema, R.A., Olsen, J.V., and Mann, M. (2011). Andromeda: a peptide search engine integrated into the MaxQuant environment. *Journal of Proteome Research* 10(4)**,** 1794-1805.

Danielsen, M., and Wind, A. (2003). Susceptibility of Lactobacillus spp. to antimicrobial agents. *Int J Food Microbiol* 82(1)**,** 1-11.

De Vuyst, L., and Degeest, B. (1999). Heteropolysaccharides from lactic acid bacteria. *FEMS Microbiol Rev* 23(2)**,** 153-177.

De Vuyst, L., Vanderveken, F., Van de Ven, S., and Degeest, B. (1998). Production by and isolation of exopolysaccharides from Streptococcus thermophilus grown in a milk medium and evidence for their growth-associated biosynthesis. *Journal of Applied Microbiology* 84(6)**,** 1059-1068.

Degeest, B., and de Vuyst, L. (1999). Indication that the nitrogen source influences both amount and size of exopolysaccharides produced by Streptococcus thermophilus LY03 and modelling of the bacterial growth and exopolysaccharide production in a complex medium. *Applied and Environmental Microbiology* 65(7)**,** 2863-2870.

Degeest, B., Vaningelgem, F., and De Vuyst, L. (2001). Microbial physiology, fermentation kinetics, and process engineering of heteropolysaccharide production by lactic acid bacteria. *International Dairy Journal* 11(9)**,** 747-757. doi: Doi 10.1016/S0958-6946(01)00118-2.

Denapaite, D., Bruckner, R., Hakenbeck, R., and Vollmer, W. (2012). Biosynthesis of teichoic acids in Streptococcus pneumoniae and closely related species: lessons from genomes. *Microb Drug Resist* 18(3)**,** 344-358. doi: 10.1089/mdr.2012.0026.

Dent, J.G., and Sun, J.D. (1982). "Development of a Novel Method for Measuring Covalent Binding and Its Application to Investigations of Bromobenzene Hepatotoxicity," in *Biological Reactive Intermediates—II: Chemical Mechanisms and Biological Effects,* eds. R. Snyder, D.J. Jollow, D.V. Parke, C.G. Gibson, J.J. Kocsis, C.M. Witmer, B.N. Engelsberg, G.F. Kalf & S.L. Longacre. (Boston, MA: Springer US), 275-285.

Deutscher, J., Küster, E., Bergstedt, U., Charrier, V., and Hillen, W. (1995). Protein kinase-dependent HPr/CcpA interaction links glycolytic activity to carbon catabolite repression in Gram-positive bacteria. *Molecular Microbiology* 15(6)**,** 1049-1053. doi: doi:10.1111/j.1365-2958.1995.tb02280.x.

Dubois, M., Gilles, K.A., Hamilton, J.K., Rebers, P.A., and Smith, F. (1956). Colorimetric Method for Determination of Sugars and Related Substances. *Analytical Chemistry* 28(3)**,** 350-356. doi: DOI 10.1021/ac60111a017.

Eid, J., Fehr, A., Gray, J., Luong, K., Lyle, J., Otto, G., et al. (2009). Real-time DNA sequencing from single polymerase molecules. *Science* 323(5910)**,** 133-138. doi: 10.1126/science.1162986.

Feiner, G. (2006). *Meat Products Handbook.* Sawston, Cambridge: Woodhead Publishing.

Fels, L., Jakob, F., Vogel, R.F., and Wefers, D. (2018). Structural characterization of the exopolysaccharides from water kefir. *Carbohydr Polym* 189, 296-303. doi: 10.1016/j.carbpol.2018.02.037.

Fernandez, M., and Zuniga, M. (2006). Amino acid catabolic pathways of lactic acid bacteria. *Crit Rev Microbiol* 32(3), 155-183. doi: 10.1080/10408410600880643.

Fialho, A.M., Moreira, L.M., Granja, A.T., Popescu, A.O., Hoffmann, K., and Sa-Correia, I. (2008). Occurrence, production, and applications of gellan: current state and perspectives. *Appl Microbiol Biotechnol* 79(6), 889-900. doi: 10.1007/s00253-008-1496-0.

Fontana, C., Li, S., Yang, Z., and Widmalm, G. (2015). Structural studies of the exopolysaccharide from Lactobacillus plantarum C88 using NMR spectroscopy and the program CASPER. *Carbohydr Res* 402, 87-94. doi: 10.1016/j.carres.2014.09.003.

Franz, C.M.A.P., Cho, G.-S., Holzapfel, W.H., and Gálvez, A. (2010). "Safety of Lactic Acid Bacteria," in *Biotechnology of Lactic Acid Bacteria*. Wiley-Blackwell), 341-359.

Fraunhofer, M.E., Geissler, A.J., Wefers, D., Bunzel, M., Jakob, F., and Vogel, R.F. (2018). Characterization of beta-glucan formation by Lactobacillus brevis TMW 1.2112 isolated from slimy spoiled beer. *Int J Biol Macromol* 107(Pt A), 874-881. doi: 10.1016/j.ijbiomac.2017.09.063.

Freitas, F., A. V. Torres, C., and A. M. Reis, M. (2017). Engineering aspects of microbial exopolysaccharide production. *Bioresource Technology*. doi: 10.1016/j.biortech.2017.05.092.

Freitas, F., Alves, V.D., and Reis, M.A. (2011). Advances in bacterial exopolysaccharides: from production to biotechnological applications. *Trends Biotechnol* 29(8), 388-398. doi: 10.1016/j.tibtech.2011.03.008.

Gorke, B., and Stulke, J. (2008). Carbon catabolite repression in bacteria: many ways to make the most out of nutrients. *Nat Rev Microbiol* 6(8), 613-624. doi: 10.1038/nrmicro1932.

Gottlieb, H.E., Kotlyar, V., and Nudelman, A. (1997). NMR chemical shifts of common laboratory solvents as trace impurities. *Journal of Organic Chemistry* 62(21), 7512-7515. doi: DOI 10.1021/jo971176v.

Groot, M.N.N., and Kleerebezem, M. (2007). Mutational analysis of the Lactococcus lactis NIZO B40 exopolysaccharide (EPS) gene cluster: EPS biosynthesis correlates with unphosphorylated EpsB. *Journal of Applied Microbiology* 103(6), 2645-2656. doi: 10.1111/j.1365-2672.2007.03516.x.

Gueimonde, M., Sanchez, B., de los Reyes-Gavilan, C.G., and Margolles, A. (2013). Antibiotic resistance in probiotic bacteria. *Frontiers in Microbiology* 4. doi: 10.3389/fmicb.2013.00202.

Hamada, S., and Slade, H.D. (1980). Biology, immunology, and cariogenicity of Streptococcus mutans. *Microbiological reviews* 44(2), 331-384.

Han, Y.W. (1990). "Microbial Levan," in *Advances in Applied Microbiology Volume 35*.), 171-194.

Hébert, E.M., Raya, R.R., and Savoy de Giori, G. (2004). "Evaluation of Minimal Nutritional Requirements of Lactic Acid Bacteria Used in Functional Foods," in *Environmental Microbiology: Methods and Protocols,* eds. J.M. Walker, J.F.T. Spencer & A.L. Ragout de Spencer. (Totowa, NJ: Humana Press), 139-148.

Hilbig, J., Gisder, J., Prechtl, R.M., Herrmann, K., Weiss, J., and Loeffler, M. (2019). Influence of exopolysaccharide-producing lactic acid bacteria on the spreadability of fat-reduced raw fermented sausages (Teewurst). *Food Hydrocolloids* 93, 422-431. doi: https://doi.org/10.1016/j.foodhyd.2019.01.056.

Ismail, B., and Nampoothiri, K.M. (2010). Production, purification and structural characterization of an exopolysaccharide produced by a probiotic Lactobacillus plantarum MTCC 9510. *Archives of Microbiology* 192(12), 1049-1057. doi: DOI 10.1007/s00203-010-0636-y.

Ito, K., Ito, S., Shimamura, T., Weyand, S., Kawarasaki, Y., Misaka, T., et al. (2011). Crystal Structure of Glucansucrase from the Dental Caries Pathogen Streptococcus mutans. *Journal of Molecular Biology* 408(2), 177-186. doi: https://doi.org/10.1016/j.jmb.2011.02.028.

Jakob, F., Pfaff, A., Novoa-Carballal, R., Rubsam, H., Becker, T., and Vogel, R.F. (2013). Structural analysis of fructans produced by acetic acid bacteria reveals a relation to hydrocolloid function. *Carbohydrate Polymers* 92(2), 1234-1242. doi: 10.1016/j.carbpol.2012.10.054.

Jolly, L., and Stingele, F. (2001). Molecular organization and functionality of exopolysaccharide gene clusters in lactic acid bacteria. *International Dairy Journal* 11(9), 733-745. doi: http://dx.doi.org/10.1016/S0958-6946(01)00117-0.

Jolly, L., Vincent, S.J.F., Duboc, P., and Neeser, J.-R. (2002). Exploiting exopolysaccharides from lactic acid bacteria. *Antonie van Leeuwenhoek* 82(1), 367-374. doi: 10.1023/a:1020668523541.

Jürgen Cox, M.Y.H.e.a. (2014). Accurate Proteome-wide Label-free Quantification by Delayed Normalization and Maximal Peptide Ratio Extraction, Termed MaxLFQ. *Molecular & Cellular Proteomics* 13(9), 2513-2526. doi: 10.1074/.

Kafka, T.A., Geissler, A.J., and Vogel, R.F. (2017). Multiple Genome Sequences of Lactobacillus plantarum Strains. *Genome Announc* 5(29). doi: 10.1128/genomeA.00654-17.

Kahm, M., Hasenbrink, G., Lichtenberg-Frate, H., Ludwig, J., and Kschischo, M. (2010). grofit: Fitting Biological Growth Curves with R. *Journal of Statistical Software* 33(7), 1-21.

Katina, K., Maina, N.H., Juvonen, R., Flander, L., Johansson, L., Virkki, L., et al. (2009). In situ production and analysis of Weissella confusa dextran in wheat sourdough. *Food Microbiology* 26(7), 734-743. doi: 10.1016/j.fm.2009.07.008.

Kim, D., Robyt, J.F., Lee, S.-Y., Lee, J.-H., and Kim, Y.-M. (2003). Dextran molecular size and degree of branching as a function of sucrose concentration, pH, and temperature of reaction of Leuconostoc mesenteroides B-512FMCM dextransucrase. *Carbohydrate Research* 338(11), 1183-1189. doi: 10.1016/s0008-6215(03)00148-4.

Kimmel, S.A., and Roberts, R.F. (1998). Development of a growth medium suitable for exopolysaccharide production by Lactobacillus delbrueckii ssp. bulgaricus RR. *Int J Food Microbiol* 40(1-2), 87-92.

Klaenhammer, T.R., Barrangou, R., Buck, B.L., Azcarate-Peril, M.A., and Altermann, E. (2005). Genomic features of lactic acid bacteria effecting bioprocessing and health. *FEMS Microbiol Rev* 29(3), 393-409. doi: 10.1016/j.femsre.2005.04.007.

Korakli, M., Pavlovic, M., Gänzle, M.G., and Vogel, R.F. (2003). Exopolysaccharide and kestose production by Lactobacillus sanfranciscensis LTH2590. *Appl Environ Microbiol* 69(4), 2073-2079.

Lamothe, G.T., Jolly, L., Mollet, B., and Stingele, F. (2002). Genetic and biochemical characterization of exopolysaccharide biosynthesis by Lactobacillus delbrueckii subsp. bulgaricus. *Arch Microbiol* 178(3), 218-228. doi: 10.1007/s00203-002-0447-x.

Landmann, J.J., Busse, R.A., Latz, J.H., Singh, K.D., Stulke, J., and Gorke, B. (2011). Crh, the paralogue of the phosphocarrier protein HPr, controls the methylglyoxal bypass of glycolysis in Bacillus subtilis. *Mol Microbiol* 82(3), 770-787. doi: 10.1111/j.1365-2958.2011.07857.x.

Leathers, T.D., and Bischoff, K.M. (2011). Biofilm formation by strains of Leuconostoc citreum and L. mesenteroides. *Biotechnol Lett* 33(3), 517-523. doi: 10.1007/s10529-010-0450-2.

Leathers, T.D., and Cote, G.L. (2008). Biofilm formation by exopolysaccharide mutants of Leuconostoc mesenteroides strain NRRL B-1355. *Appl Microbiol Biotechnol* 78(6), 1025-1031. doi: 10.1007/s00253-008-1384-7.

Leemhuis, H., Pijning, T., Dobruchowska, J.M., van Leeuwen, S.S., Kralj, S., Dijkstra, B.W., et al. (2013). Glucansucrases: three-dimensional structures, reactions, mechanism, alpha-glucan analysis and their implications in biotechnology and food applications. *J Biotechnol* 163(2), 250-272. doi: 10.1016/j.jbiotec.2012.06.037.

Liu, X., Hu, Y., Pai, P.J., Chen, D., and Lam, H. (2014). Label-free quantitative proteomics analysis of antibiotic response in Staphylococcus aureus to oxacillin. *J Proteome Res* 13(3), 1223-1233. doi: 10.1021/pr400669d.

Looijesteijn, P.J., and Hugenholtz, J. (1999). Uncoupling of growth and exopolysaccharide production by Lactococcus lactis subsp. cremoris NIZO B40 and optimization of its synthesis. *Journal of Bioscience and Bioengineering* 88(2), 178-182. doi: http://dx.doi.org/10.1016/S1389-1723(99)80198-4.

Lovett, S.T., Drapkin, P.T., Sutera, V.A., Jr., and Gluckman-Peskind, T.J. (1993). A sister-strand exchange mechanism for recA-independent deletion of repeated DNA sequences in Escherichia coli. *Genetics* 135(3), 631-642.

Maina, N.H., Virkki, L., Pynnonen, H., Maaheirno, H., and Tenkanen, M. (2011). Structural Analysis of Enzyme-Resistant Isomaltooligosaccharides Reveals the Elongation of alpha-(1 -> 3)-Linked Branches in Weissella confusa Dextran. *Biomacromolecules* 12(2), 409-418. doi: 10.1021/bm1011536.

Marshall, V.M., Cowie, E.N., and Moreton, R.S. (1995). Analysis and Production of 2 Exopolysaccharides from Lactococcus-Lactis Subsp Cremoris Lc330. *Journal of Dairy Research* 62(4), 621-628. doi: Doi 10.1017/S0022029900031356.

McLeod, A., Snipen, L., Naterstad, K., and Axelsson, L. (2011). Global transcriptome response in Lactobacillus sakei during growth on ribose. *BMC Microbiol* 11**,** 145. doi: 10.1186/1471-2180-11-145.

Mende, S., Peter, M., Bartels, K., Rohm, H., and Jaros, D. (2013). Addition of purified exopolysaccharide isolates from S. thermophilus to milk and their impact on the rheology of acid gels. *Food Hydrocolloids* 32(1)**,** 178-185. doi: 10.1016/j.foodhyd.2012.12.011.

Miao, M., Huang, C., Jia, X., Cui, S.W., Jiang, B., and Zhang, T. (2015). Physicochemical characteristics of a high molecular weight bioengineered α-D-glucan from Leuconostoc citreum SK24.002. *Food Hydrocolloids* 50**,** 37-43. doi: https://doi.org/10.1016/j.foodhyd.2015.04.009.

Moller, M.S., Fredslund, F., Majumder, A., Nakai, H., Poulsen, J.C., Lo Leggio, L., et al. (2012). Enzymology and structure of the GH13_31 glucan 1,6-alpha-glucosidase that confers isomaltooligosaccharide utilization in the probiotic Lactobacillus acidophilus NCFM. *J Bacteriol* 194(16)**,** 4249-4259. doi: 10.1128/JB.00622-12.

Monsan, P., Bozonnet, S., Albenne, C., Joucla, G., Willemot, R.-M., and Remaud-Siméon, M. (2001). Homopolysaccharides from lactic acid bacteria. *International Dairy Journal* 11(9)**,** 675-685. doi: 10.1016/s0958-6946(01)00113-3.

Montel, M.C., and Champomier, M.C. (1987). Arginine catabolism in Lactobacillus sake isolated from meat. *Applied and Environmental Microbiology* 53(11)**,** 2683-2685.

Mozzi, F., Vaningelgem, F., Hebert, E.M., Van der Meulen, R., Foulquie Moreno, M.R., Font de Valdez, G., et al. (2006). Diversity of heteropolysaccharide-producing lactic acid bacterium strains and their biopolymers. *Appl Environ Microbiol* 72(6)**,** 4431-4435. doi: 10.1128/AEM.02780-05.

Nacher-Vazquez, M., Iturria, I., Zarour, K., Mohedano, M.L., Aznar, R., Pardo, M.A., et al. (2017a). Dextran production by Lactobacillus sakei MN1 coincides with reduced autoagglutination, biofilm formation and epithelial cell adhesion. *Carbohydr Polym* 168**,** 22-31. doi: 10.1016/j.carbpol.2017.03.024.

Nacher-Vazquez, M., Ruiz-Maso, J.A., Mohedano, M.L., Del Solar, G., Aznar, R., and Lopez, P. (2017b). Dextransucrase Expression Is Concomitant with that of Replication and Maintenance Functions of the pMN1 Plasmid in Lactobacillus sakei MN1. *Front Microbiol* 8**,** 2281. doi: 10.3389/fmicb.2017.02281.

Nunes, F.M., Reis, A., Silva, A.M., Domingues, M.R., and Coimbra, M.A. (2008). Rhamnoarabinosyl and rhamnoarabinoarabinosyl side chains as structural features of coffee arabinogalactans. *Phytochemistry* 69(7)**,** 1573-1585. doi: 10.1016/j.phytochem.2008.01.021.

Peant, B., LaPointe, G., Gilbert, C., Atlan, D., Ward, P., and Roy, D. (2005). Comparative analysis of the exopolysaccharide biosynthesis gene clusters from four strains of Lactobacillus rhamnosus. *Microbiology* 151(Pt 6)**,** 1839-1851. doi: 10.1099/mic.0.27852-0.

Perry, D.B., McMahon, D.J., and Oberg, C.J. (1997). Effect of exopolysaccharide-producing cultures on moisture retention in low fat mozzarella cheese. *Journal of Dairy Science* 80(5)**,** 799-805. doi: DOI 10.3168/jds.S0022-0302(97)76000-4.

Petersen, T.N., Brunak, S., von Heijne, G., and Nielsen, H. (2011). SignalP 4.0: discriminating signal peptides from transmembrane regions. *Nat Methods* 8(10), 785-786. doi: 10.1038/nmeth.1701.

Pham, P.L., Dupont, I., Roy, D., Lapointe, G., and Cerning, J. (2000). Production of exopolysaccharide by Lactobacillus rhamnosus R and analysis of its enzymatic degradation during prolonged fermentation. *Appl Environ Microbiol* 66(6), 2302-2310.

Polak-Berecka, M., Wasko, A., and Kubik-Komar, A. (2014). Optimization of Culture Conditions for Exopolysaccharide Production by a Probiotic Strain of Lactobacillus rhamnosus E/N. *Polish Journal of Microbiology* 63(2), 253-257.

Prechtl, R.M., Janssen, D., Behr, J., Ludwig, C., Küster, B., Vogel, R., et al. (2018a). Sucrose-induced proteomic response and carbohydrate utilization of Lactobacillus sakei TMW 1.411 during dextran formation. *Frontiers in Microbiology* 9, 2796. doi: 10.3389/fmicb.2018.02796.

Prechtl, R.M., Wefers, D., Jakob, F., and Vogel, R.F. (2018b). Cold and salt stress modulate amount, molecular and macromolecular structure of a Lactobacillus sakei dextran. *Food Hydrocolloids.* doi: 10.1016/j.foodhyd.2018.04.003.

Prechtl, R.M., Wefers, D., Jakob, F., and Vogel, R.F. (2018c). Structural characterization of the surface-associated heteropolysaccharide of Lactobacillus plantarum TMW 1.1478 and genetic analysis of its putative biosynthesis cluster. *Carbohydrate Polymers* 202, 236-245. doi: 10.1016/j.carbpol.2018.08.115.

R Development Core Team (2010). "R: A language and environment for statistical computing". (Vienna, Austria: R Foundation for Statistical Computing).

Remus, D.M., van Kranenburg, R., van, S., II, Taverne, N., Bongers, R.S., Wels, M., et al. (2012). Impact of 4 Lactobacillus plantarum capsular polysaccharide clusters on surface glycan composition and host cell signaling. *Microb Cell Fact* 11, 149. doi: 10.1186/1475-2859-11-149.

Rimaux, T., Riviere, A., Illeghems, K., Weckx, S., De Vuyst, L., and Leroy, F. (2012). Expression of the arginine deiminase pathway genes in Lactobacillus sakei is strain dependent and is affected by the environmental pH. *Appl Environ Microbiol* 78(14), 4874-4883. doi: 10.1128/AEM.07724-11.

Rimaux, T., Vrancken, G., Pothakos, V., Maes, D., De Vuyst, L., and Leroy, F. (2011). The kinetics of the arginine deiminase pathway in the meat starter culture Lactobacillus sakei CTC 494 are pH-dependent. *Food Microbiol* 28(3), 597-604. doi: 10.1016/j.fm.2010.11.016.

RStudio Team (2016). "RStudio: Integrated Development for R". (Boston, MA: RStudio, Inc.).

Ruas-Madiedo, P., Hugenholtz, J., and Zoon, P. (2002). An overview of the functionality of exopolysaccharides produced by lactic acid bacteria. *International Dairy Journal* 12(2-3), 163-171. doi: 10.1016/S0958-6946(01)00160-1.

Rühmkorf, C. (2012). *Molecular background, in situ production and structure/function relation of bacterial exopolysaccharides in gluten-free dough and bread.* Doctoral Thesis, TU Munich.

Rühmkorf, C., Bork, C., Mischnick, P., Rübsam, H., Becker, T., and Vogel, R.F. (2013). Identification of Lactobacillus curvatus TMW 1.624 dextransucrase and comparative characterization with Lactobacillus reuteri TMW 1.106 and Lactobacillus animalis TMW 1.971 dextransucrases. *Food Microbiol* 34(1)**,** 52-61. doi: 10.1016/j.fm.2012.11.002.

Rühmkorf, C., Rübsam, H., Becker, T., Bork, C., Voiges, K., Mischnick, P., et al. (2012). Effect of structurally different microbial homoexopolysaccharides on the quality of gluten-free bread. *European Food Research and Technology* 235(1)**,** 139-146. doi: 10.1007/s00217-012-1746-3.

Ryan, P.M., Ross, R.P., Fitzgerald, G.F., Caplice, N.M., and Stanton, C. (2015). Sugar-coated: exopolysaccharide producing lactic acid bacteria for food and human health applications. *Food Funct* 6(3)**,** 679-693. doi: 10.1039/c4fo00529e.

Saulnier, D.M., Molenaar, D., de Vos, W.M., Gibson, G.R., and Kolida, S. (2007). Identification of prebiotic fructooligosaccharide metabolism in Lactobacillus plantarum WCFS1 through microarrays. *Appl Environ Microbiol* 73(6)**,** 1753-1765. doi: 10.1128/AEM.01151-06.

Schellhaass, S., and Morris, H. (1985). Rheological and scanning electron microscopic examination of skim milk gels obtained by fermenting with ropy and non-ropy strains of lactic acid bacteria. *Food Structure* 4(2)**,** 11.

Schmid, J., Sieber, V., and Rehm, B. (2015). Bacterial exopolysaccharides: biosynthesis pathways and engineering strategies. *Frontiers in Microbiology* 6. doi: ARTN 496

10.3389/fmicb.2015.00496.

Schott, A.S., Behr, J., Geissler, A.J., Kuster, B., Hahne, H., and Vogel, R.F. (2017). Quantitative Proteomics for the Comprehensive Analysis of Stress Responses of Lactobacillus paracasei subsp. paracasei F19. *J Proteome Res* 16(10)**,** 3816-3829. doi: 10.1021/acs.jproteome.7b00474.

Schwab, C., and Gänzle, M.G. (2006). Effect of membrane lateral pressure on the expression of fructosyltransferases in Lactobacillus reuteri. *Syst Appl Microbiol* 29(2)**,** 89-99. doi: 10.1016/j.syapm.2005.09.005.

Schwanhausser, B., Busse, D., Li, N., Dittmar, G., Schuchhardt, J., Wolf, J., et al. (2011). Global quantification of mammalian gene expression control. *Nature* 473(7347)**,** 337-342. doi: 10.1038/nature10098.

Shamala, T.R., and Prasad, M.S. (1995). Preliminary Studies on the Production of High and Low Viscosity Dextran by Leuconostoc spp. *Process Biochemistry* 30(3)**,** 237-241.

Stingele, F., Neeser, J.R., and Mollet, B. (1996). Identification and characterization of the eps (Exopolysaccharide) gene cluster from Streptococcus thermophilus Sfi6. *J Bacteriol* 178(6)**,** 1680-1690.

Stingele, F., Vincent, S.J., Faber, E.J., Newell, J.W., Kamerling, J.P., and Neeser, J.R. (1999). Introduction of the exopolysaccharide gene cluster from Streptococcus thermophilus Sfi6 into Lactococcus lactis MG1363: production and characterization of an altered polysaccharide. *Mol Microbiol* 32(6)**,** 1287-1295.

Stolz, P., Bocker, G., Hammes, W.P., and Vogel, R.F. (1995). Utilization of Electron-Acceptors by Lactobacilli Isolated from Sourdough. *Zeitschrift Fur Lebensmittel-Untersuchung Und-Forschung* 201(1), 91-96. doi: Doi 10.1007/Bf01193208.

Sutherland, I.W. (1979). Microbial exopolysaccharides. *Trends in Biochemical Sciences* 4(3), 55-59. doi: https://doi.org/10.1016/0968-0004(79)90262-7.

Sweet, D.P., Shapiro, R.H., and Albersheim, P. (1975). Quantitative analysis by various g.l.c. response-factor theories for partially methylated and partially ethylated alditol acetates. *Carbohydrate Research* 40(2), 217-225. doi: https://doi.org/10.1016/S0008-6215(00)82604-X.

Tatusova, T., DiCuccio, M., Badretdin, A., Chetvernin, V., Nawrocki, E.P., Zaslavsky, L., et al. (2016). NCBI prokaryotic genome annotation pipeline. *Nucleic Acids Res* 44(14), 6614-6624. doi: 10.1093/nar/gkw569.

Tieking, M., Ehrmann, M.A., Vogel, R.F., and Gänzle, M.G. (2005). Molecular and functional characterization of a levansucrase from the sourdough isolate Lactobacillus sanfranciscensis TMW 1.392. *Appl Microbiol Biotechnol* 66(6), 655-663. doi: 10.1007/s00253-004-1773-5.

Tieking, M., Korakli, M., Ehrmann, M.A., Gänzle, M.G., and Vogel, R.F. (2003). In situ production of exopolysaccharides during sourdough fermentation by cereal and intestinal isolates of lactic acid bacteria. *Applied and Environmental Microbiology* 69(2), 945-952. doi: 10.1128/Aem.69.2.945-952.2003.

Torino, M.I., Font de Valdez, G., and Mozzi, F. (2015). Biopolymers from lactic acid bacteria. Novel applications in foods and beverages. *Front Microbiol* 6, 834. doi: 10.3389/fmicb.2015.00834.

Tozzi, M.G., Camici, M., Mascia, L., Sgarrella, F., and Ipata, P.L. (2006). Pentose phosphates in nucleoside interconversion and catabolism. *FEBS J* 273(6), 1089-1101. doi: 10.1111/j.1742-4658.2006.05155.x.

Tyanova, S., Temu, T., Sinitcyn, P., Carlson, A., Hein, M.Y., Geiger, T., et al. (2016). The Perseus computational platform for comprehensive analysis of (prote)omics data. *Nat Methods* 13(9), 731-740. doi: 10.1038/nmeth.3901.

Ua-Arak, T., Jakob, F., and Vogel, R.F. (2016). Characterization of growth and exopolysaccharide production of selected acetic acid bacteria in buckwheat sourdoughs. *Int J Food Microbiol* 239, 103-112. doi: 10.1016/j.ijfoodmicro.2016.04.009.

Ua-Arak, T., Jakob, F., and Vogel, R.F. (2017a). Fermentation pH Modulates the Size Distributions and Functional Properties of Gluconobacter albidus TMW 2.1191 Levan. *Frontiers in Microbiology* 8. doi: 10.3389/fmicb.2017.00807.

Ua-Arak, T., Jakob, F., and Vogel, R.F. (2017b). Influence of levan-producing acetic acid bacteria on buckwheat-sourdough breads. *Food Microbiology* 65, 95-104. doi: 10.1016/j.fm.2017.02.002.

Usbeck, J.C., Kern, C.C., Vogel, R.F., and Behr, J. (2013). Optimization of experimental and modelling parameters for the differentiation of beverage spoiling yeasts by Matrix-Assisted-Laser-Desorption/Ionization–Time-of-Flight Mass Spectrometry (MALDI–

TOF MS) in response to varying growth conditions. *Food Microbiology* 36(2)**,** 379-387. doi: https://doi.org/10.1016/j.fm.2013.07.004.

Van Calsteren, M.R., Pau-Roblot, C., Begin, A., and Roy, D. (2002). Structure determination of the exopolysaccharide produced by Lactobacillus rhamnosus strains RW-9595M and R. *Biochem J* 363(Pt 1)**,** 7-17.

van Geel-Schutten, G.H., Faber, E.J., Smit, E., Bonting, K., Smith, M.R., Ten Brink, B., et al. (1999). Biochemical and structural characterization of the glucan and fructan exopolysaccharides synthesized by the Lactobacillus reuteri wild-type strain and by mutant strains. *Applied and Environmental Microbiology* 65(7)**,** 3008-3014.

van Geel-Schutten, G.H., Flesch, F., ten Brink, B., Smith, M.R., and Dijkhuizen, L. (1998). Screening and characterization of Lactobacillus strains producing large amounts of exopolysaccharides. *Applied Microbiology and Biotechnology* 50(6)**,** 697-703. doi: 10.1007/s002530051353.

van Hijum, S.A., Kralj, S., Ozimek, L.K., Dijkhuizen, L., and van Geel-Schutten, I.G. (2006). Structure-function relationships of glucansucrase and fructansucrase enzymes from lactic acid bacteria. *Microbiol Mol Biol Rev* 70(1)**,** 157-176. doi: 10.1128/MMBR.70.1.157-176.2006.

van Kranenburg, R., Marugg, J.D., van, S., II, Willem, N.J., and de Vos, W.M. (1997). Molecular characterization of the plasmid-encoded eps gene cluster essential for exopolysaccharide biosynthesis in Lactococcus lactis. *Mol Microbiol* 24(2)**,** 387-397.

Vandenberg, D.J.C., Robijn, G.W., Janssen, A.C., Giuseppin, M.L.F., Vreeker, R., Kamerling, J.P., et al. (1995). Production of a Novel Extracellular Polysaccharide by Lactobacillus-Sake 0-1 and Characterization of the Polysaccharide. *Applied and Environmental Microbiology* 61(8)**,** 2840-2844.

Vignolo, G.M., Fontana, C., and Cocconcelli, P.S. (2010). "New Approaches for the Study of Lactic Acid Bacteria Biodiversity: A Focus on Meat Ecosystems," in *Biotechnology of Lactic Acid Bacteria*. Wiley-Blackwell), 251-271.

Vujicic-Zagar, A., Pijning, T., Kralj, S., Lopez, C.A., Eeuwema, W., Dijkhuizen, L., et al. (2010). Crystal structure of a 117 kDa glucansucrase fragment provides insight into evolution and product specificity of GH70 enzymes. *Proc Natl Acad Sci U S A* 107(50)**,** 21406-21411. doi: 10.1073/pnas.1007531107.

Walter, J., Schwab, C., Loach, D.M., Gänzle, M.G., and Tannock, G.W. (2008). Glucosyltransferase A (GtfA) and inulosucrase (Inu) of Lactobacillus reuteri TMW1.106 contribute to cell aggregation, in vitro biofilm formation, and colonization of the mouse gastrointestinal tract. *Microbiology* 154(Pt 1)**,** 72-80. doi: 10.1099/mic.0.2007/010637-0.

Xu, D., Fels, L., Wefers, D., Behr, J., Jakob, F., and Vogel, R.F. (2018). Lactobacillus hordei dextrans induce Saccharomyces cerevisiae aggregation and network formation on hydrophilic surfaces. *Int J Biol Macromol* 115**,** 236-242. doi: 10.1016/j.ijbiomac.2018.04.068.

Xu, Y., Coda, R., Shi, Q., Tuomainen, P., Katina, K., and Tenkanen, M. (2017). Exopolysaccharides Production during the Fermentation of Soybean and Fava Bean Flours by Leuconostoc mesenteroides DSM 20343. *Journal of Agricultural and Food Chemistry* 65(13)**,** 2805-2815. doi: 10.1021/acs.jafc.6b05495.

Yother, J. (2011). Capsules of Streptococcus pneumoniae and other bacteria: paradigms for polysaccharide biosynthesis and regulation. *Annu Rev Microbiol* 65**,** 563-581. doi: 10.1146/annurev.micro.62.081307.162944.

Zannini, E., Waters, D.M., Coffey, A., and Arendt, E.K. (2016). Production, properties, and industrial food application of lactic acid bacteria-derived exopolysaccharides. *Appl Microbiol Biotechnol* 100(3)**,** 1121-1135. doi: 10.1007/s00253-015-7172-2.

Zarour, K., Llamas, M.G., Prieto, A., Ruas-Madiedo, P., Duenas, M.T., de Palencia, P.F., et al. (2017). Rheology and bioactivity of high molecular weight dextrans synthesised by lactic acid bacteria. *Carbohydr Polym* 174**,** 646-657. doi: 10.1016/j.carbpol.2017.06.113.

Zeidan, A.A., Poulsen, V.K., Janzen, T., Buldo, P., Derkx, P.M.F., Oregaard, G., et al. (2017). Polysaccharide production by lactic acid bacteria: from genes to industrial applications. *FEMS Microbiol Rev* 41(Supp_1)**,** S168-S200. doi: 10.1093/femsre/fux017.

Zhu, M., Ajdić, D., Liu, Y., Lynch, D., Merritt, J., and Banas, J.A. (2009). Role of the Streptococcus mutans irvA Gene in GbpC-Independent, Dextran-Dependent Aggregation and Biofilm Formation. *Applied and Environmental Microbiology* 75(22)**,** 7037-7043. doi: 10.1128/AEM.01015-09.

Zúñiga, M., Champomier-Verges, M., Zagorec, M., and Pérez-Martínez, G. (1998). Structural and Functional Analysis of the Gene Cluster Encoding the Enzymes of the Arginine Deiminase Pathway of Lactobacillus sake. *Journal of Bacteriology* 180(16)**,** 4154-4159.
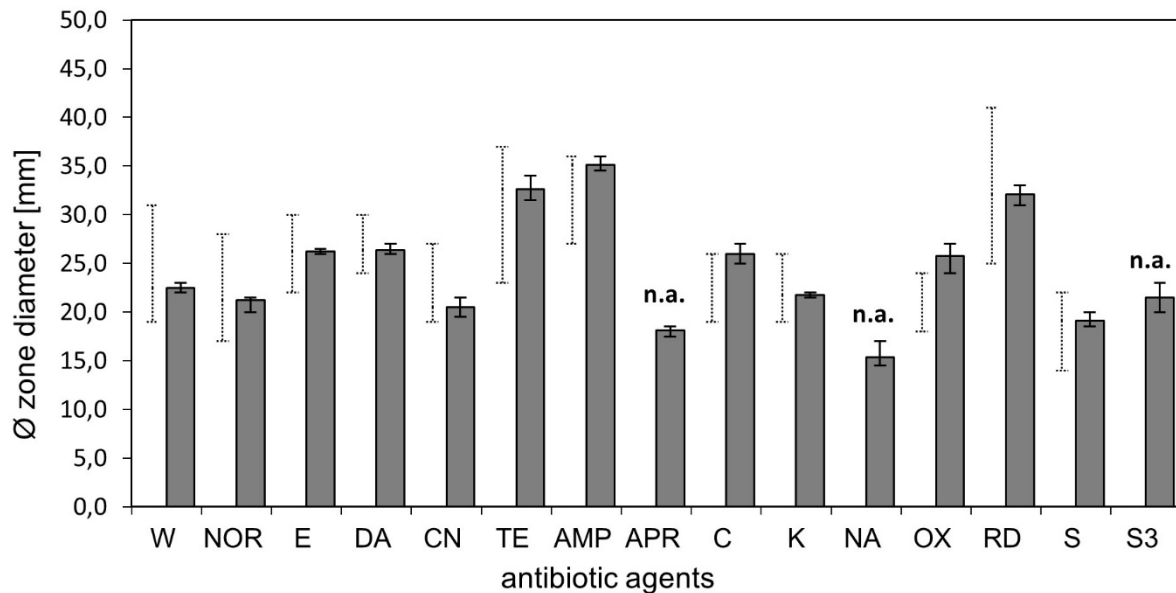
9. APPENDIX

9.1. Figures

Figure A 1: Inhibition zone diameters of the control strain *Staphylococcus aureus* ATCC 52923 and control ranges (dashed lines) for 15 antibiotics according to the CLSI M100-S22 document (2012). The control ranges are depicted as the interval of minimum and maximum reported values, respectively. The error bars indicate standard deviations calculated from duplicates of two biological replicates. Abbreviations: W, Trimethoprim; NOR, Norfloxacin; E, Erythromycin; DA, Clindamycin; CN, Gentamycin; TE, Tetracycline; AMP, ampicillin; APR, Apramycin; C, Chloramphenicol; K, Kanamycin; NA, Nalidixic acid; OX, Oxacillin; RD, Rifampicin; S, Streptomycin; S3, Sulfonamide; n.a., not available.
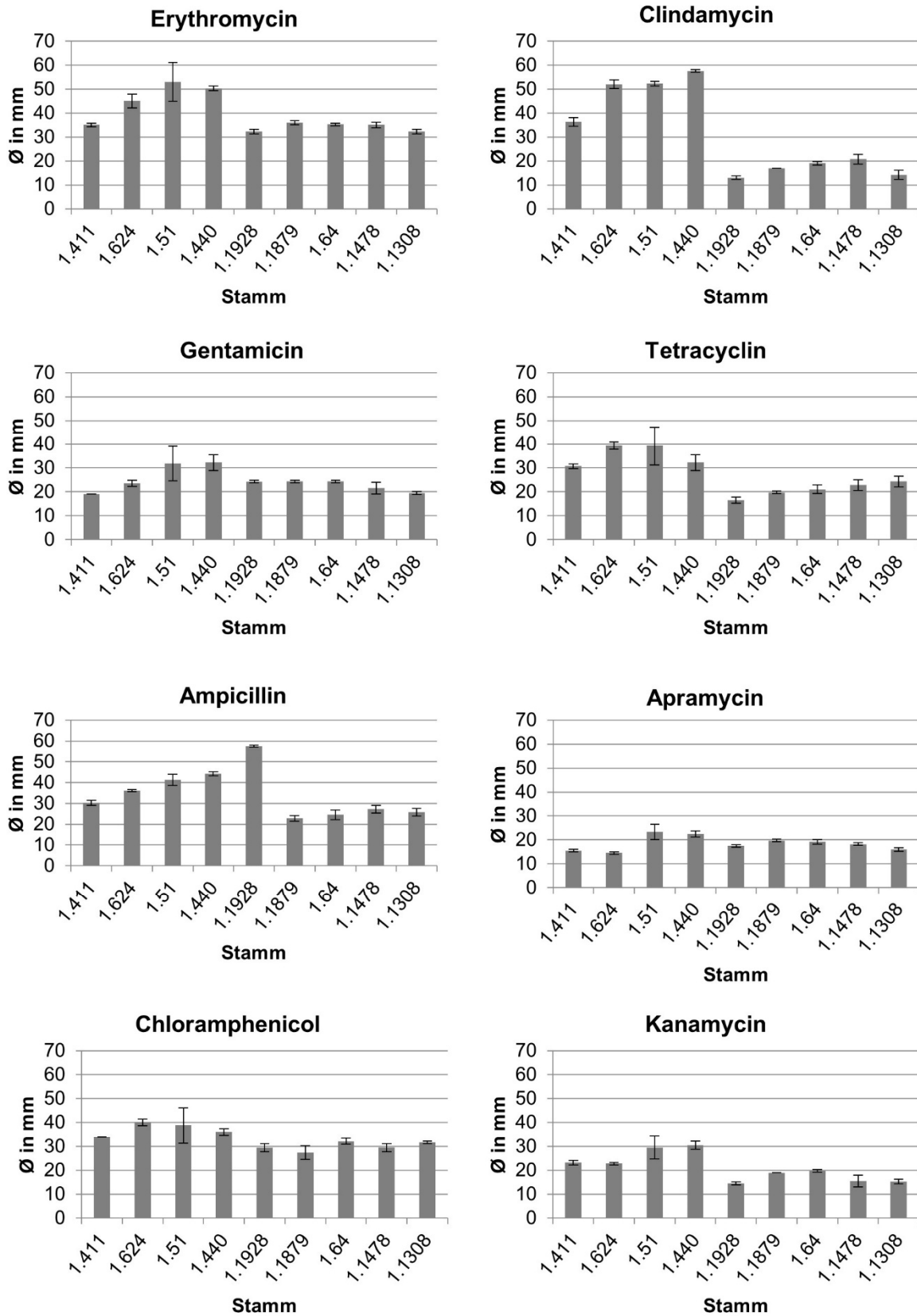
Figure A 2 Inhibition zone diameters of antibiotic agents for the nine selected LAB strains. The error bars indicate standard deviations calculated from duplicates of two biological replicates. Species: *L. sakei* **(TMW 1.411);** *L. curvatus* **(TMW 1.440, 1.624, 1.51, 1.1928);** *L. plantarum* **(TMW 1.1308, 1.1478, 1.1879, 1.64).**
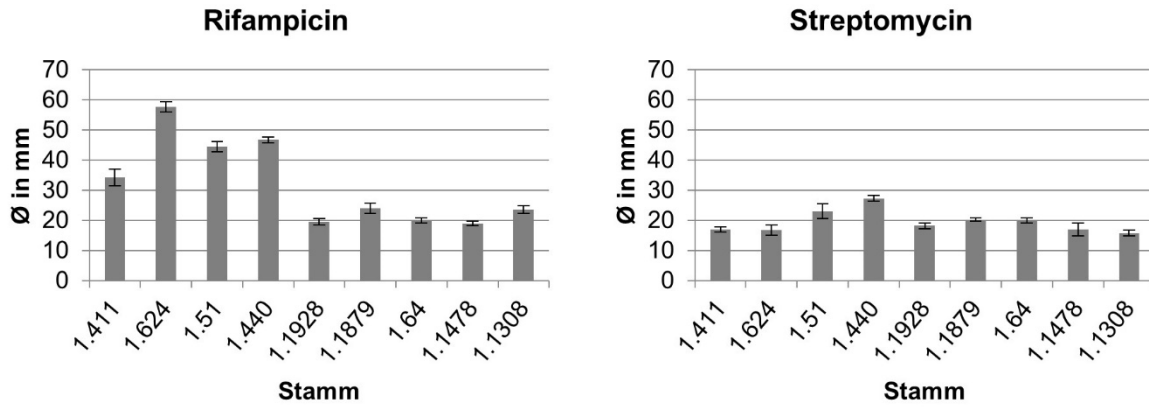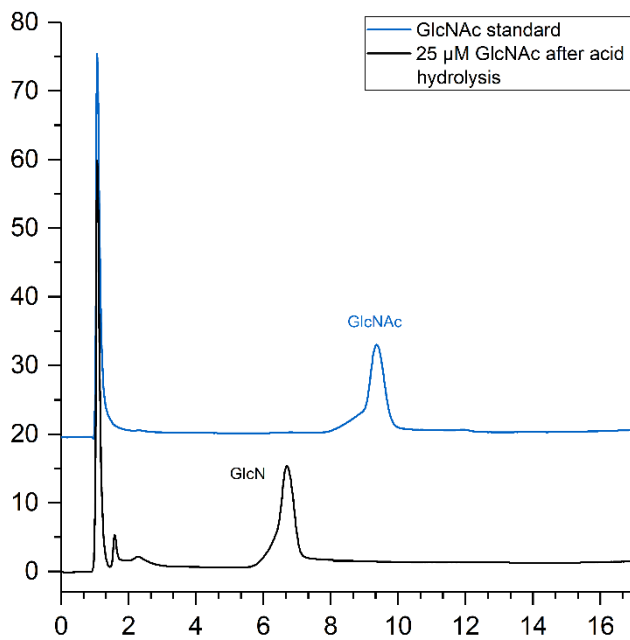
Figure A 3 Inhibition zone diameters of antibiotic agents for the nine selected LAB strains (continued). The error bars indicate standard deviations calculated from duplicates of two biological replicates. Species: *L. sakei* (TMW 1.411); *L. curvatus* (TMW 1.440, 1.624, 1.51, 1.1928); *L. plantarum* (TMW 1.1308, 1.1478, 1.1879, 1.64).

Figure A 4 HPAEC-PAD chromatograms of a GlcNAc standard solution (100 µM, blue line) and a GlcNAc solution which had been subjected to acid hydrolysis (25 µM, black line). This figure was published as Fig. S2 in Prechtl et al. (2018c).
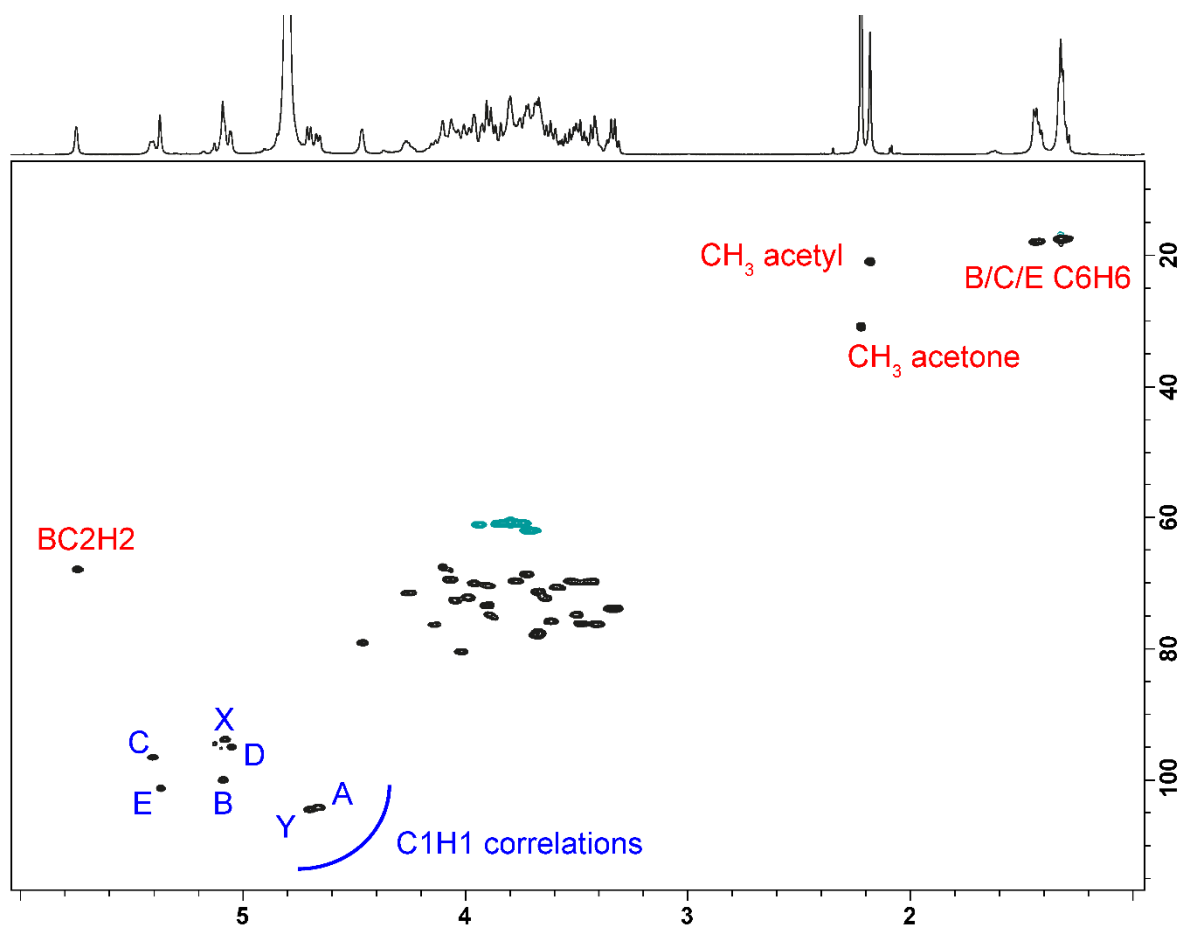
Figure A 5 HSQC spectrum of the HePS produced by *L. plantarum* TMW 1.1478 after 72 h at 20 °C. The nature of the spin systems is indicated in Table A 2 and Figure A 6. Further assignments can be found in Figure A 7. This figure was created by Dr. Daniel Wefers and published as Fig. 3 in Prechtl et al. (2018c).
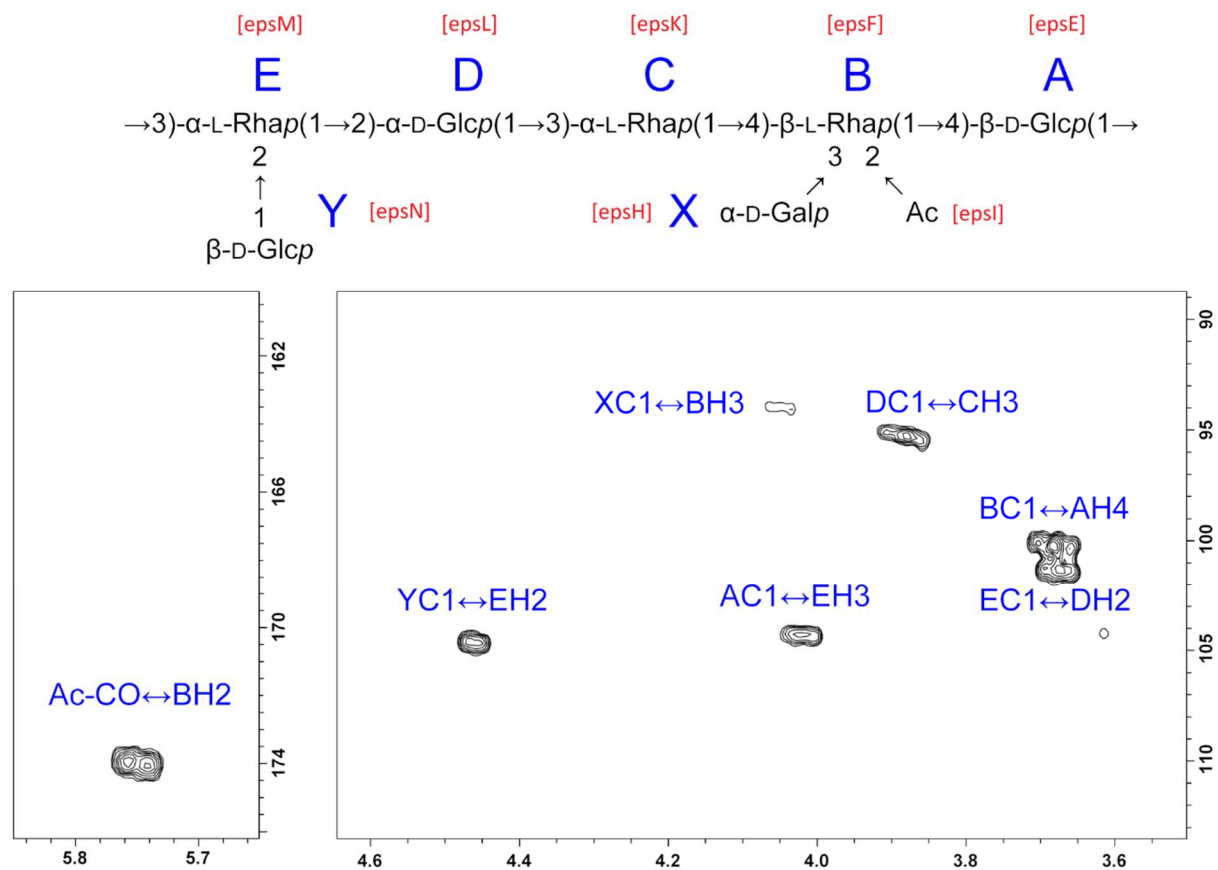
Figure A 6 Diagnostic signals in the HMBC spectrum and proposed structure of the repeating unit of the HePS produced by *L. plantarum* TMW 1.1478. The start of the repeating unit (descriptor A) was derived from genetic cluster analysis, and the suggested enzymes responsible for the transfer of the particular units are indicated in red according to Table 11. This figure was created by Dr. Daniel Wefers and published as Fig. 4 in Prechtl et al. (2018c).
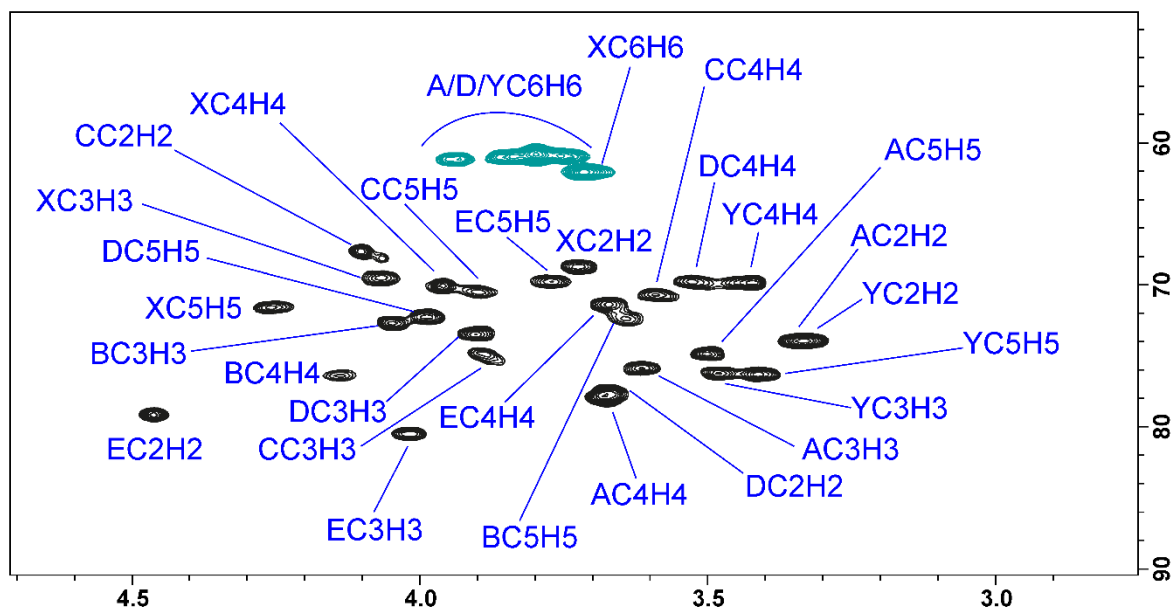
Figure A 7 HSQC spectrum of the HePS produced by *L. plantarum* TMW 1.1478 after 72 h at 20°C with the assignments of the ring protons. The nature of the spin systems is indicated in Table A 2 and Figure A 6. This figure was created by Dr. Daniel Wefers and published as Fig. S4 in Prechtl et al. (2018c).
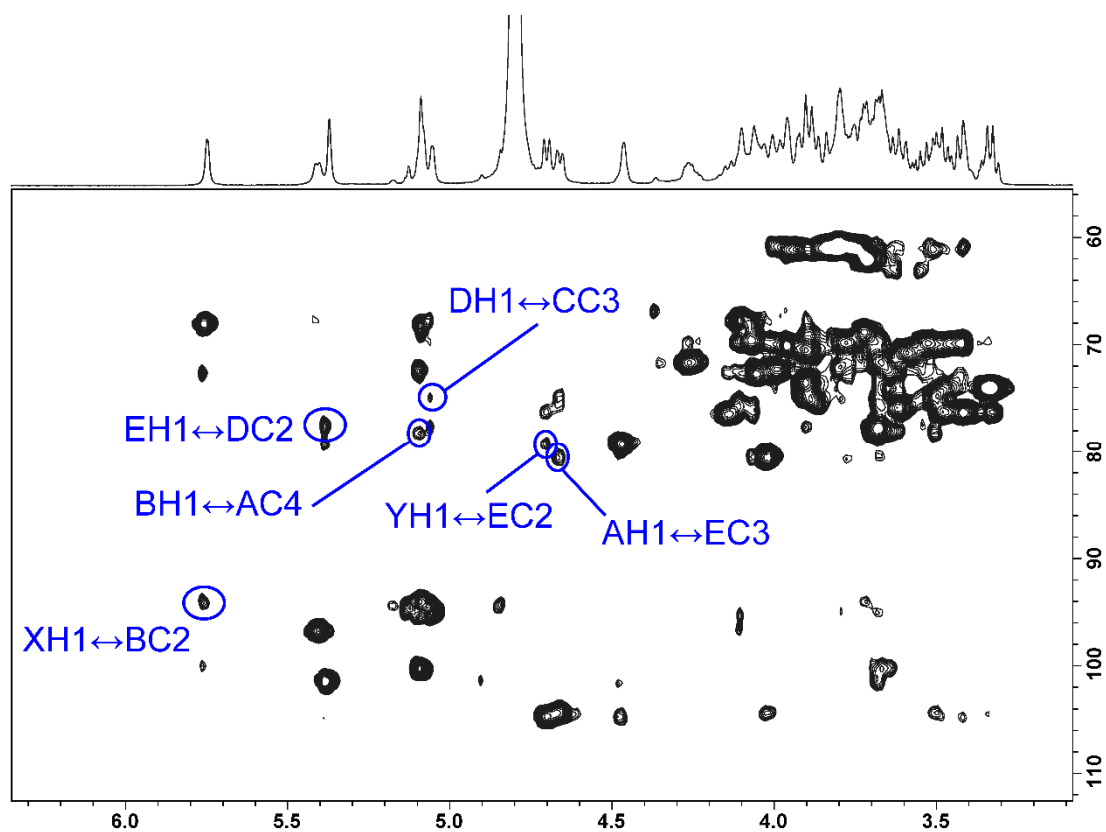

Figure A 8 HSQC-NOESY spectrum of the HePS produced by *L. plantarum* TMW 1.1478 after 72 h at 20°C with the most relevant inter-residual assignments. The nature of the spin systems is indicated in Table A 2 and Figure A 6. This figure was created by Dr. Daniel Wefers and published as Fig. S5 in Prechtl et al. (2018c).
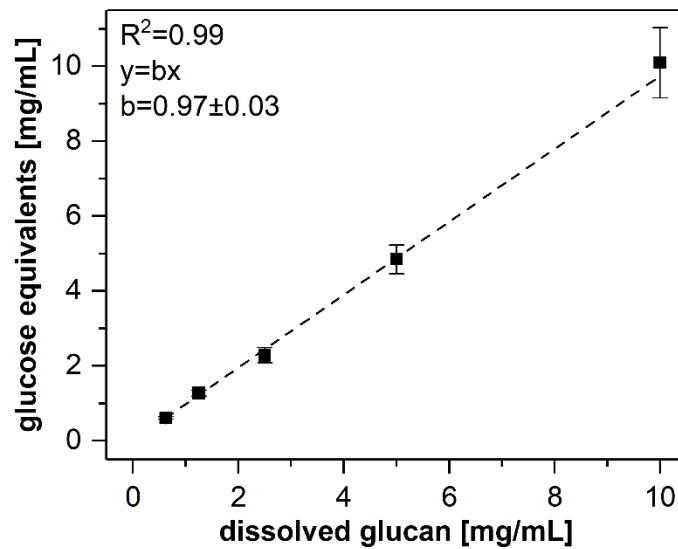
Figure A 9 Validation of phenol sulfuric acid method. Dextran amount in solutions of known concentration (x-axis) was quantified using the phenol sulfuric acid method as described and the results were expressed as mg/mL glucose equivalents (y-axis). All values are expressed as mean ±SD from three replicates. This figure was published as Fig. S2 in Prechtl et al. (2018b).
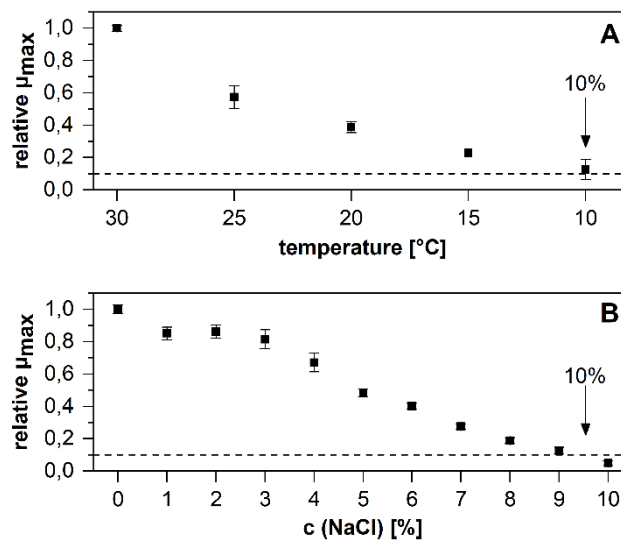

Figure A 10 Relative µmax of *L. sakei* TMW 1.411 for varying temperatures (A) and NaCl concentrations (B). All values were related to the standard condition of 30 °C/0% NaCl and are expressed as mean ±SD of three replicates. This figure was published as Fig. 1 in Prechtl et al. (2018b).
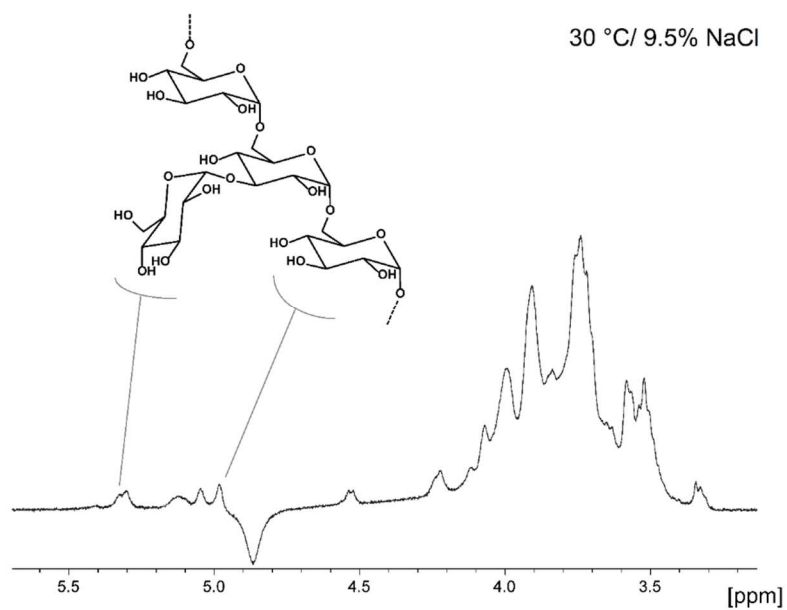
Figure A 11 Figure A 12 Proton spectrum of the dextrans produced at 30 °C/9.5% NaCl. This figure was created by Dr. Daniel Wefers and published as Fig. S1 in Prechtl et al. (2018b).

9.2. Tables

Table A 1 Glycosidic linkages (mol%) of the HePS produced by *L. plantarum* TMW 1.1478 after 72 h at 20 °C as determined by methylation analysis. This table was created by Dr. Daniel Wefers and published as Table 1 in Prechtl et al. (2018c).

Glycosidic linkage	Portion [%]
1,2,3-Rhap	8.5
1,3,4-Rhap	1.9
1,3-Rhap	4.9
1,2-Rhap	0.6
1,4-Glcp	18.1
1,2-Glcp	22.8
t-Glcp	25.5

t = terminal, Rha = rhamnose, Glc = glucose, Gal = galactose, *p* = pyranose. Numbers indicate the substituted positions of a sugar unit, which are derived from the acetylated positions of the corresponding PMAA (e.g. 1,4-Glc*p* is derived from 1,4,5-tri-*O*-acetyl-(1-deuterio)-2,3,6-tri-*O*-methylglucitol).

Table A 2 ^{1}H and ^{13}C chemical shifts of the structural units of the HePS produced by *L. plantarum* TMW 1.1478 after 72 h at 20°C. The proposed structure of the HePS and the corresponding descriptors are shown in Figure 11. This table was created by Dr. Daniel Wefers and published as Table 2 in Prechtl et al. (2018c).

Structural unit	1	2	3	4	5	6
A	4.66	3.35	3.61	3.67	3.50	3.80/3.93
→4)-β-D-Glc*p*(1→	104.23	73.96	75.87	78.22	74.90	60.99
	(164)					
B	5.09	5.75	4.05	4.14	3.64	1.43
→2,3,4)-β-L-Rha*p*(1→	100.06	68.00	72.69	76.41	72.40	17.96
	(164)					
C	5.41	4.10	3.88	3.59	3.90	1.32
→3)-α-L-Rha*p*(1→	96.58	67.64	74.88	70.71	70.55	17.53
	(178)					
D	5.05	3.68	3.90	3.53	3.99	3.80
→2)-α-D-Glc*p*(1→	95.04	77.57	73.51	69.78	72.25	60.81
	(173)					
E	5.37	4.46	4.02	3.67	3.77	1.32
→2,3)-α-L-Rha*p*(1→	101.31	79.16	80.51	71.39	69.79	17.56
	(178)					
X	5.08	3.73	4.07	3.96	4.26	3.71
α-D-Gal*p*(1→	93.87	68.73	69.49	70.08	71.59	62.06
	(173)					
Y	4.70	3.33	3.48	3.42	3.41	3.76/3.84
β-D-Glc*p*(1→	104.58	73.95	76.25	69.84	76.31	61.00
	(164)					
Ac		2.18				
	173.92	21.01				

Table A 3 Statistical t-Test analysis of the pH values measured prior to protein isolation

	pH values prior to protein isolation	
	mMRS-glucose	**mMRS-sucrose**
Replicates		
#1	4,09	4,14
#2	4,11	4,18
#3	4,09	4,18
#4	4,09	4,16
Average	4,10	4,17
StDev.	0,01	0,02

Two sample T-Test (assuming equal variances)

	Variable 1	*Variable 2*
Average	4,095	4,165
Variance	0,0001	0,000366667
Observables	4	4
Pooled Variance	0,000233333	
Hypothesis (Mean difference)	0	
dF	6	
t-statistic	-6,480740698	
P(T<=t) two sided	0,000641313	(<0.01)
critical t value (two sided)	3,707428021	

Table A 4 Log$_2$ FCs, p-values (-log$_{10}$) and related information of differentially expressed proteins (Benjamini-Hochberg FDR ≤ 0.01). Negative log$_2$ FC values indicate higher abundance in glucose treated cells, whereas positive values indicate higher abundance in sucrose treated cells. The predicted functions and assigned SEED subsystems were derived from RAST annotation (FIG identifiers). The gene loci refer to the deposited WGS sequence (accession number QOSE00000000). This table was published as Table 4 in Prechtl et al. (2018a).

Log$_2$ FC	-log$_{10}$ (p-value)	Function	SEED Subsystem	FIG identifier	Gene loci
-3.8	5.03	Arginine deiminase	Arginine Deiminase Pathway	fig|1664.9.peg.1732	DT321_05025
-2.9	5.13	Ornithine carbamoyl transferase	Arginine Deiminase Pathway	fig|1664.9.peg.1733	DT321_05030
-2.5	5.01	Carbamate kinase	Arginine Deiminase Pathway	fig|1664.9.peg.1734	DT321_05035
1.5	5.37	Predicted hydrolase	n.a.	fig|1664.9.peg.175	DT321_00915
1.5	3.85	Deoxyribose-phosphate aldolase	Deoxyribose and Deoxynucleoside Catabolism	fig|1664.9.peg.1010	DT321_08545
1.7	4.43	Trehalose-6-phosphate hydrolase	Trehalose Uptake and Utilization	fig|1664.9.peg.1859	DT321_05660
2.2	6.08	Sucrose operon repressor ScrR	Sucrose utilization	fig|1664.9.peg.1584	DT321_04270
2.2	4.44	Purine nucleoside phosphorylase	Deoxyribose and Deoxynucleoside Catabolism	fig|1664.9.peg.1008	DT321_08535
2.4	3.74	Pyrimidine-nucleoside phosphorylase	Deoxyribose and Deoxynucleoside Catabolism	fig|1664.9.peg.1004	DT321_08515
2.8	6.91	PTS system, fructose-specific IIABC components	Fructose utilization	fig|1664.9.peg.1236	DT321_02745
3.2	4.92	Glucan 1,6-alpha-glucosidase	n.a.	fig|1664.9.peg.1587	DT321_04285
3.2	4.03	1-phosphofructokinase	Fructose utilization	fig|1664.9.peg.1237	DT321_04250
3.2	5.98	Transcriptional repressor of the fructose operon	Fructose utilization	fig|1664.9.peg.1238	DT321_04255
4.5	3.75	Fructokinase	Fructose/Sucrose utilization	fig|1664.9.peg.1588	DT321_04290
5.9	6.20	Sucrose-6-phosphate hydrolase	Sucrose utilization	fig|1664.9.peg.1585	DT321_04275
7.1	7.62	PTS system, sucrose-specific IIBCA components	Sucrose utilization	fig|1664.9.peg.1586	DT321_04280
-0.4	3.74	3-ketoacyl-CoA thiolase	Biotin biosynthesis; Butanol Biosynthesis; Fatty acid metabolism; Isoprenoid Biosynthesis	fig|1664.9.peg.116	DT321_00615
0.5	6.14	Pyruvate formate-lyase	Butanol Biosynthesis; Fermentations: Mixed acid	fig|1664.9.peg.1310	DT321_03110
-0.9	4.61	Dihydrofolate reductase	5-FCL-like protein; Folate Biosynthesis	fig|1664.9.peg.1437	DT321_03535
-0.4	4.01	dipeptidase	n.a.	fig|1664.9.peg.402	DT321_06170
0.8	4.33	Inosine-uridine preferring nucleoside hydrolase	Purine conversions; Queuosine-Archaeosine Biosynthesis	fig|1664.9.peg.662	DT321_07450

9.3. List of publications derived from this work

Peer-reviewed journals

- Prechtl, R. M., Wefers, D., Jakob, F., and Vogel, R. F. (2018). **Cold and salt stress modulate amount, molecular and macromolecular structure of a *Lactobacillus sakei* dextran**. *Food Hydrocolloids*. doi: 10.1016/j.foodhyd.2018.04.003.
- Prechtl, R. M., Wefers, D., Jakob, F., and Vogel, R. F. (2018). **Structural characterization of the surface-associated heteropolysaccharide of *Lactobacillus plantarum* TMW 1.1478 and genetic analysis of its putative biosynthesis cluster**. *Carbohydrate Polymers* 202**,** 236-245. doi: 10.1016/j.carbpol.2018.08.115.
- Prechtl, R. M., Janssen, D., Behr, J., Ludwig, C., Küster, B., Vogel, R. F., and Jakob, F. (2018). **Sucrose-induced proteomic response and carbohydrate utilization of *Lactobacillus sakei* TMW 1.411 during dextran formation.** *Frontiers in Microbiology* 9, 2796. doi: 10.3389/fmicb.2018.02796.
- Hilbig, J., Gisder, J., Prechtl, R.M., Herrmann, K., Weiss, J., and Loeffler, M. (2019). **Influence of exopolysaccharide-producing lactic acid bacteria on the spreadability of fat-reduced raw fermented sausages (Teewurst).** *Food Hydrocolloids* 93**,** 422-431. doi: https://doi.org/10.1016/j.foodhyd.2019.01.056..

Oral presentations and posters

- Prechtl, R. M., Jakob, F., Vogel, R.F. (2017). **Influence of cold and osmotic stress on the macromolecular structure of a Lactobacillus sakei glucan**, LAB12 Symposium, Egmond aan Zee
- Jakob, F., Prechtl, R. M., Vogel, R. F. (2018). **Entwicklung und Einsatz von Exopolysaccharid bildenden Starterkulturen in Fleischwaren**. Lebensmitteltagung 2018 in Wädenswil (Schweiz).
- Jakob, F., Brandt, J., Ua-Arak, T., Prechtl, R. M., Vogel, R. F. (2018). **Mechanistic and ecological insights into polysaccharide formation from sucrose by specialized acetic acid bacteria**. 5th International Conference on Acetic Acid Bacteria (AAB), Freising.
- Jakob, F., Prechtl, R. M., Fraunhofer, M., Brandt, J., Ua-Arak, T., Vogel, R. F. (2018). **Exopolysaccharide production by food-grade lactic and acetic acid bacteria**. CDZ-Symposium der Universität Hohenheim.

9.4. Curriculum vitae

Personal data

Roman Maximilian Prechtl

Born on 19.06.1989 in Trostberg, Germany

Education

06/2015 – 04/2018 Doctoral thesis at the Chair of Technical Microbiology, TU Munich, Germany

10/2012 – 05/2015 Master studies Molecular Biotechnology, TU Munich, Germany

10/2009 – 09/2012 Bachelor studies Molecular Biotechnology, TU Munich, Germany

09/1999 – 06/2008 Gymnasium (Abitur), Hertzhaimer Gymnasium Trostberg, Germany